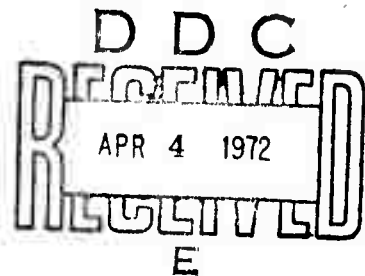


AD 739340

TECHNICAL REPORT

**CENTER FOR
MATERIALS SCIENCE AND ENGINEERING**



**Massachusetts Institute of Technology
Cambridge, Massachusetts 02139**

Reproduced by
**NATIONAL TECHNICAL
INFORMATION SERVICE**
Springfield, Va. 22151



130 R

**BEST
AVAILABLE COPY**

DOCUMENT CONTROL DATA - R & D

(Security classification of title, body of abstract and indexing annotation must be entered when the overall report is classified)

1. ORIGINATING ACTIVITY (Corporate author)

Massachusetts Institute of Technology
Cambridge, Massachusetts 02139

2a. REPORT SECURITY CLASSIFICATION

Unclassified

2b. GROUP

3. REPORT TITLE

Structure and Property Control Through Rapid Quenching of Liquid Metals

4. DESCRIPTIVE NOTES (Type of report and inclusive dates)

Semi-Annual Technical Report #3, (July 1, 1971-December 31, 1971)

5. AUTHOR(S) (First name, middle initial, last name)

Grant, Nicholas J.; Pelloux, Regis M.N.; Flemings, Merton C.; Argon, Ali S.

6. REPORT DATE

January 1, 1972

7a. TOTAL NO. OF PAGES

129

7b. NO. OF REFS

8a. CONTRACT OR GRANT NO.

DAHC15 70 C 0283

b. PROJECT NO.

ARPA Order #1608

c.

Program Code #0D10

d.

9a. ORIGINATOR'S REPORT NUMBER(S)

9b. OTHER REPORT NO(S) (Any other numbers that may be assigned this report)

10. DISTRIBUTION STATEMENT

11. SUPPLEMENTARY NOTES

12. SPONSORING MILITARY ACTIVITY

Advanced Research Projects Agency
1400 Wilson Blvd.
Arlington, Virginia 22209

13. ABSTRACT

This report presents the results and accomplishments of the third six-month period of a three year research program investigating the processing of billets from rapidly quenched liquid metals.

Various powder metallurgy (P/M) and quench-casting techniques have been employed to generate extremely fine dendrite arm spacings and homogeneous structures. Iron, nickel and cobalt-base alloy powders, produced by steam atomization (coarse powders), argon atomization, vacuum atomization, and the rotating electrode process, have been consolidated into dense billets by hot isostatic pressing (HIP) and/or extrusion. New powder processes based on separating solid nodules from a liquid-solid mixture and random break up of a fine stream of liquid metal into spherical particles are being evaluated.

The hot working properties of P/M billets and quench-cast bars have been evaluated by hot rolling, high strain rate tests, and creep (superplastic) testing. Two P/M superalloys, MAR-M-509 (cobalt-base) and IN-100 (nickel-base) after HIP and hot extrusion demonstrated excellent hot workability under high strain rate and creep forming conditions, respectively.

Detailed analyses of microstructure, heat treatment, and mechanical properties are presented for all P/M alloys and compared to equivalent cast materials. Room temperature properties of P/M alloys continue to be far superior to their cast counterparts. Elevated temperature properties are significantly improved by proper heat treatments.

Rapid Quenching Structure and Segregation Control Powder Metallurgy

[illegible]

10. AVAILABILITY/LIMITATION NOTICES: Enter any limitations on further dissemination of the report, other than those

14. **KEY WORDS:** Key words are technically meaningful terms or short phrases that characterize a report and may be used as index entries for cataloging the report. Key words must be selected so that no security classification is required. Identifiers, such as equipment model designation, trade name, military project code name, geographic location, may be used as key words but will be followed by an indication of technical context. The assignment of links, rules, and weights is optional.

For period - July 1, 1971 to Dec. 31, 1971

Semi-Annual Technical Report No. 3

STRUCTURE AND PROPERTY CONTROL THROUGH
RAPID QUENCHING OF LIQUID METALS

Sponsored by
Advanced Research Projects Agency
Contract No.: DAHC15 70 C 0283

ARPA Order No.: 1608
Program Code No.: OD10

Contractor:
Massachusetts Institute of Technology
Cambridge, Mass. 02139

Principal Investigator:
N.J. Grant
(617) 864-6900 Ext. 5638

Effective date of Contract: June 22, 1970
Contract Expiration Date: July 21, 1972

Total Amount of Contract: \$470,300

ARPA Order No. 1608

The views and conclusions contained in this document are those of the authors and should not be interpreted as necessarily representing the official policies, either expressed or implied, of the Advanced Research Projects Agency or the U.S. Government.

TABLE OF CONTENTS

	<u>Page Number</u>
TASK I PROCESSING OF ALLOYS	1
I. Introduction	1
II. Experimental Work	1
A. Melting and Atomization	1
B. Powder Characterization	2
1. Maraging Steels	2
2. Cobalt Base Superalloys	3
C. Powder Consolidation	3
1. Objectives	3
2. Hot Isostatic Pressing Runs	3
3. HIP Microstructures	3
4. Extrusion Runs	5
III. Conclusions	5
Tables	7
Figures	15
TASK II SOLIDIFICATION RESEARCH	21
I. Introduction	21
II. Results	24
1. High Temperature Homogenization Treatment of Consolidated Billets of Maraging 300 and IN-100 Alloys	24

TASK II - SOLIDIFICATION RESEARCH cont'd

2. Rapid Solidification of a Cobalt Base Alloy	25
3. Rheoatomization and Refining by Partial Solidification	26
Tables	31
Figures	33

TASKS III and IV THERMOMECHANICAL TREATMENT, MICROSTRUCTURE AND MECHANICAL PROPERTIES 39

I. Mechanical Properties of 300 Grade Maraging Steel	40
A. Introduction	40
B. Tensile Properties	41
C. Fracture Toughness Properties	41
D. Stretched Zones	43
E. Fatigue Properties	44
Tables	45
Figures	48
II. Microstructure and Mechanical Properties of IN-100 Processed By Powder Metallurgy	54
A. Introduction	54
B. Powder Characterization	55
C. Microstructure	55
D. Grain Coarsening	56

TASKS III and IV - THERMOMECHANICAL TREATMENT,
MICROSTRUCTURE AND MECHANICAL PROPERTIES cont'd

E. Mechanical Properties	57
F. Creep Testing	59
References	61
Tables	62
Figures	65
III. Thermomechanical Treatment, Microstructure and Mechanical Properties of Cobalt-Base Superalloys	77
A. Introduction	77
B. Composition and Processing History	79
C. Thermomechanical Treatment	81
D. Heat Treatment	82
E. Atomized Cobalt-Hafnium Powders	84
F. Mechanical Properties	86
References	88
Tables	89
Figures	98

LIST OF TABLES

<u>Table No.</u>	<u>Title</u>	<u>Page No.</u>
<u>TASK I</u>		
I	Atomization Runs	7
II	Chemistry	8
III	Hot Isostatic Pressing Runs	12
<u>TASK II</u>		
I	Rheoatomized Sn-14.4% Pb Alloy	31
II	Results of Refining Experiments Done on Al-30% Si-6% Fe-1% Ti Alloy	32
<u>TASKS III and IV</u>		
<u>Maraging Steels</u>		
I	Summary of Tensile Properties	45
II	Summary of Fracture Toughness Properties	46
III	Tension-Compression Fatigue Testing	47
<u>IN-100</u>		
I	IN-100 Chemistries (w/o)	62
II	Size Range and Screen Analysis (%) Retained) of the Powders as Received from the Manufacturers	63
III	IN-100 Room Temperature Properties	64

LIST OF TABLES - cont'd

<u>Table No.</u>	<u>Title</u>	<u>Page No.</u>
<u>Cobalt-Base Alloys</u>		
i	MAR-M-509 Cobalt-Base P/M Alloy Compositions and Processing History	89
II	Co-Hf P/M and Cast Alloy Compositions and Processing History	90
III	Cobalt-Base Alloys - Heat Treatment and Hardness Data	91
IV	Dendrite Arm Spacing Measurements in Co-Hf Alloy	92
V	Cobalt Alloy - Room Temperature Tensile Properties	93
VI	Stress Rupture Data	94
VII	Cobalt Alloys - 1800°F, 100 Hour Life Stress Rupture Data	96
VIII	Cobalt Alloys - Hot Plasticity Data	97

LIST OF FIGURES

<u>Figure No.</u>	<u>Title</u>	<u>Page No.</u>
<u>TASK I</u>		
1.	Maraging steel VM-300. Oil quench atomization. Heat No. 230. -25/+30 mesh. Oxide inclusions. Unetched. 500x.	15
2.	Ni-Co-Mo maraging steel. Heat No. 231. Cleaned. Mesh fractions -4/+5, -8/+10, -16/+18. and -25/+30. 1x.	15
3.	Ni-Co-Mo maraging steel. Heat No. 231. -8/+10 mesh. Oxide inclusions. Unetched. 500x.	16
4.	Cobalt-hafnium alloy +Si and B additions. Heat No. 228. As atomized. 1x.	16
5.	IN-100, low carbon, R.E.P. powder, -35 mesh. HIP @ 1825°F, 27,700 psi, 1 hr. As pressed. Etched. 100x.	17
6.	IN-100, low carbon, R.E.P. powder, -35 mesh. HIP @ 1825°F, 27,700 psi, 1 hr. As pressed. Etched. 1000x.	17
7.	IN-100, low carbon, R.E.P. powder, -35 mesh. HIP @ 2300°F, 27,700 psi, 1 hr. As pressed. Etched. 100x.	18
8.	IN-100, normal carbon, R.E.P. powder, -35 mesh. HIP @ 2300°F, 27,700 psi, 1 hr. As pressed. Etched. 100x.	18

LIST OF FIGURES - cont'd

<u>Figure No.</u>	<u>Title</u>	<u>Page No.</u>
9.	IN-100, normal carbon, R.E.P. powder, -35 mesh. HIP @ 1900°F, 26,300 psi, 1 hr. Etched. 1000x.	19
10.	IN-100, low carbon, R.E.P. powder, -35 mesh. HIP @ 1900°F, 26,300 psi, 1 hr. Etched. 1000x.	19
11.	IN-100, low carbon, R.E.P. powder, -35 mesh. HIP @ 2320°F, 27,300 psi, 1 hr. IN-100/low carbon steel can inter-diffusion zone \approx .020". Etched. 100x.	20

TASK II

1.	Effect of high temperature homogenization on composition variations across nickel plated interfaces of consolidated rods of maraging 300 alloy.	33
2.	Composition variations across a nickel plated interface of consolidation rods of IN-100, homogenized at 2100°F for 3 hrs.	34
3.	Photomicrographs showing structure of a rapidly solidified rod of Co-Hf alloy. (a) 300x, (b) 1500x.	35
4.	Sketch of apparatus for mixing and atomization of liquid-solid slurries of alloys.	36

LIST OF FIGURES - cont'd

<u>Figure No.</u>	<u>Title</u>	<u>Page No.</u>
5.	Microstructures of powders obtained from rheoatomization of Sn-15% Pb alloy; (a) structure of a "primary" solid particle (b) structure of atomized liquid (liquid existing in the slurry before atomization) particles. 100x.	37
6.	Microstructure of a vigorously agitated slurry of Al-4% Si alloy cast in a chill mold at 0.5 volume fraction solid. 50x.	38

TASKS III
and IV

Maraging Steels

1.	Commercial 300 grade maraging steel - 15% Nital etch 1 minute. 150x.	48
2.	Hot isostatically pressed and hot rolled Nuclear Metals powder of 300 grade maraging steel - Nital 15%. 150x.	48
3.	Compact tensile fracture toughness specimen. The dimensions are for a 0.25 inch thick specimen.	49

LIST OF FIGURES - cont'd

<u>Figure No.</u>	<u>Title</u>	<u>Page No.</u>
4.	Fracture surfaces of fracture toughness specimen. Top: VASCOMAX 300, Middle: HIP 69 perpendicular to the rolling direction, Bottom: HIP 69 parallel to the rolling direction. Note the particle delamination in the last two specimens. 1.5x.	50
5.	Stereo pairs (0° and 7°) of matching surfaces (A and B) of the stretched zone in 300 grade maraging steel. Magnification 1225x.	51
6.	Tension-compression fatigue specimen.	52
7.	S-N curve tension-compression maraging steel 300.	53
<u>IN-100</u>		
1a.	As-received Federal Mogul IN-100 powders. SEM 140x.	65
1b.	Polished and etched sections of above powders. 500x.	65
2a.	As-received Homogeneous Metals IN-100 powders. SEM 24x.	66
2b.	Polished and etched sections of above powders. 200x.	66
3a.	As-received Nuclear Metals IN-100 powders. SEM 63x.	67
3b.	Polished and etched sections of above powders. 350x.	67

LIST OF FIGURES - cont'd

<u>Figure No.</u>	<u>Title</u>	<u>Page No.</u>
4.	Longitudinal section of as-extruded Federal Mogul powders. 200x.	68
5.	Grain-coarsened Nuclear Metals powder extrusion. 24 hours at 2270°F. 500x.	68
6.	High strain rate log stress vs. log rupture time at various temperatures for as-cast IN-100.	69
7.	High strain rate log stress vs. log rupture time at various temperatures for as-extruded IN-100.	70
8.	High strain rate log stress vs. log deformation rate at various temperatures for as-extruded IN-100.	71
9.	High strain rate effect of deformation rate on elongation at various temperatures for as-extruded IN-100.	72
10.	High strain rate fracture cross-section of extruded Federal Mogul powder test bar. 200x.	73
11.	As-extruded tensile bars superplastically deformed at 1900°F at indicated strain rates.	74
12.	Microstructure of a superplastically deformed as-extruded IN-100 tensile bar. 1000x.	74

LIST OF FIGURES - cont'd

<u>Figure No.</u>	<u>Title</u>	<u>Page No.</u>
13.	Superplastic deformation of as-extruded IN-100 at various temperatures plotted as log true flow stress vs. log strain rate.	75
14.	1800°F stress-rupture properties for various grain sizes of cast IN-100 and extruded IN-100 powders.	76
<u>Cobalt-Base Alloys</u>		
1.	Effect of tap temperature and chemistry on the morphology of steam atomized coarse cobalt powders.	98
2.	Stoichiometric mono-carbides in cobalt alloys.	99
3.	Cobalt-1 atom % HfC P/M alloy comparing HIP + Extr. structure with the HIP + Extr. + RE-HIP structure.	100
4.	Coarsening rate of fine grains in secondary recrystallized (2280°F and 2225°F) and in uniform (2170°F) MAR-M-509 (P/M) alloy structures.	101
5.	Abnormal grain growth in MAR-M-509 P/M alloys heat treated at 2280 ± 10°F.	102
6.	Microstructures of MAR-M-509 P/M alloys heat treated for 121 hours at approximately 25°F above and below the secondary recrystallization temperature.	103

LIST OF FIGURES - cont'd

<u>Figure No.</u>	<u>Title</u>	<u>Page No.</u>
7.	Grain coarsening behavior of as-extruded Co-1 atom % HfC alloy.	104
8.	The radial fraction liquid (or vol % solid) versus free-fall time or distance for spherical liquid droplets of steel.	105
9.	Fracture topography and profile of MAR-M-509 P/M alloy HIP at 2000°F and 28 Ksi for 2 hours and subsequently tensile tested at room temperature.	106
10.	Fracture topography and profile of MAR-M-509 P/M alloy HIP at 2150°F and 27 Ksi for 2 hours and subsequently tensile tested at room temperature.	107
11.	Fracture topography and profile of MAR-M-509 P/M alloy HIP at 2300°F and 28 Ksi for 2 hours and subsequently tensile tested at room temperature.	108
12.	MAR-M-509 and HiZr-509 stress rupture data at 1800°F and 1850°F.	109
13.	Cobalt-Hafnium alloys stress rupture data at 1800°F.	110
14.	High strain rate stress-rupture data for MAR-M-509 P/M alloys in the as-HIP condition.	111

LIST OF FIGURES - cont'd

<u>Figure No.</u>	<u>Title</u>	<u>Page No.</u>
15.	High strain rate stress-rupture data for cobalt-base alloys in the cast or extr. condition.	112

- TASK I -

Processing of Alloys

P. E. Price

R. Widmer

J. Blucher

TASK I

Processing of Alloys

I. INTRODUCTION

In the past six months Task I work on structure and property control through rapid quenching of liquid metals has continued past efforts in production of coarse powders of iron and cobalt base alloys. Emphasis has increased on hot isostatic pressing of larger billets for subsequent hot working. Coarse powder atomization work was carried out with Mar M 509 to produce material for sheet bar rolling. New compositions of cobalt base alloys utilizing hafnium as a major alloying element were steam atomized. Several maraging steel atomization runs were conducted with the primary goal of decreasing oxygen pickup in the coarse powder particles. An extended series of experiments reported earlier showed that oxygen appears in part as spherical oxide inclusions. For maraging steels containing titanium and aluminum as essential strengthening elements, oxygen pickup in atomization makes the recovery of these strengthening elements unpredictable. Current work has utilized several methods in attempts to produce an oxide free coarse maraging steel powder.

Consolidation of powders has been carried out by hot isostatic pressing and extrusion. The largest HIP billets and sheet bars of IN-100 and Mar M 509 produced to date in the program were processed and forwarded to Task III. With normal carbon (~ 0.15 wt. %) IN-100 from several commercial sources, earlier HIP processing showed that carbide films invariably form at prior particle boundaries limiting grain growth and hot ductility. Current work has included investigation of the hot isostatic pressing response of low carbon IN-100 rotating electrode powder.

II. EXPERIMENTAL WORK

A. Melting and Atomization

A summary of all melting and atomization runs is given in Table I. Atomization runs were carried out routinely with the exception of IMT Ht. No. 230 which involved

quenching the VM-300 coarse powder in heat treating type quenching oil (Thermoquench). Surface flaming occurred during entry of the metal spray into the oil bath, but extinguished immediately at the end of the atomization.

B. Powder Characterization

1. Maraging Steels

Chromium containing maraging steel (see Table II for composition) was atomized with the objective of utilizing the chromium for oxidation protection of the liquid metal droplets. The overall metal chemistry resulted, however, in production of twisted flaky particles unsuitable for further processing in spite of a high tap temperature of 3030°F.

Conventional maraging steel, VM-300, which has been investigated using coarse powder techniques, was atomized (Ht. No. 230) and oil quenched with the objective of maintaining relatively oxygen free conditions during the quenching step. Chemical analysis (Table II) of separate size fractions of cleaned powder showed that oxygen pickup was similar to that previously found for VM-300. Oxide inclusions were also found in all separate size fractions. Figure 1 is an example. Carbon analysis (Table II) of these same size fractions showed varying degrees of carbon pickup presumably from the quenching oil.

One heat of a "state of the art" 400 KSI maraging steel containing solely nickel, cobalt and molybdenum as alloying elements was steam atomized, Ht. No. 231. In the absence of reactive elements such as titanium and aluminum, the coarse powder morphology was nearly ideal, see Figure 2. Metallographic examination showed oxide inclusions, Figure 3. Chemical analysis, Table II, showed oxygen levels in the 1000 - 2000 ppm range. Since reactive elements were not present, the data suggests that the oxygen levels (inclusions plus solid solution oxygen) found in the coarse powder are a result of fundamental mechanisms in the steam atomization process as currently operated. It is also interesting to note that the carbon levels of the various mesh fractions are below that of the melt dip sample. This finding indicates that there is sufficient time between atomization and droplet solidification for chemical reactions in the liquid metal

droplets to take place to a measurable extent. Quenching rates thus are not fast enough to completely prevent reactions required by the thermodynamics of the liquid metal droplet/atomization environment "system".

2. Cobalt Base Alloys

Both Mar M 509 and two cobalt-hafnium alloys were steam atomized in this reporting period. The cobalt-hafnium alloys as steam atomized were predominantly twisted flake, coarse "powder" particles. Additions of boron and silicon to modify oxide forming characteristics (Ht. No. 228)(Figure 4) did not produce rounded particles. The cobalt-hafnium alloys also resisted chemical cleaning action previously used successfully for cobalt alloys. Chemistry is given in Table II.

Mar M 509 steam atomized to produce material for HIP billets and sheet bars resulted in coarse rounded powder with "shells" and "nested" particles. Chemistry of these heats is given in Table II.

C. Powder Consolidation

1. Objectives

Powders were consolidated by hot isostatic pressing and extrusion.

Objectives were:

- a. to produce material for test,
- b. to produce billets and sheet bar for further processing,
- c. to investigate the effects of HIP parameters on microstructure.

2. Hot Isostatic Pressing Runs

All hot isostatic pressing runs completed in the present reporting period are summarized in Table III.

3. HIP Microstructures

The majority of microstructure investigations were on IN-100 compacts. One sample of oil quenched coarse powder VM-300 was investigated.

The structure of oil quenched VM-300 after HIP was examined. Carbon pickup (see Table II) in the coarse powder partly manifested itself as white patches of retained austenite ($M_s \ll \text{room temperature}$) in the etched microstructure.

Hot isostatic pressing of IN-100 in the 1800 - 1900°F range has for the first time disclosed the nature of the compaction process. As Figure 5 shows, some powder particles fill space with little or no deformation. Their cast grain structure remains intact. Other particles are partially or completely deformed. The result is a highly mixed grain size. One interesting additional feature is that a spherical void in a particle which was not deformed to fill space remained intact, Figure 5, lower right. The nature of the deformation structure is more clearly shown in Figure 6, 1000X, where both the cast structure and the deformation structure may be seen interspersed.

The next significant feature established for HIP'ed IN-100 is the marked effect of carbon level on the grain growth response. Figure 7 shows an ASTM grain size of $\sim 1 \frac{1}{2}$ established by HIP @ 2300°F for a low carbon R.E.P. powder. Liquation at triple points has occurred. This should be expected since the melting range for the alloy (C .15 - .20) is 2305-2435°F. 1000X magnification shows the white patches at triple points at 100X to be eutectic solidification structures.

Normal carbon R.E.P. IN-100 HIP'ed at the same time as the above material responds with an ASTM grain size of ~ 5 , Figure 8. Carbide particle clusters in curvilinear arrays prevent grain growth across prior particle boundaries. Even within prior particle boundaries, grain growth has been inhibited by dispersed discrete carbides. Liquation did not occur to as great an extent as in the low carbon compact.

In the lower temperature (1900°F) HIP compaction range, interparticle carbide films still occur, Figure 9. Aside from larger discrete carbides, unrefined in R.E.P. atomization, particles are outlined in places by thin sharp lines, presumed to be carbides. By contrast, low carbon material HIP'ed at the same time shows particles outlined by a small scale blocky phase, Figure 10. There is nearly complete absence of carbides. In both the low and normal carbon structures, the cast dendrites remain unhomogenized. Where deformation has occurred, the structure has changed from aligned dendrite arms to a "blocky" structure.

Hot isostatic pressing at 2150°F of low carbon IN-100 results in coarsening of the deformation structure. Prior particle boundaries are outlined by a larger scale blocky structure. Carbides are nearly completely absent. The cast structure is not completely homogenized.

The extent of interaction of the can and the powder during HIP was investigated. Low carbon steel (1020) was used to can the low carbon IN-100 R.E.P. powder and HIP was carried out at 2320°F. Since 2320°F can be considered close to a limiting case for nickel base alloys, i.e. higher process temperatures would rarely be used, the depth of the interaction zone with a carbon steel can would usually be less than that of the present case. Figure 11 shows an interdiffusion zone of $\leq 2''$ @ 100X, actual $\leq .020''$. The .020" zone is defined on the basis that inside this zone grain growth has occurred unimpeded by carbide formation and to an extent identical to that of the center of the compact, i.e. ASTM $\sim 1\ 1/2$. It is to be noted that at least .020" of material would normally be allowed for finish machining of a part pressed to "shape".

4. Extrusion Runs

Extruded bars of normal carbon IN-100 R.E.P. powder and argon atomized IN-100 fine powder (normal carbon, Federal Mogul - 60 mesh) were processed and forwarded to Task III for test.

III. CONCLUSIONS

With the cobalt base alloys and maraging steels atomized in this period, the liquid metal droplets have, in general, interacted strongly with the environment resulting in unfavorable particle geometry, oxidation of reactive elements, and oxide inclusions in the case of a "non-reactive" Ni-Co-Mo maraging steel.

Hot isostatic pressing of low carbon IN-100 has demonstrated the feasibility of producing large grain size material. Particle boundaries have been shown to have a distinct behavior in low carbon and normal carbon IN-100 powders. Under identical pressing conditions at 2300°F, grain growth is inhibited at particle boundaries in

compacts with normal carbon powder, whereas with low carbon powder grain growth is inhibited at a larger grain size by grain boundary liquation. The use of low carbon steel cans for HIP of IN-100 at $\sim 2300^{\circ}\text{F}$ produces an interaction zone of the order of .020".

TABLE I

Atomization Runs

Heat No.	Alloy	Atomization Steam, Argon	Nozzles, Pressure		Tundish Nozzle	Tap Temp.	Objective	Result
			Top Pressure	Side Pressure				
224	Co - Hf	S	60 mmg 8 psig	2 1/2 x 100 mmf 10 psig	13/32"	3050°F	Produce powder for cleaning & consolidation.	Sharp, flaky powder.
225	Mar M 509	S	60 mmg 9 psig	2 1/2 x 100 mmf 12 psig	13/32"	2980°F	Produce powder for cleaning & HIP.	Rounded, oxidized powder. Shells.
226	Mar M 509	S	60 mmg 9 psig	2 1/2 x 100 mmf 12 psig	13/32"	3000°F	Produce powder for cleaning & HIP.	Rounded, oxidized powder. Shells.
227	Mar M 509	S	60 mmg 9 psig	2 1/2 x 100 mmf 13 psig	13/32"	2950°F	Produce powder for cleaning & HIP.	Rounded, oxidized powder. Shells.
228	Co - Hf	S	60 mmg 9 psig	2 1/2 x 100 mmf 12 psig	13/32"	3100°F	Test effects of Si, B on powder particle shape.	Some rounding. Mostly irregular flake.
229	Cr-Maraging Steel	S	60 mmg 9 psig	2 1/2 x 100 mmf 12 psig	13/32"	3030°F	Test effect of Cr on oxide pickup.	Sharp, flaky, irregular powder. Tundish freeze up.
230	VM-300 Maraging Steel	A		Unijet "U" 55 psig	-----	2950°F	Test effect of oil quench on oxide pickup.	Coarse, rounded powder. Chemistry, Table II,
231	Ni-Co-Mo Maraging Steel	S	60 mmg 9 psig	2 1/2 x 100 mmf 12 psig	13/32"	2960°F	Produce Ti, Al free maraging steel powder for test.	Coarse, rounded powder. Median particle size, 1150 microns, $\sigma = 2.0$.

TABLE II

Chemistry1. Maraging Steels

Heat No.	Sample Description	Analysis	
229	Chromium containing maraging steel. <u>Aim composition.</u>	10 Ni, 10 Cr, 2 Mo, .2 Ti, .4 Al, Bal Fe	
230	VM-300 Argon atomized. Oil quench. -4/+5 mesh. 5 cleaning cycles + HCl etch.	<u>O</u> (ppm)	<u>C</u> (wt. %)
	Same as above except -8/+10 mesh.	530	0.12
	Same as above except -16/+18 mesh.	530	0.24
	Same as above except -25/+30 mesh.	1400	0.12
	Melt dip sample.	2200	0.090
231	Ni-Co-Mo maraging steel. <u>Aim composition.</u>	30	0.020
		12 Ni, 15 Co, 10 Mo, <.02 C, Bal Fe	

Chemistry

Page 9

1. Moroging Steels (Continued)

Heat No.	Sample Description	Analysis	
231	Ni-Co-Mo moroging steel. Steam atomized. -4/+5 mesh, 5 cleaning cycles + HCl etch. Same as above except -8/+10 mesh. Same as above except -16/+18 mesh. Same as above except -25/+30 mesh. Melt dip sample.	<u>O</u> (ppm) 1300 1900 2400 2300 270	<u>C</u> (wt. %) 0.0098 0.0074 0.0095 0.0095 0.012
224	Co-Hf alloy. <u>Nominal</u> composition. -3 1/2 mesh powder, 11 cycles chemical cleaning.	<u>O</u> (ppm) 3300	<u>C</u> (wt. %) 0.55
228	Co-Hf alloy. <u>Aim</u> composition.	11.8 Hf, 20.0 Cr, 5.0 Mo, 9.0 Ni, 0.6 C, 1.0 Si, Bal Co, .05 B added.	
225	Mar M 509. <u>Aim</u> composition. - 3 1/2 mesh. 6 cycles chemical cleaning + 1 cycle aqua-regia. <u>Analyzed values.</u> Melt dip sample.	0.65 C, 24.0 Cr, 11.0 Ni, 7.5 W, 4.0 Ta, .25 Ti, 0.6 Zr, Bal Co, .05 B added. 0.60 C, 22.9 Cr, 11.4 Ni, 7.5 W, 2.8 Ta, .15 Ti, 0.27 Zr, .031 B, Bal Co. <u>O</u> (ppm) 960 <u>O</u> (ppm) 140	

2. Cobalt Base Alloys

2. Cobalt Base Alloys (Continued)

Heat No.	Sample Description	Analysis
226	Mar M 509. <u>Aim composition.</u> - 3 1/2 mesh. 6 cycles chemical cleaning + 1 cycle oquo-regia. Analyzed values. Melt dip sample.	0.65 C, 24.0 Cr, 11.0 Ni, 7.5 W, 4.0 Ta, .25 Ti, 0.6 Zr, Bal Co. .05 B added. 0.47 C, 22.9 Cr, 11.5 Ni, 7.5 W, 2.4 Ta, .14 Ti, 0.30 Zr, 0.023 B, Bal Co. <u>O</u> (ppm) 1000 <u>O</u> (ppm) 14
227	Mar M 509. <u>Aim composition.</u> Melt dip sample.	0.65 C, 24.0 Cr, 11.0 Ni, 7.5 W, 4.0 Ta, .25 Ti, 0.6 Zr, Bal Co. .05 B Added. <u>O</u> (ppm) 21
<u>Hot Isostatic Pressing Runs</u>		
<u>HIP Run No.</u> 1.	VM-300 R.E.P. powder. Lot No. 8494-00849. -20/+35 mesh. Vasco Hr. No. 1503-A. Mill analysis.	.009 C, .01 Si, .02 Mn, .006 S, .004 P, 4.88 Mo, 9.04 Co, 18.33 Ni, .11 Al, .64 Ti, .003 B, .011 Zr, .05 Ca (added).
4.	IN-100 R.E.P. powder. Lot No. 4521. -35/+325 mesh.	.178 C, .0015, <.01 Mn, <.01 Si, <.40 Cr, 3.08 Mo, 15.18 Co, 4.82 Ti, 5.81 Al, .016 B, .05 Zr, <.01 Fe, Bal Ni, Al + Ti 10.63, .99 V, 74 ppm <u>O</u> .

Hot Isostatic Pressing Runs

HIP Run No.	Sample Description	Analysis
7.	IN-100 R.E.P. powder. Lot No. 4529. -35 mesh. <u>Ingot analysis.</u>	.176 C, .001 S, <.01 Mn, .02 Si, 9.52 Cr, 3.07 Mo, 15.01 Co, 4.71 Ti, 5.73 Al, .018 B, .05 Zr, <.01 Fe, Bal Ni, Al + Ti, 10.44, .98 V.
9.	IN-100. Low carbon R.E.P. powder. Lot No. 6140. -35 mesh <u>Ingot analysis.</u>	.02 C, .006 S, <.10 Mn, <.10 Si, 9.20 Cr, 2.92 Mo, 14.9 Co, 4.68 Ti, 5.65 Al, .014 B, .07 Zr, .46 Fe, Bal Ni, .94 V.

TABLE III

Hot Isostatic Pressing Runs

No.	Can No.	Powder	Billet Size at Start	Pressing Conditions	Remarks
1.	1E30	VM-300 Nuclear Metals R.E.P. Lot No. 8494-00849. Vasco Ht. No. 1503-A, -20/+35 mesh.	2" x 3" x 11 7/8" sheet bar.	2150°F, 28,400 psi, 2 hr.	To Task III intact. Chemistry Table II.
2.	1G07	VM-300 Nuclear Metals R.E.P. Lot No. 8494-00849. Vasco Ht. No. 1503-A, -20/+35 mesh.	2" x 3" x 12" sheet bar.	2200°F, 28,100 psi, 1 hr.	To Task III intact.
3.	1H28	Mar M 509, IMT 30-225, - 3 1/2 mesh.	6" ϕ x 6"	2300°F, 28,400 psi, 2 hr.	To Task III intact. Chemistry Table II.
4.	1H29	Mar M 509, IMT 30-226, - 3 1/2 mesh.	6" ϕ x 6"	2150°F, 26,600 psi, 2 hr.	To Task III intact. Chemistry Table II.
4.	1H22	IN-100 Nuclear Metals R.E.P. Lot. No. 4521, -35/+325 mesh.	6" ϕ x 6"	2150°F, 26,600 psi, 2 hr.	To Task III intact. Chemistry Table II.
5.	1H27	Mar M 509, IMT 30-225, 226 comb. - 3 1/2 mesh.	6" ϕ x 6"	2000°F, 28,000 psi, 2 hr.	To Task III intact.
5.	1H20	IN-100 Nuclear Metals R.E.P. Lot No. 4521, -35/+325 mesh.	6" ϕ x 6"	2000°F, 28,000 psi, 2 hr.	To Task III intact.
6.	1H21	IN-100 Nuclear Metals R.E.P. Lot. No. 4521, -35/+325 mesh.	6" ϕ x 6"	2300°F, 27,400 psi, 2 hr.	To Task III intact.
7.	1114	IN-100 Nuclear Metals R.E.P. Lot No. 4529, -35 mesh.	2" x 5" x 13 1/8" sheet bar.	2300°F, 27,700 psi, 1 hr.	To Task III intact. Chemistry Table II.

Hot Isostatic Pressing Runs (Continued)

Page 13

No.	Can No.	Powder	Billet Size of Start	Pressing Conditions	Remarks
6.	1116	Mar M 509, IMT 227, - 3 1/2 mesh.	2" x 5" x 12 1/4" sheet bar.	2300°F, 28,000 psi, 1 hr.	To Task III intact.
8.	1118	VM-300, IMT 197, Oil quench. Cleaned + H2 anneal.	1" ϕ x 6 1/2"	2300°F, 28,000 psi, 1 hr.	
9.	1K21	IN-100, Low carbon Nuclear Metals R.E.P. Lot No. 6140, -35 mesh.	1" ϕ x 13"	1825°F, 27,700 psi, 1 hr.	Chemistry Table II.
10.	1K20	IN-100, Low carbon Nuclear Metals R.E.P. Lot No. 6140, -35 mesh.	1" ϕ x 13"	2300°F, 27,700 psi, 1 hr.	
10.	1K26	IN-100, Nuclear Metals P.E.P. Lot No. 4529, -35 mesh.	1" ϕ x 7"		Table II Chemistry,
10.	1K28	6 pieces Co-Hf alloy extrusion. IMT 30-217.	1/2" ϕ x 9"	2300°F, 27,700 psi, 1 hr.	HIP of extrusion for densification of internal tears. To Task III intact.
11.	1K27	IN-100, Nuclear Metals R.E.P. Lot No. 4529, -35 mesh.	1" ϕ x 7"	1900°F, 26,300 psi, 1 hr.	Leaked. Can No. 1K18
	1K18	IN-100, Low carbon.	1" ϕ x 13"		
12.	1K17	IN-100, Low carbon. Nuclear Metals R.E.P. Lot No. 6140, -35 mesh.	1" ϕ x 13"	1900°F, 26,300 psi, 1 hr.	

Hot Isostatic Pressing Runs (Continued)

No.	Can No.	Powder	Billet Size at Start	Pressing Conditions	Remarks
13.	1K17 1K21 (1K19)	Small pieces from previous runs. IN-100, Low carbon Nuclear Metals R.E.P. Lot No. 6140, -35 mesh.	7/8" ϕ x 1" pieces 1" ϕ x 13"	2150°F, 27,700 psi, 1 hr.	Repress of lower temperature pressed material. Can No. 1K19 leaked.
14.	1K18	IN-100, Low carbon Nuclear Metals R.E.P. Lot No. 6140, -35 mesh.	1" ϕ x 13"	2320°F, 27,300 psi, 1 hr.	Repress after pumping and sealing of previously leaky can.
14.	1K19	IN-100, Low carbon.	1" ϕ x 13"	2320°F, 27,300 psi, 1 hr.	Repress after pumping and sealing of previously leaky can.
14.	1L04	Ni-Co-Mo, Maraging steel, IMT 30-231, -14/+35 mesh.	1" ϕ x 13"	2320°F, 27,300 psi, 1 hr.	
14.	1L05	Ni-Co-Mo, Maraging steel, IMT 30-231, -3 1/2/+12 mesh.	1" ϕ x 13"	2320°F, 27,300 psi, 1 hr.	
14.	1L23	Ni-Co-Mo, Maraging steel, IMT 30-231. 2 1/2" length (net) of -3 1/2/+12, 6 3/4" length (net) of -12/+35.	2" x 3" x 12" sheet bar.	2320°F, 27,300 psi, 1 hr.	To Task III intact.

Figure 1. Maraging steel VM-300. Oil quench atomization. Heat No. 230. -25/+30 mesh. Oxide inclusions. Unetched. 500X.



Figure 2. Ni-Co-Mo maraging steel. Heat No. 231. Cleaned. Mesh fractions -4/+5, -8/+10, -16/+18, and -25/+30. 1X.



Figure 3. Ni-Co-Mo maraging steel. Heat No. 231.
-8/+10 mesh. Oxide inclusions. Unetched.
500X.

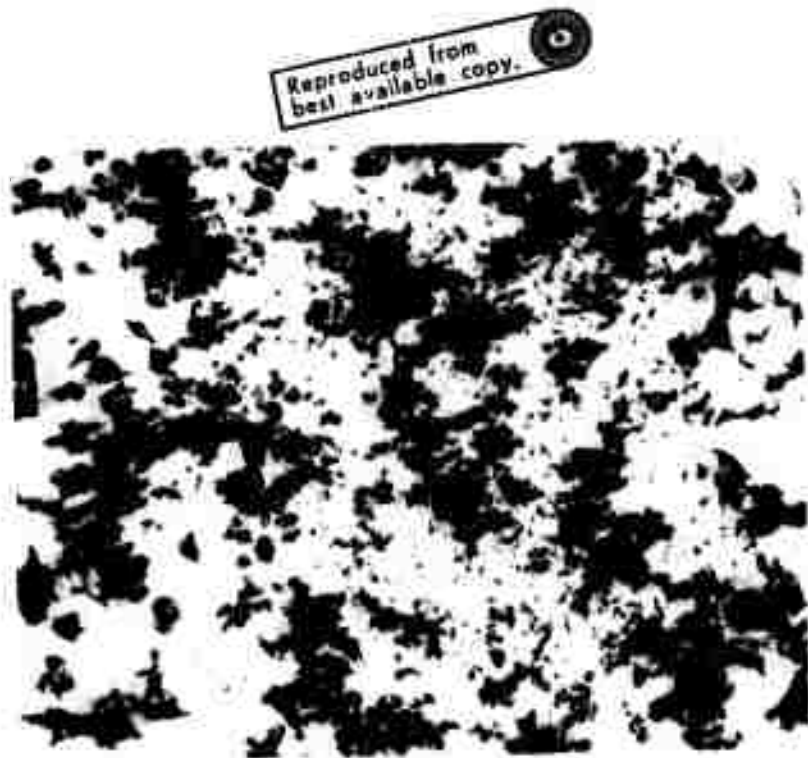


Figure 4. Cobalt-hafnium alloy +Si and B additions.
Heat No. 228. As atomized. 1X.

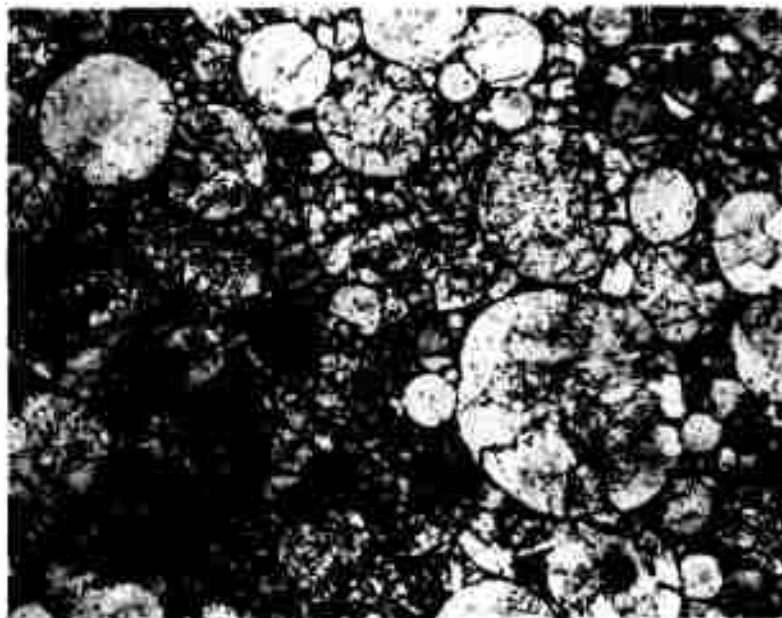


Figure 5. IN-100, low carbon, R.E.P. powder, -35 mesh.
HIP @ 1825°F, 27,700 psi, 1 hr. As pressed.
Etched. 100X.

Reproduced from
best available copy.



Figure 6. IN-100, low carbon, R.E.P. powder, -35 mesh.
HIP @ 1825°F, 27,700 psi, 1 hr. As pressed.
Etched. 1000X.



Figure 7. IN-100, low carbon, R.E.P. powder, -35 mesh.
HIP @ 2300°F, 27,700 psi, 1 hr. As pressed.
Etched. 100X.

Reproduced from
best available copy.

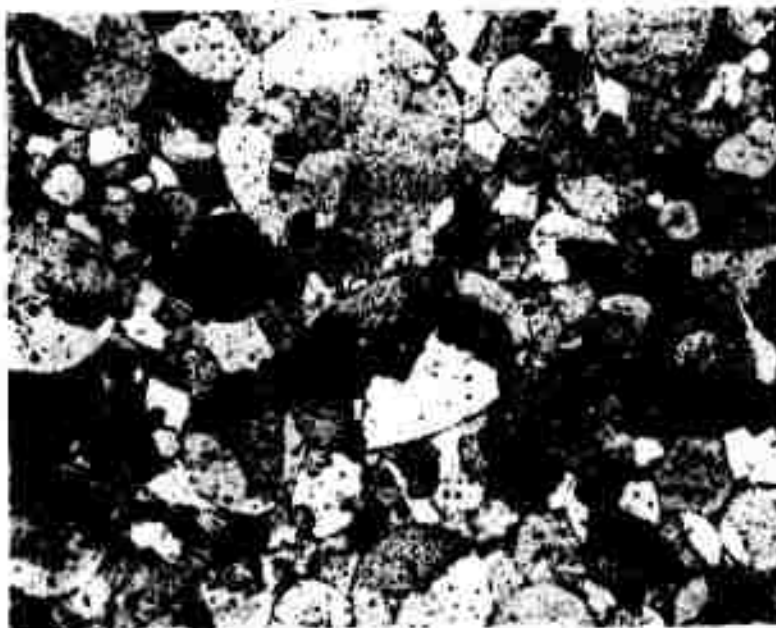


Figure 8. IN-100, normal carbon, R.E.P. powder, -35 mesh.
HIP @ 2300°F, 27,700 psi, 1 hr. As pressed.
Etched. 100X.

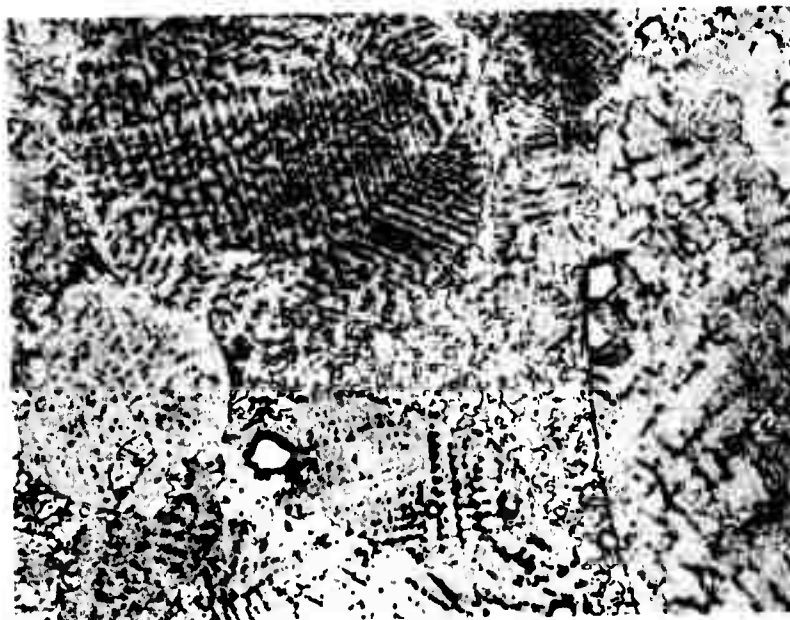


Figure 9. IN-100, normal carbon, R.E.P. powder, -35 mesh.
HIP @ 1900°F, 26,300 psi, 1 hr. Etched. 1000X.

Reproduced from
best available copy.

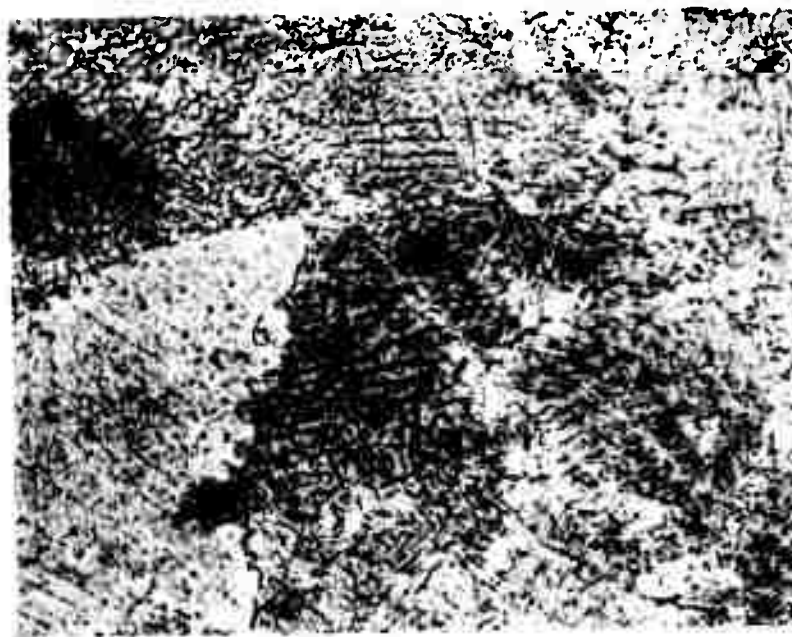


Figure 10. IN-100, low carbon, R.E.P. powder, -35 mesh.
HIP @ 1900°F, 26,300 psi, 1 hr. Etched. 1000X.

Reproduced from
best available copy.



Figure 11. IN-100, low carbon, R.E.P. powder, -35 mesh.
HIP @ 2320°F, 27,300 psi, 1 hr. IN-100/low
carbon steel can interdiffusion zone ~ .020".
Etched. 100X.

TASK II - SOLIDIFICATION RESEARCH

by

D. R. Geiger, P. A. Joly, R. Mehrabian, M. C. Flemings

INTRODUCTION

In the last six months of this program, Task II (Solidification Group) has conducted research on the bonding characteristics of rapidly solidified rods during consolidation and "rheoatomization" (atomization of vigorously agitated, partially solid-partially liquid mixtures of alloys). Specific aspects of these investigations have included:

1. High temperature homogenization characteristics of thin nickel platings, used in consolidation of Maraging 300 and IN-100 alloys, were studied using the electron microprobe technique for determination of composition variations.
2. Rods of a cobalt base alloy containing 10% hafnium were cast in chill molds and sent out to be consolidated into a billet by the closed die forging process.

- 3.(a) An apparatus was constructed to enable vigorous agitation of low melting point alloys (i.e., Pb-Sn and Al-Si) in the liquid-solid "mushy" range. Inert gas atomization equipment was built in the lower section of this apparatus to permit atomization of the liquid-solid slurries obtained by vigorous agitation.
- (b) Application of atomization to vigorously agitated alloys in the solidification range was investigated. Several experiments were carried out on Pb-15% Sn alloy where the vigorously agitated slurry was pushed out a tap hole in bottom of the crucible and atomized. The gas jets atomized the liquid portion of the slurry separating the "primary" solid (that existing before atomization) from the liquid. Initial indications are that this technique might lend itself to production of extremely homogeneous powders with negligible microsegregation. Alternatively, the process can be used as a refining method.
- (c) In a second set of experiments carried out on an Al-Si alloy containing Fe and Ti, a new process was developed

for refining of metal alloys. In these experiments, the vigorously agitated slurry was again cooled to a temperature in the liquid-solid range. The tap hole in the bottom of the crucible was opened, and the mixing blades were moved so that only the liquid portion of the slurry went through the tap hole, and the bulk of the solid phase remained in the crucible.

4. Presently, a patent application, based on the above-mentioned processes for refining of metal alloys is being written and will be filed by the M.I.T. patent office under the sponsorship of this program.

RESULTS

1. High Temperature Homogenization Treatment of Consolidated Billets of Maraging 300 and IN-100 Alloys

Rods of Maraging 300 and IN-100 alloys were chill cast by methods described previously⁽¹⁾. The as-cast rods were machined to remove surface imperfections and polished down to 600 grid paper. The polished rods were nickel plated, canned, and extruded at 2000°F at 135 tons pressure and a rate of 70-80 inches/min. Both the plating and the extrusion processes were as previously described⁽¹⁾.

Cross-sectional structures of the consolidated billets were studied using the electron microprobe technique to determine composition variations across the thin nickel platings. Subsequently, sections of each billet were homogenized at 2100°F for three to five hours in an argon atmosphere and variations were redetermined across the nickel-plated interfaces. Figure 1 shows the composition variations obtained across a nickel-plated interface of Maraging 300 alloy with homogenization times of 0, 3, and 5 hours. Both the nickel and iron profiles flatten out considerably with five hours of homogenization at 2100°F. As expected, rate of decrease in the nickel and iron peaks is dependent on the concentration gradient and decreases with increasing homogenization time. Figure 2 shows the concentration profiles obtained across a similar interface of IN-100 alloy billet that was homogenized for three hours at 2100°F.

Billets produced from consolidated rods of rapidly solidified nickel-plated, Maraging 300 and IN-100 alloys are presently being homogenized at 2100°F. Sections of these billets will subsequently be tested for low and high temperature mechanical properties.

2. Rapid Solidification of a Cobalt Base Alloy

Rapidly solidified rods of a cobalt base alloy (10% Hf, 21% Cr, 6.75% Mo, 10.0% Ni, 0.65% C, balance Co) were chill cast using the copper chill mold described previously⁽¹⁾. The 5/16" by 5/16" by 5" long rods were ground flat, polished, etched and metallographically examined. Figure 3 shows the cast dendritic structure of one such rod. The secondary dendrite arms spacings were measured across the cross-section of the rods. This spacing varied from 1.7 to 5 microns.

Surfaces of a set of rods were chemically polished and sent out to be vacuum die forged into a billet, at 1200°C and 240,000 psi punch pressure.

3. Rheoatomization and Refining by Partial Solidification

One of the objectives of this program has been to develop new or improved techniques of production of rapidly solidified small to medium size homogeneous powders of metal alloys. Over the last six months, partial solidification accompanied by vigorous agitation of alloys and subsequent atomization of the resulting alloy slurries has been investigated. The particulate suspension of "primary" solid particles, obtained in an alloy melt by vigorous agitation⁽²⁾ could lend itself to production of homogeneous powders free of microsegregation and undesirable second phases (i.e., eutectics) that form at the end of solidification.

During the course of this investigation, we discovered that atomization of liquid-solid mixtures of alloys (rheoatomization) may also be a useful technique for refining of metal alloys. Hence, some further experiments were carried out on the refining of aluminum alloys where only the liquid in the liquid-solid slurry was drained out of the crucible.

In both of the processes that have emerged from this work, the alloy is partially solidified while it is vigorously agitated by a rotating

blade. The vigorous agitation causes the liquid-solid mixture to behave as a fluid slurry to fractions solid as high as about 0.5. A combination of the vigorous agitation and relatively slow rate of heat removal from the solidifying slurry causes it to be essentially isothermal and to have uniform distribution of fraction solid throughout.

The structure of the solid grains that form during this vigorous agitation is very different from the usual dendritic structure that forms during usual solidification of castings and ingots. The solid particles are, or approach, small spheroids, and this is an important aspect of the processes to be described. Because the fine dendritic structure is absent, the segregated liquid is much easier to separate from the solid than in existing processes - there is, ideally, no liquid in small interdendritic "pockets".

Figure 4 is a schematic illustration of the basic mixing apparatus, used in experiments on Sn-15% Pb alloy and an Al-Si alloy. In one process, after the agitated slurry has reached a desired temperature (and so desired fraction solid), a tap hole is opened. Vigorous agitation is maintained especially in the vicinity of the tap hole and the slurry then flows out this hole. On leaving the hole, it is struck by a series of gas jets to "atomize" it as is done in standard commercial practice with fully liquid melts. In this case, the gas jets atomize the fully liquid portion of the

melt to a very fine particle size which subsequently solidify. These fine particles, having formed from fully liquid material, possess the average composition of the liquid (usually enriched in impurity). The gas jet cannot, of course, atomize the solid particles of metal entrained in the stream. These particles, larger than those of the atomized liquid, are low in impurity.

Separation of the "primary" solid particles from the atomized liquid powders is now accomplished by screening. Table 1 summarizes results of one such test on Sn-15% Pb alloy. The smaller size fractions contain approximately 23% Pb which is about that given by the equilibrium liquidus temperature of atomization (202°C). The larger size fractions (that which was solid before atomization and some adhering liquid) contain about 12% Pb. Figure 5 shows the microstructures of the resulting powders. The "primary" solid particles, Figure 2a, trap some of the liquid, while the particles obtained by atomization of the liquid are almost entirely free of "primary" solid.

Experiments presently under way show that by choosing proper mixing speeds and holding times in the liquid-solid range, "primary" solid particles can be coarsened, resulting in more spheroidal shaped particles and in the elimination of entrapped liquid in each individual particle. Figure 6 shows microstructure of an Al-4% Si alloy rapidly solidified after

vigorous agitation up to 0.5 fraction solid. Here, individual "primary" solid particles are more spheroidal in shape and less remaining liquid is entrapped in each individual particle.

Further experiments on rheoatomization (atomization of liquid-solid slurries) will be carried out in the future with special emphasis on obtaining homogeneous particles free of entrapped liquid.

The second process described here was an outgrowth of experiments done on rheoatomization. The discovery that the liquid portion of a vigorously agitated liquid-solid slurry could be easily drained from the container, makes this technique a very attractive refining process. Here, again, the alloy is mixed and cooled as described above, to obtain a partially solid slurry. A tap hole is again opened in the crucible but this time, the blades are moved so the metal in the immediate vicinity of the tap hole is not vigorously agitated. Now, a metal stream again flows through the tap hole but this time only the liquid portion goes through the hole; the bulk of the solid phase stays behind. Our conjecture as to the reason for this behavior is that the solid particles give the slurry a "thixotropic" nature. A semi-rigid skeleton of the solid grains forms in regions of the melt that are not vigorously agitated. This rigid skeleton then effectively acts as a fine filter, holding back the particles from the more vigorously agitated portion of the melt.

Table 2 shows results of three experiments carried out on aluminum base alloy containing 30% Si, 6.0%Fe, and 1% Ti. The experiments were done at 750°C, 650°C, and 600°C, corresponding to increasing fraction solid with decreasing test temperature. As to be expected, for this system, the effluent liquid was purified in all alloy elements, the amount of purification increasing with decreasing temperature. As example, at 600°C, silicon content was reduced from 30 to 13%, iron from 6.2 to 1.8% and titanium from 0.94 to 0.15%.

REFERENCES

1. Semi-Annual Technical Report No. 2, Task II, ARPA Order No. 1608.
2. "Rheological Behavior of Tin-15% Lead in the Crystallization Range", D. B. Spencer, R. Mehrabian, and M. C. Flemings. Submitted for publication to Met. Trans.

TABLE 1

Rheoatomized Sn - 14.4% Pb Alloy

<u>Sample</u>	<u>Particles Collected</u>	<u>Weight</u>	<u>%Pb</u>
D-4-14	10 Mesh Screen	195.5 g	
	14 Mesh Screen	103.0	12.1
	20 Mesh Screen	192.0	11.6
D-4-30	30 Mesh Screen	250.0	12.1
	50 Mesh Screen	110.5	17.4
D-4-100	100 Mesh Screen	199.5	21.5
	140 Mesh Screen	125.0	22.6
D-4-200	200 Mesh Screen	64.5	22.9
	200 Mesh Screen	86.5	23.0
D-4-C	left in Crucible	623.5	10.7
	Initial Charge	2050.0	14.4

TABLE 2

Results of Refining Experiments Done on Al-30% Si - 6% Fe - 1% Ti Alloy

(A) 750°C = Temperature When Tapped

		<u>Silicon</u>	<u>Iron</u>	<u>Titanium</u>
Initial	1025.9 grams	29.8%	6.10%	1.08%
Left in crucible	573.0 grams	31.0%	6.21%	1.58%
Drained	411.0 grams	22.6%	4.64%	.43%
Samples	5.0 grams			

(B) 650°C = Temperature When Tapped

		<u>Silicon</u>	<u>Iron</u>	<u>Titanium</u>
Initial	966.5 grams	25.3%	4.18%	0.88%
Left in crucible	695.5 grams	28.0%	6.53%	1.40%
Drained	183.0 grams	15.2%	1.77%	0.16%
Samples	65.8 grams			

(C) 600°C = Temperature When Tapped

		<u>Silicon</u>	<u>Iron</u>	<u>Titanium</u>
Initial	1035.0 grams	30.0%	6.19%	0.94%
Left in crucible	874.0 grams	31.4%	6.95%	1.32%
Drained	133.0 grams	13.1%	1.77%	0.15%
Samples	12.5 grams			

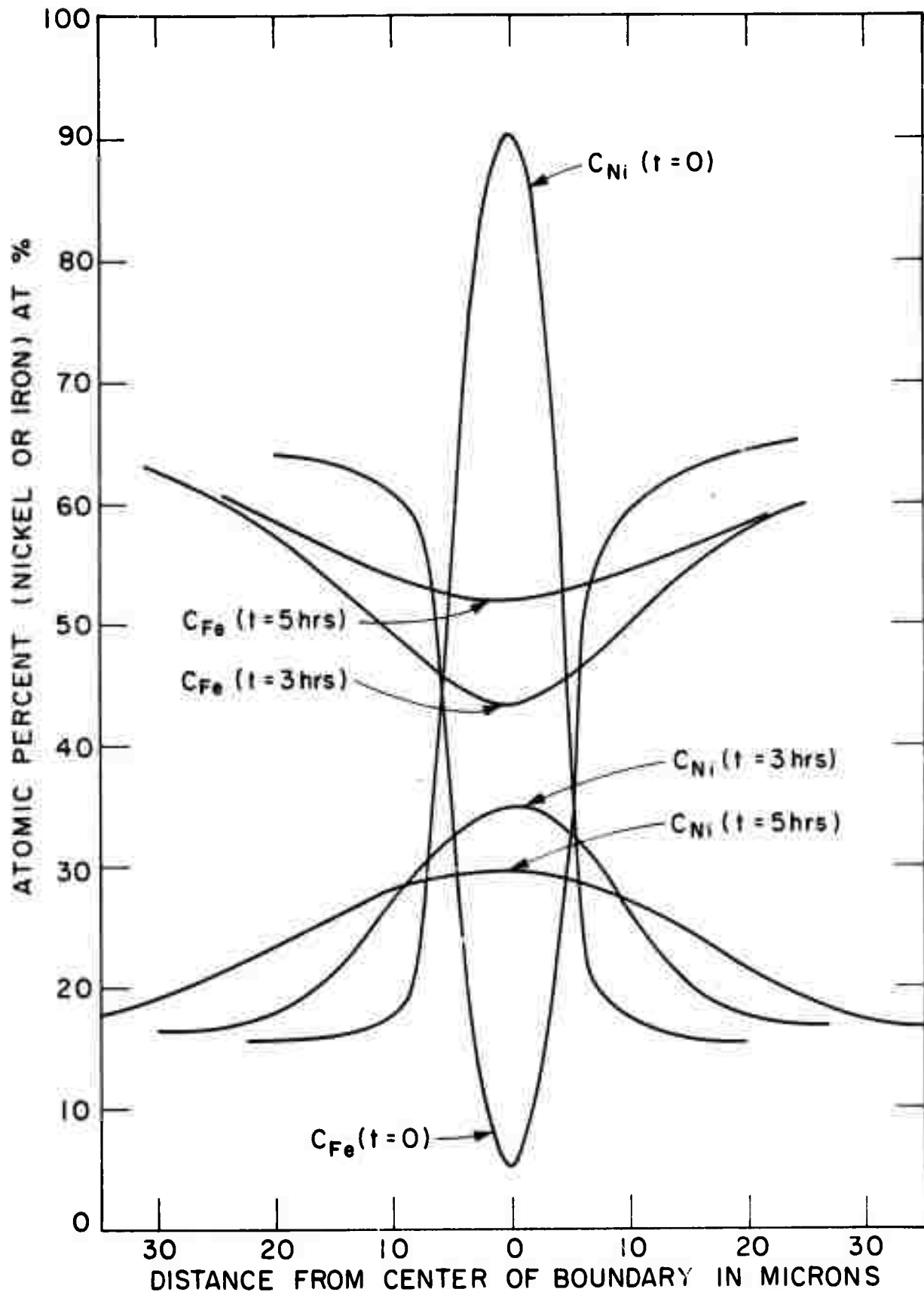


Figure 1. Effect of high temperature homogenization on composition variations across nickel plated interfaces of consolidated rods of Maraging 300 alloy.

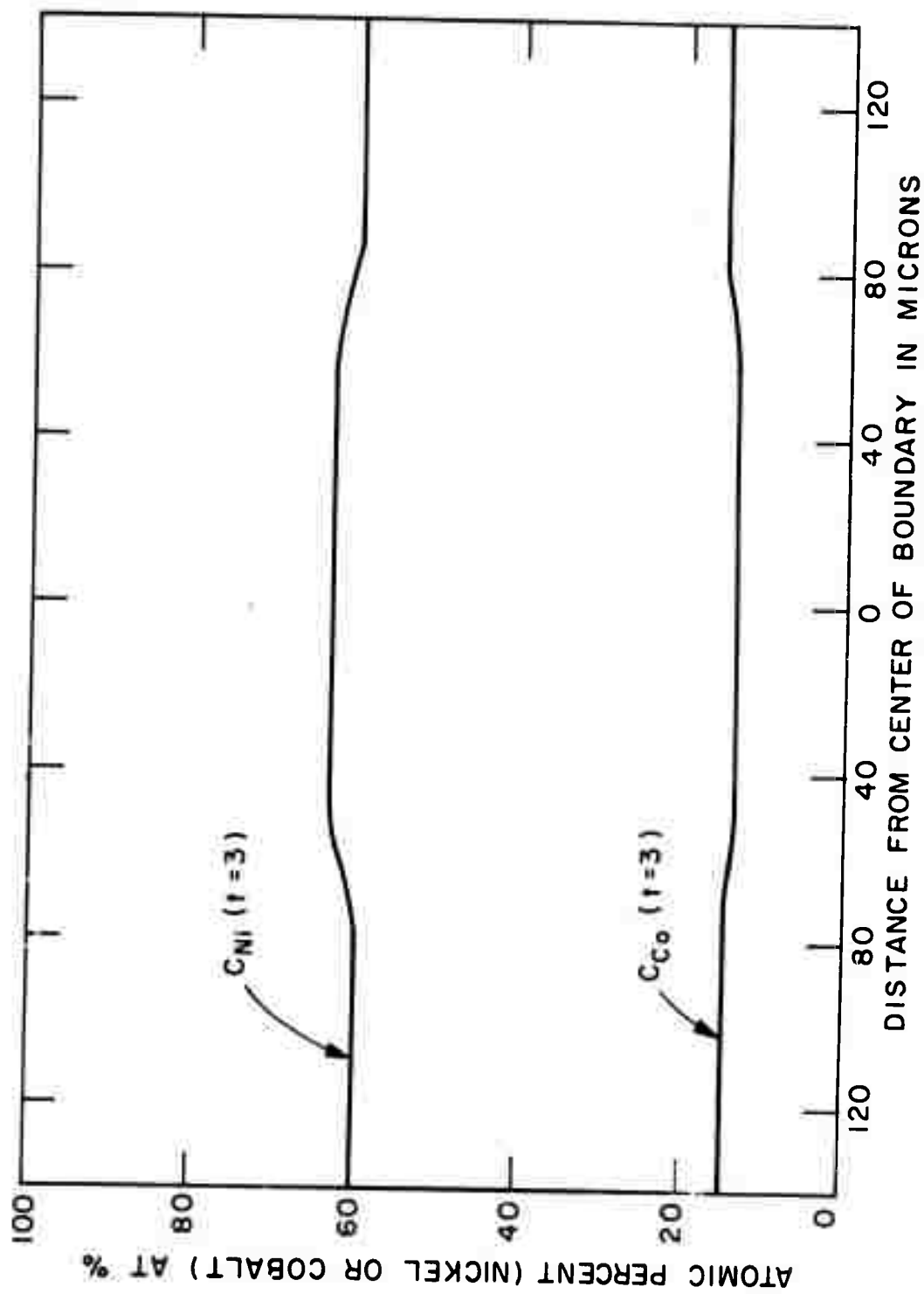


Figure 2. Composition variation across a nickel plated interface of consolidated rods of IN-100, homogenized at 2100°F for 3 hours.



(a)



(b)

Figure 3. Photomicrographs showing structure of a rapidly solidified rod of Co-Hf alloy, (a) 300X, (b) 1500X.

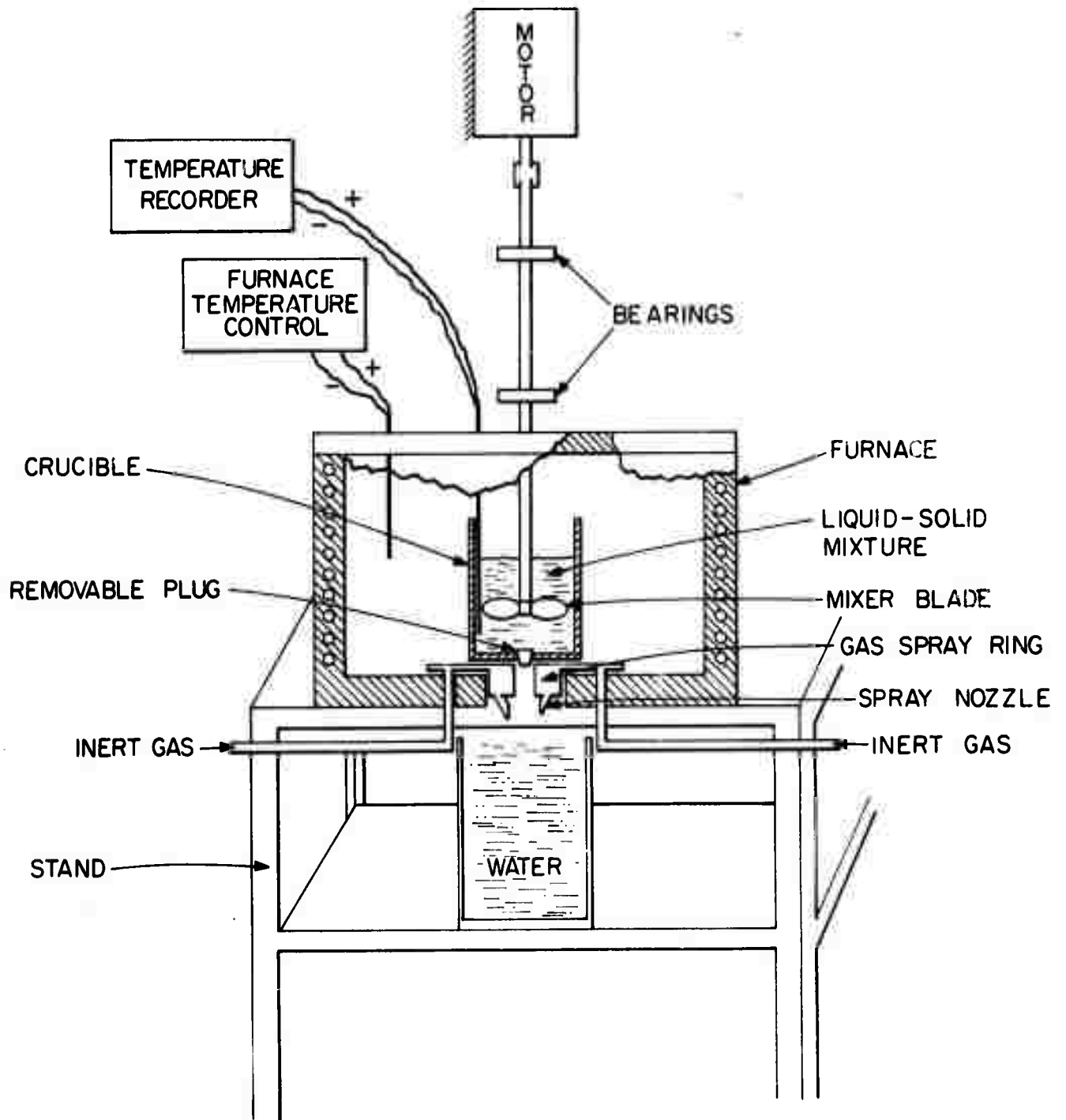
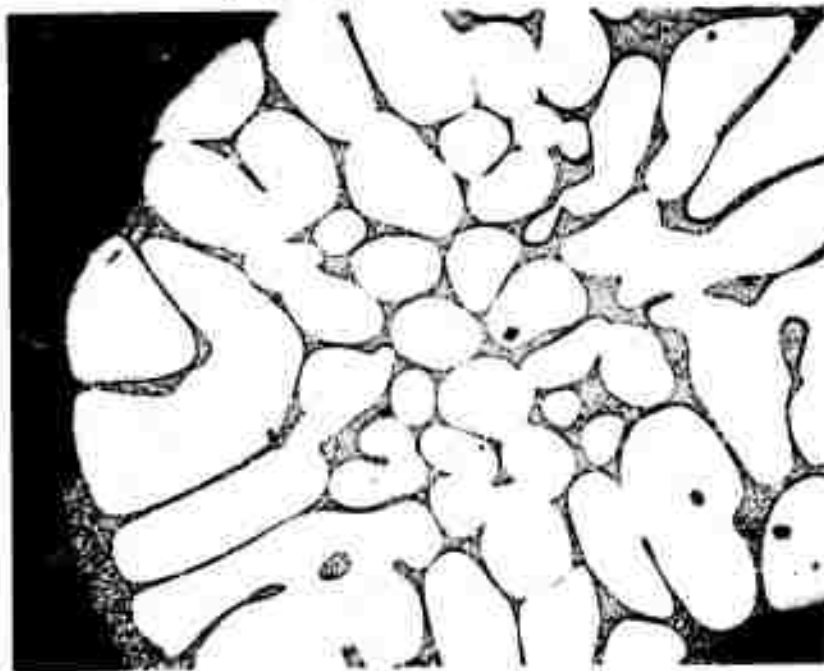
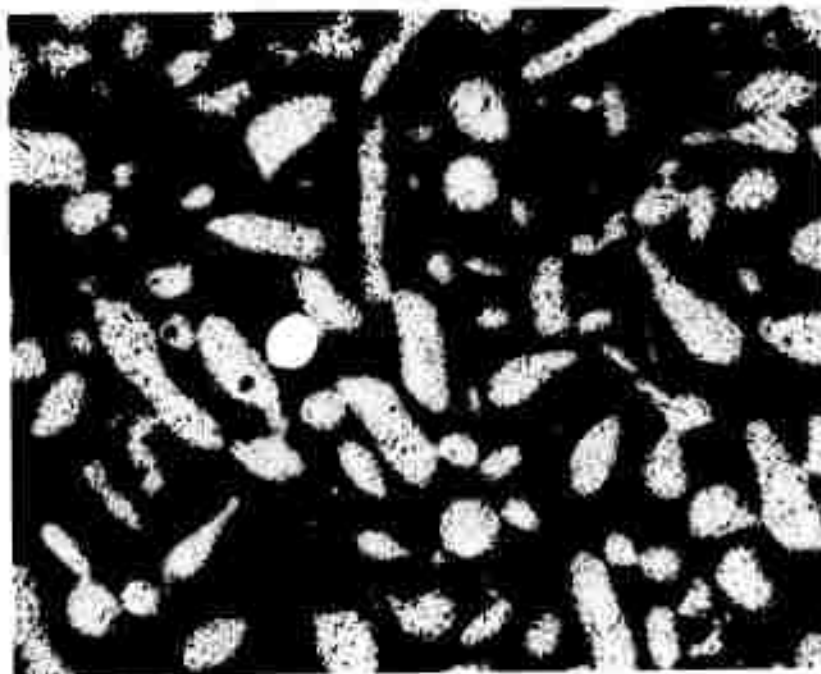


Figure 4. Sketch of apparatus for mixing and atomization of liquid-solid slurries of alloys.

Reproduced from
best available copy.



(a)



(b)

Figure 5. Microstructures of powders obtained from rheoatomization of Sn-15% Pb alloy; (a) structure of a "primary" solid particle, (b) structure of atomized liquid (liquid existing in the slurry before atomization) particles. 100X.

Reproduced from
best available copy.

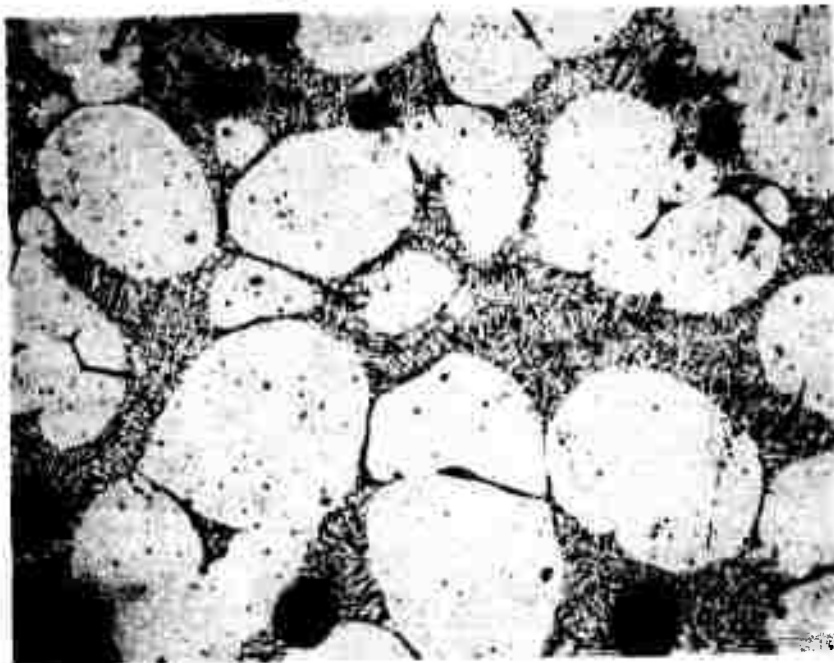


Figure 6. Microstructure of a vigorously agitated slurry of Al-4% Si alloy cast in a chill mold at 0.5 volume fraction solid. 50X.

- TASKS III and IV -

Thermomechanical Treatment, Microstructure
and Mechanical Properties

N.J. Grant

R.M.N. Pelloux

L.F.P. van Swam

L.N. Moskowitz

R.K. Robinson

MECHANICAL PROPERTIES OF 300 GRADE MARAGING STEELS

INTRODUCTION

Materials produced by conventional ingot and rolling procedures and by powder metallurgical methods have now undergone extensive testing. Commercial material in the form of 4" wide by 1-1/4" thick bar was obtained from VASCO. The material was received in the annealed condition. Powders produced by Nuclear Metals (spinning electrode process) were consolidated by hot isostatic pressing (HIP) extrusion or hot rolling. This particular powder was chosen because of its cleanliness and uniform size. The final products are designated as follows:

- HE, hot isostatic pressed billet followed by extrusion ratio 11.5:1 to obtain 1/2" rod
- E, direct powder extrusion (ratio 11.5:1)
- HR 69, hot isostatic pressed billet followed by hot rolling at 2000°F 69% reduction of area
- HR 83, same except 83% reduction of area.

The powder metallurgical products are very similar in structure to the commercial material. Compare Figures 1 and 2. Banding of course is completely eliminated in the powder products which are also free from Ti_2S inclusions. The grain sizes of all materials after annealing are roughly the same.

Tensile testing was performed on all materials, both in the annealed and the aged (3 hours at 900°F in air) condition. Tension-compression fatigue testing on aged commercial stock in air and dry argon and on extruded stock in air was done on a Baldwin SF-1 machine. Fracture toughness testing on commercial material and both hot rolled products was carried out according to ASTM E399 70T testing procedure using the compact tensile specimen.

TENSILE PROPERTIES

The specimen size used in all tensile tests has a 1" gauge length and 0.160" gauge diameter. The 1" gauge length was necessary to facilitate the use of a 1" long extensometer which was used in all tensile testing. Reduction in area, U.T.S., and 0.2% offset are reported for annealed and aged material and are summarized in Table I. The powder products have slightly higher tensile strengths than the commercial material in the aged condition, while retaining the same reduction of area values. All materials in the aged condition show a low work hardening exponent (about 0.02) and the powder materials show some delamination along the powder particle boundaries. The particle boundaries can be etched in 10% HNO_3 propanol mixture for several minutes. See Figure 2 for a longitudinal section of HIP 83.

FRACTURE TOUGHNESS PROPERTIES

It has been realized for some time that the design criteria

for the use of high strength materials should include fracture toughness as well as tensile strength. The American Society for Testing and Materials has proposed a tentative testing procedure under the designation E399-70T (volume 31). Both 3 point bending and compact tensile specimens can be used to measure the fracture toughness. We have found the compact tensile specimen to be easier to use. This specimen also requires less material. A drawing of the specimen is given in Figure 3. The critical dimensions of the specimen are its thickness and crack length. Both should be larger than $2.5 \frac{K_{IC}^2}{\sigma_y}$, where K_{IC} is the plane strain fracture toughness and σ_y the yield strength (0.2% offset) of the material. For 300 grade maraging steel in the aged condition this gives a value of approximately 0.1". Testing was carried out on 0.5" and 0.25" thick specimens with crack lengths of 1" and 0.5" respectively. All testing was performed on a MTS systems machine. A clip on gauge to measure the crack tip opening displacement was used. The length of the fatigue crack was 0.1" in all cases. The specimen size to test the materials in the annealed condition would be prohibitively large and all reported fracture toughness values were measured on material aged for 3 hours at 900°F.

Since it can be expected that the fracture toughness will be different when measured in different directions of the rolling plane, all testing was done on specimens with the crack either parallel or perpendicular to the rolling direction. All fracture

toughness values are summarized in Table II. Also shown in this table are the maximum fatigue load used to propagate the last .05" of fatigue crack and the total number of cycles spent in fatigue. Hardness measurements on each specimen were made to check for proper heat treatment and an average of 3 values is reported in the table.

The hot isostatic pressed and hot rolled powder products shows lower fracture toughness values than the commercial steel in both directions. A picture of the fracture surface after testing is shown in Figure 4. The powder material shows a large amount of delamination of the powder particles and the lower toughness values obtained for this material must be attributed to it.

STRETCHED ZONES

The fracture area bounded by the fatigue crack front on one side and the onset of the fracture surface characterized by voids on the other side is commonly called the stretched zone. It is important to study the size and shape of this zone which might explain the difference in fracture toughness for materials with the same yield-strength, work hardening exponent and elastic modulus as is the case for commercial stock and powder products.

A number of stereopair pictures of matching fracture surfaces of the stretched zone of commercial 300 grade maraging steel were taken on the SEM. Two stereo pairs are shown in Figure 5. The stereophotographs were taken with the fatigue fracture

surfaces making angles of 0° and 7° with the electron beam. The stretched zone is approximately 1 micron wide and makes an angle of anywhere between 0° and 90° with the rest of the fracture surface. An angle of 45° is frequently observed. No comparable pictures of the powder products are available as yet.

FATIGUE PROPERTIES

Fatigue testing was done on a Baldwin SF-1 machine. All testing is in tension-compression with a zero mean load. A constant load is maintained throughout the test. A drawing of the fatigue specimen is shown in Figure 6. The specimens have a 0.3" gauge length 0.15" in diameter. The specimens are heat treated and polished with 600 carbide paper and 1 micron diamond paste. Possible scratches are at 45° angles to the tensile axis.

The results of 14 tests of commercial material in the aged condition and of 16 tests of HE material tested in air together with 12 tests of commercial steel tested in dry argon (dewpoint- -70°F) are given in Table III and are plotted on a S-N curve in Figure 7. Specimens tested in dry argon show a much larger fatigue limit and much less scatter in the data than similar specimens tested in laboratory air. The scatter obtained by testing in air is most probably due to large fluctuations in humidity. It seems clear that properly reported fatigue data should include a statement about the testing environment.

Table I - Summary of Tensile Properties

	Annealed			Aged		
	U.T.S.	0.2 %	R.A.*	U.T.S.	0.2 %	R.A.
VASCOMAX 300	145.8	138.8	76.0	274.0	269.0	48.5
	145.0	120.0	72.1	280.0	272.5	53.6
HE	151.0	125.0	65.6	291.0	285.0	47.3
E	153.0	125.0	68.6	290.0	285.0	48.4
HR 69	148.0	112.5	62.0	271.0	263.0	38.8
HR 83	146.0	112.5	70.3	287.0	280.0	53.5

$$*R.A. = \frac{A_0 - A_f}{A_0}$$

Table II - Summary of Fracture Toughness Properties

Crack // R.D.					Crack ⊥ R.D.				
	Load lbs.	N cycles	K_{IC} ksi $\sqrt{\text{in.}}$	R_c	Load lbs.	N cycles	K_{IC} ksi $\sqrt{\text{in.}}$	R_c	
Commercial 0.5" spec	2,000	47,000	63.2	53	2,000	48,000	71	53	
	2,000	43,000	62.1	54					
HR 69 0.5" spec	1,750	34,000	49.3	53	1,500	34,000	62.2	53	
	1,500	34,500	52.5	51	1,500	40,500	67.0	55	
	1,500	40,000	51.4	54	1,500	38,500	59.4	55	
Commercial 0.25" spec	700	17,000	61.6	53					
	625	19,500	62.7	53					
	625	20,500	63.3	54					
HR 83 0.25" spec	625	24,000	53.9	52	625	24,500	63.5	53	
	625	20,000	53.7	54	625	19,500	68.7	52	
	625	21,500	56.9	54	625	21,500	63.7	53	

Table III - Tension-Compression Fatigue Testing

Stress ksi	200	150	130	120	110	100	90	80	70
VASCOMAX 300	15	20		41		80	72	116	1053
							218	423	5330*
							274	498	
							2273	937	
Life cycles x 10 ³									
HE		8		21		89	87	98	267
						885	109	334	514
							343	416	662
							1907	5060*	5860*
VASCOMAX 300 tested in argon	58	64	255	623	4180				
		109	487	753	8269				
			529	997					
				1184					

* specimen did not break



Figure 1 - Commercial 300 grade maraging steel - 15% Nital etch
1 minute, 150x.

Reproduced from
best available copy.

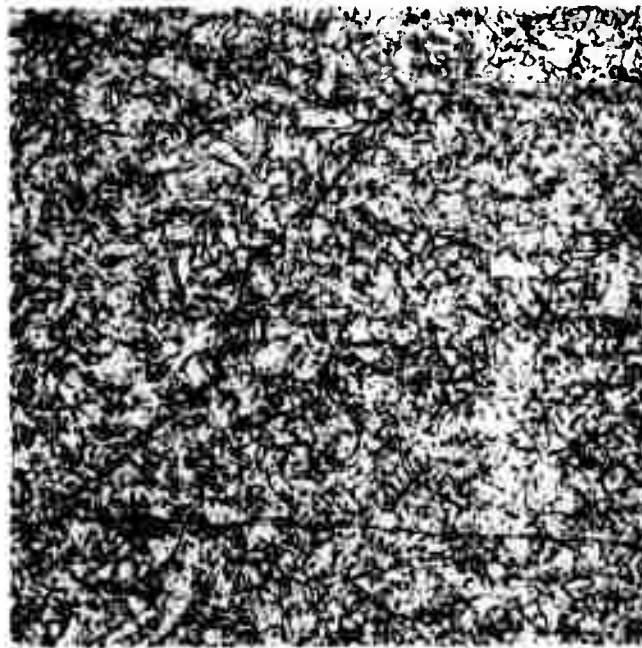


Figure 2 - Hot isostatically pressed and hot rolled Nuclear Metals
powder of 300 grade maraging steel - Nital 15%, 150x.

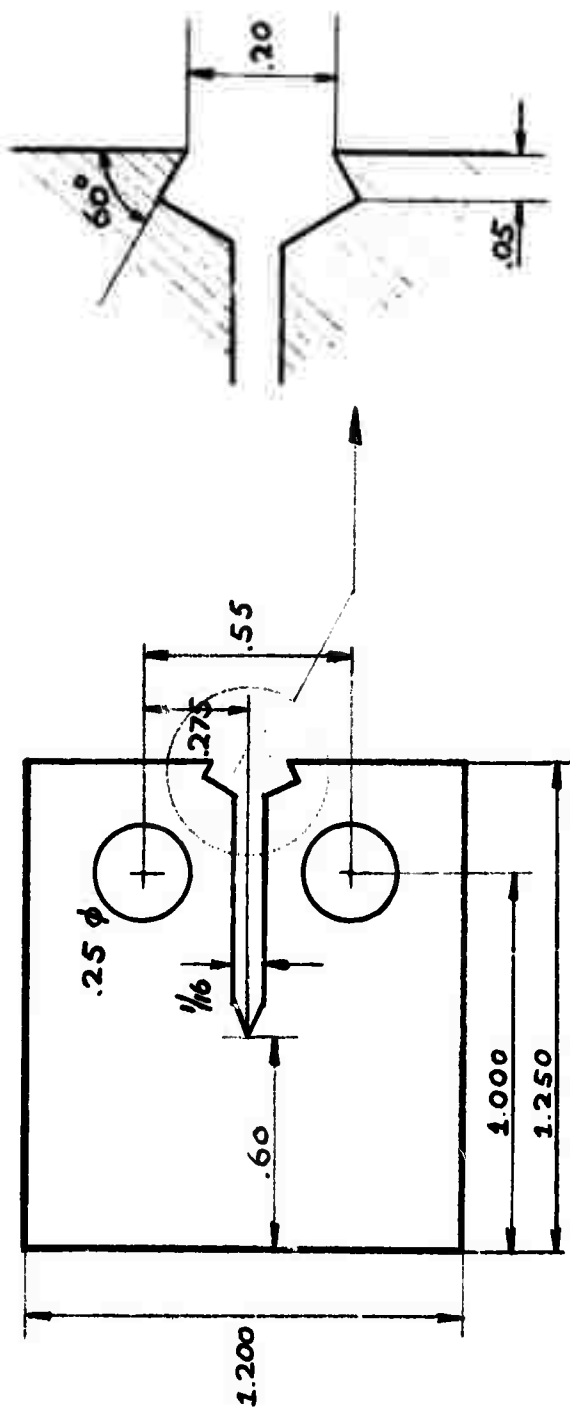


Figure 3 - Compact tensile fracture toughness specimen. The dimensions are for a 0.25 inch thick specimen.



Figure 4 - Fracture surfaces of fracture toughness specimen.
Top: VASCOMAX 300, Middle: HIP 69 perpendicular to the rolling
direction, Bottom: HIP 69 parallel to the rolling direction.
Note the particle delamination in the last two specimens. 1.5x

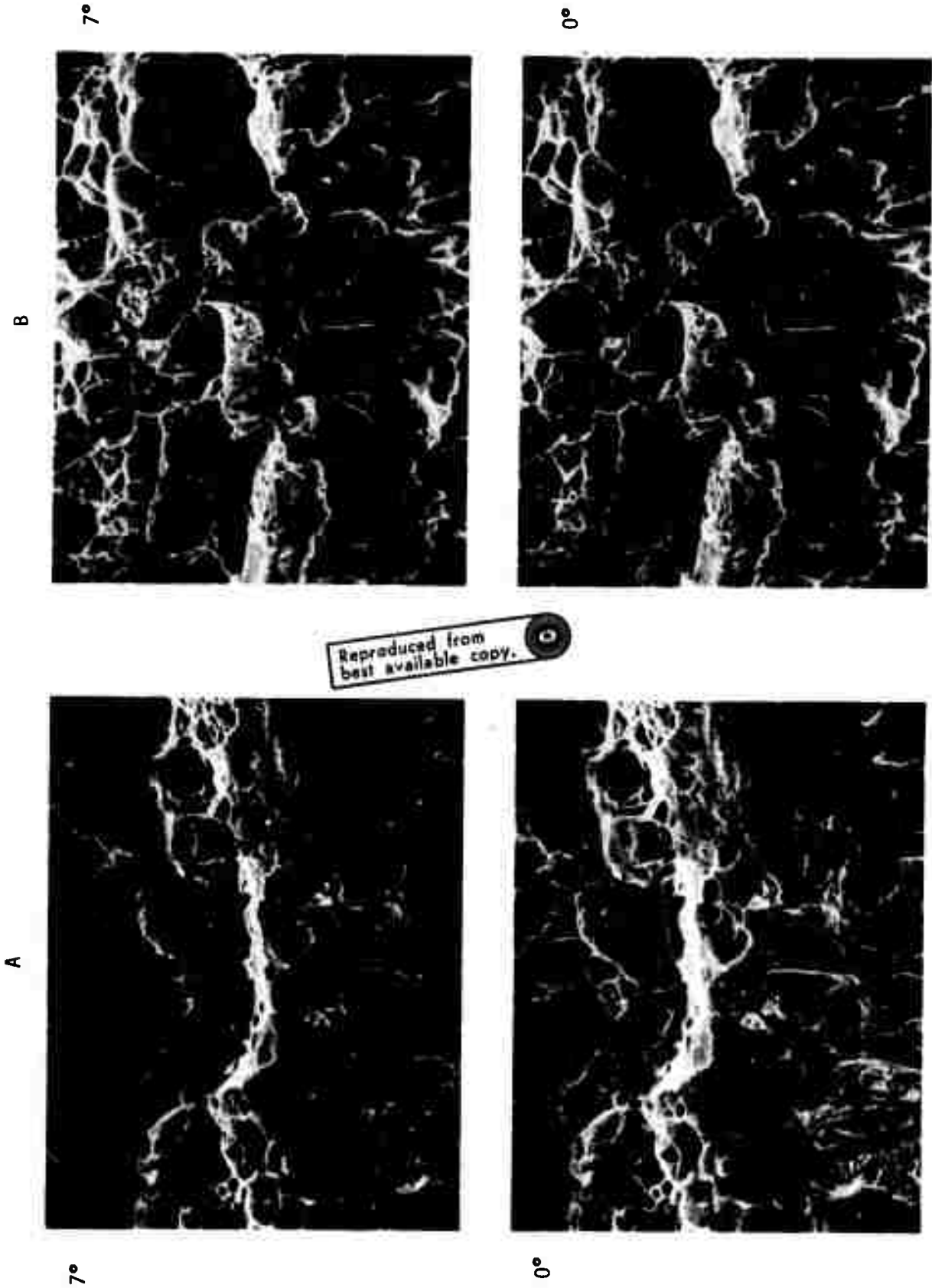


Figure 5 - Stereo pairs (0° and 7°) of matching surfaces (A and B) of the stretched zone in 300 grade maraging steel. Magnification 1225x.

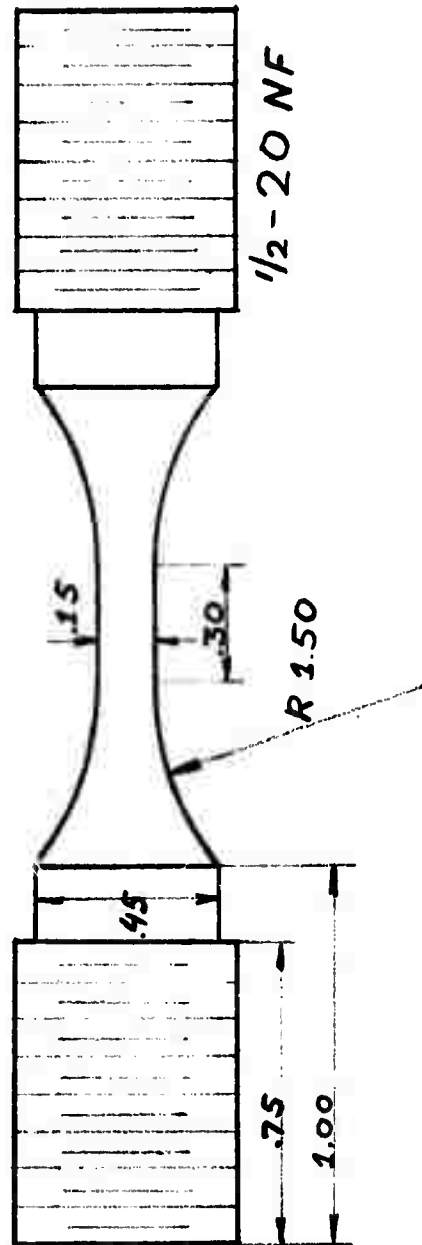
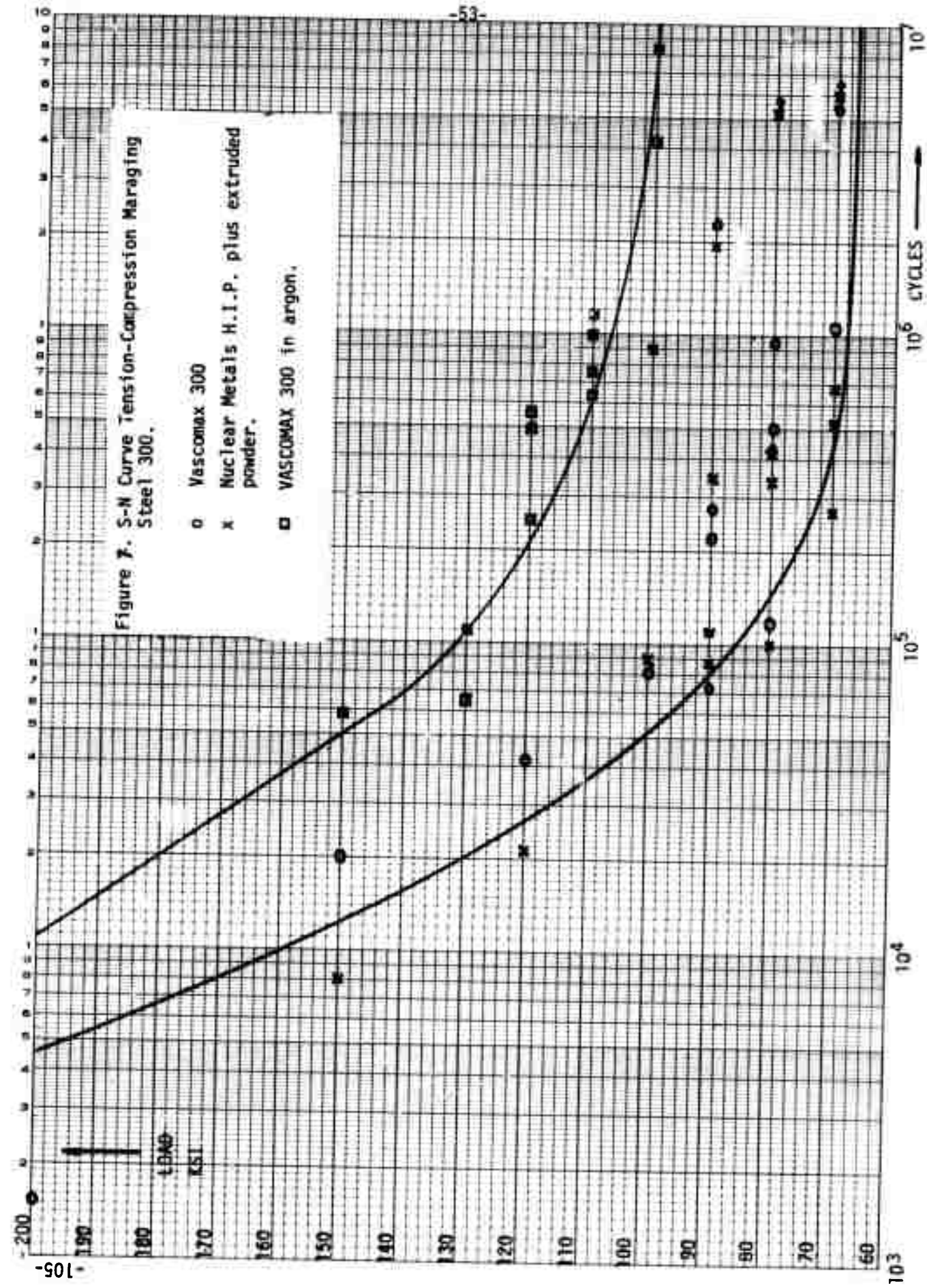


Figure 6 - Tension-Compression fatigue specimen.

Figure 7. S-N Curve Tension-Compression Maraging Steel 300.

- o Vascomax 300
- x Nuclear Metals H.I.P. plus extruded powder.
- VASCOMAX 300 in argon.



MICROSTRUCTURE AND MECHANICAL
PROPERTIES OF IN-100 PROCESSED
BY POWDER METALLURGY

INTRODUCTION

Three types of prealloyed IN-100 powders were evaluated. They were produced by Federal Mogul (inert-gas atomization), Homogeneous Metals (vacuum atomization), and Nuclear Metals (rotating electrode process). A 20-inch bar of rectangular cross-section, 1" x 1-1/2" was prepared from Federal Mogul powder, canned in carbon steel, by hot isostatic pressing. The HIP processing was carried out at 2320°F and 25,000 psi for one hour. Another bar of Homogeneous Metals powder was hot isostatically pressed at 2300°F and 15,000 psi for one hour, and then extruded at 2000°F, with a 12:1 reduction ratio, to a 3/4" diameter rod. Finally, two 7-foot long, 1/2-inch diameter bars were produced by direct extrusion of FM and NM powders evacuated in stainless steel cans. They were both processed at 2150°F with a 20:1 reduction.

In order to compare the structures and properties of the powder product to the cast alloy, an investment casting of IN-100 was made into twenty-four 1/4-inch diameter, 3/8-inch x 16 thread, tensile bars. The casting was made from a vacuum cast ingot of IN-100 (see Table I for the chemical analysis). The bar was remelted under an argon atmosphere, and cast at 2730°F

into a mold at 1500°F. The average grain size in the cast bars is 1500 microns, with about five grains per diameter.

POWDER CHARACTERIZATION

Chemistries, size ranges and screen analyses of the three powders used are presented in Tables I and II. With the exception of FM powder, all contain less than 100 ppm of oxygen and show little oxygen pick-up during powder production. Typical powder particles viewed by scanning electron microscopy are shown in Figures 1, 2, and 3 along with polished and etched cross-sections. The average secondary dendrite arm spacing in the Federal Mogul powder is 2 microns, in the Homogeneous Metals powder is 6 microns, and in the Nuclear Metals powder is 3 microns. There was little variation throughout each heat.

MICROSTRUCTURE

The average secondary dendrite arm spacing in the cast IN-100 tensile bars is 28 microns and a typical cast nickel-base superalloy structure was evident. The average size of the matrix gamma prime particles is about 1.5 microns.

The microstructures of the HIP Federal Mogul powders and the HIP and extruded Homogeneous Metals powders were presented in the previous semi-annual Technical Report. Carbide extraction replicas were made of the continuous film of second phase precipitates surrounding the original powder particles. Electron diffraction of the extracted replicas showed the phase to be

titanium carbide.

The microstructure of an as-extruded bar is shown in Figure 4. The particles have been well deformed, and a recrystallized grain size of about 8 microns is evident in both bars. Large carbides within the particle boundaries can be seen in the bar extruded from Nuclear Metals powders. These carbides were present in the original powders as shown in Figure 3b. The prior particle boundaries of the Federal Mogul powder extrusion are still delineated by a second phase, although not to the extent that is was in the HIP material. In the Nuclear Metals powder bar, this effect is even smaller. The average gamma prime particle size after extrusion is about 0.2 microns in each alloy.

GRAIN COARSENING

In order to see if significant grain growth could easily occur past the prior particle boundaries, a series of grain coarsening experiments were run. Tests initially performed at 2300°F showed evidence of incipient melting, and 2270°F was selected as an optimum coarsening temperature. The samples from the Federal Mogul powder extrusion showed substantially less grain growth than those from the Nuclear Metals powder, indicating that the surrounding carbide phase can slow down grain growth markedly. In both alloys, however, grain boundaries were able to grow past the prior particle boundaries. For the Federal Mogul powder extrusion, the average grain size was about 50 microns after 24 hours at 2270°F, with grains as large as 100

microns. For the Nuclear Metals extrusion, after the same treatment, an average grain size of about 100 microns was measured, with grains as large as 200 microns (Figure 5).

MECHANICAL PROPERTIES

The room temperature tensile properties and Rockwell C hardness values for the different materials are presented in Table 3. The excellent room temperature tensile properties of the as-extruded material are attributed to the refinement of the microstructure during atomization and hot extrusion. The tensile ductility of all the P/M alloys are excellent considering the strength levels and compared to the ductility of the as-cast material.

Characterization of the hot workability of the powder processed IN-100 was first done by high strain rate testing and finally by an investigation of the superplastic behavior at low strain rates. A description of the high speed tensile testing can be found in the previous semi-annual Technical Report, along with the results for the HIP Federal Mogul powder material. The stress versus rupture time for the as-cast alloy and for the as-extruded alloys show suitable linear relationships on log-log plots (Figures 6 and 7). The ductility, measured as elongation after fracture, is presented for each test. The extruded product shows a change in slope at rates below about 10^{-1} sec^{-1} as seen in the log stress vs. log average deformation rate plot of Figure

8. This break in slope, indicating a change in structure, deformation or fracture mode, was not exhibited by either the cast or HIP alloys. The ductility of the extruded material is seen to increase markedly at slower deformation rates, especially at 2100°F. Total elongations as a function of deformation rate are plotted in Figure 9. A cross-section of an extruded Federal Mogul powder test bar is shown in Figure 10. The material exhibits its extensive intergranular cracking, accounting for its higher ductility. At deformation rates below about 10^{-1} sec^{-1} , the high strain rate stress levels in the extruded product fall rapidly below both of the other materials, an effect also most pronounced at 2100°F.

This extreme sensitivity of the deformation stress and ductility on temperature, strain rate and structure led to a series of low strain rate tensile tests, to investigate the superplastic behavior of the extruded material. High temperature tensile tests were performed on the as-extruded alloys over a range of strain rates from .005 to .5 min^{-1} at 1800°F, 1900°F, 2000°F and 2100°F. Figure 11 shows the total elongations that can be obtained at different strain rates at 1900°F, as compared to an undeformed tensile bar of a one-inch gauge length. The results are plotted on log-log coordinates as true flow stress vs. strain rate in Figure 13. The slopes of the curves are approximately the same and equal to 0.5 below about 10^{-1} min^{-1} . This value of the slope was taken as the strain rate sensitivity exponent,

m, in

$$\sigma = K\epsilon^m,$$

where σ = flow stress, K = constant, and ϵ = strain rate. The activation energy for the deformation process was determined from an Arrhenius plot at two stress levels. A constant activation energy of approximately 98 kcal/mole was found. These results are in agreement with similar work by Reichman et.al.¹.

The microstructure of a superplastically deformed tensile bar is shown in Figure 12. The most noticeable change exhibited is the extreme growth of the gamma prime particles, from about 0.2 microns to an average size of one micron.

CREEP TESTING

1800°F stress-rupture tests were conducted on the extruded material, and the grain-coarsened (24 hours at 2270°F - air cooled) Nuclear Metals powder material. To optimize the creep strength, the as-extruded material was overaged at 1800°F for 24 hours, and the grain-coarsened material at 1825°F for 20 hours. The stress-rupture results are compared to stress-rupture properties of fine and coarse-grained cast IN-100² in Figure 14. The extruded material (average grain size of 8 microns) exhibits stress-rupture properties far inferior to that of the cast material, as a result of superplastic deformation. The 100 micron grain-coarsened material shows stress-rupture properties beginning to approach those of the cast material, and the absence of superplasticity. The total elongations observed in this material,

-60-

however, are below those of the cast alloy.

REFERENCES

1. Reichman, Smythe, "Superplasticity in P/M IN-100 Alloy",
Int. J. of Powder Metallurgy, 6, 1970, p. 65.
2. "Engineering Properties of IN-100", International Nickel
Company.

Table I - IN-100 Chemistries (w/o)

	N	Cr	Co	Mo	Al	Ti	C	B	Zr	V	Fe	Mn	Si	S	Oxygen (ppm)	
															Ingot	Powder
As-Cast	Bal.	10.5	15.4	3.02	5.55	4.72	.16	.015	.06	1.05	.94	<.10	.05	.007	108	158
Fl Powder	Bal.	9.54	13.97	3.70	5.65	4.82	.17	.014	--	--	--	--	--	--	50	53
HT Powder	Bal.	10.5	15.4	3.02	5.55	4.72	.16	.015	.06	1.05	.94	<.10	.05	.007	74	79
HT Powder	Bal.	9.40	15.18	3.08	5.81	4.82	.178	.016	.06	.99	<.01	<.10	<.10	.001		

Table II - Size Range and Screen Analysis (% retained)
of the Powders as Received from the Manufacturers

	FM POWDER	HM POWDER	NM POWDER
Size Range (microns):	-250+44	-707+74	-500+44
Mesh:			
-25+35	0.0	4.6	0.0
-35+60	0.5	43.0	4.3
-60+100	1.3	24.0	58.0
-100+200	43.3	28.4	29.5
-200+325	23.3	0.0	6.6
-325	31.6	0.0	1.6

Table **JMC** - IN-100 Room Temperature Properties

Material	Hardness (R_c)	.2% YS (ksi)	UTS (ksi)	% elong.	% RA
As-Cast	32	136	143	4	8
As-HIP + EXTR (HM)	41	-	-	-	-
As-HIP (FM)	49	137	163	8	10
As-EXTR (FM)	43	175	244	20	16
As-EXTR (NM)	43	171	238	21	17
As-Grain Coarsened (NM)	33	137	188	14	7



Figure 1a - As-received Federal Mogul IN-100 powders. SEM 140x.

Reproduced from
best available copy.



Figure 1b - Polished and etched sections of above powders. 500x.



Figure 2a - As-received Homogeneous Metals IN-100 powders. SEM 24x.

Reproduced from
best available copy.

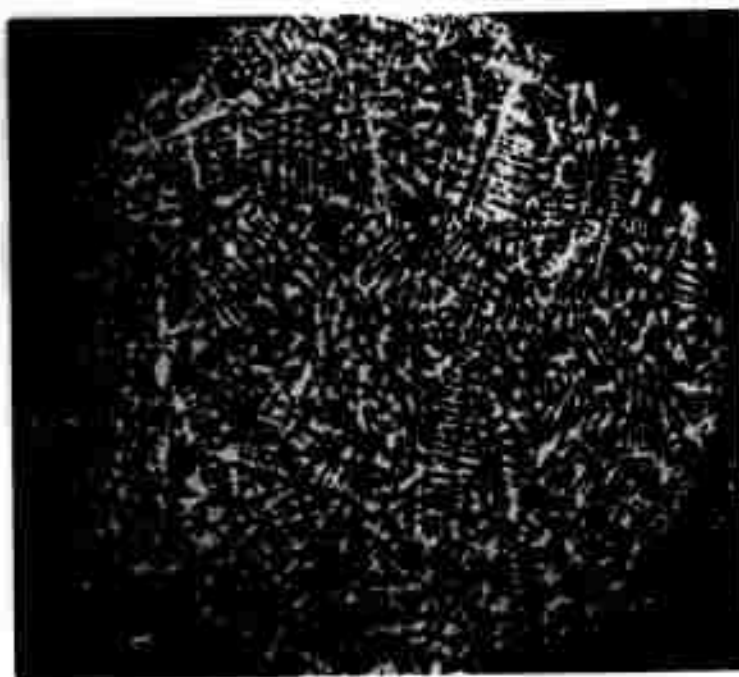


Figure 2b - Polished and etched sections of above powders. 200x.

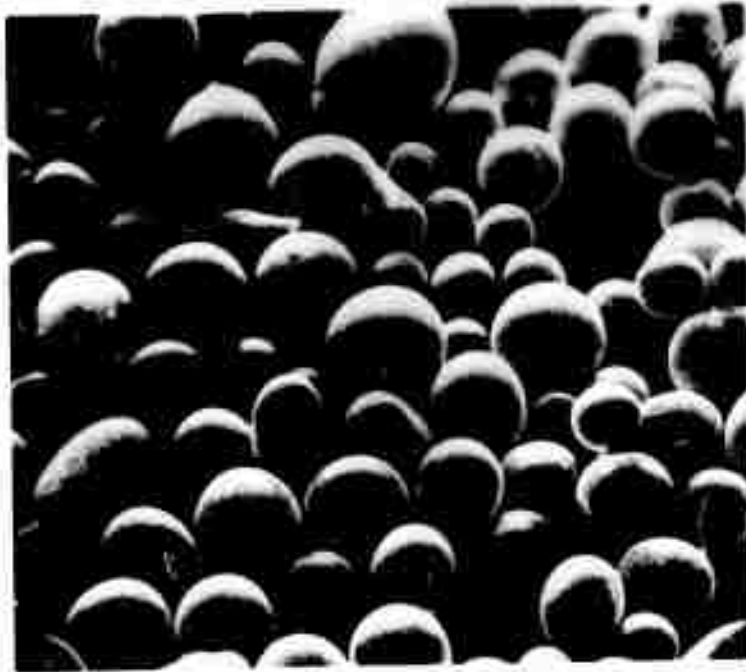


Figure 3a - As-received Nuclear Metals IN-100 powders. SEM 63x.

Reproduced from
best available copy.

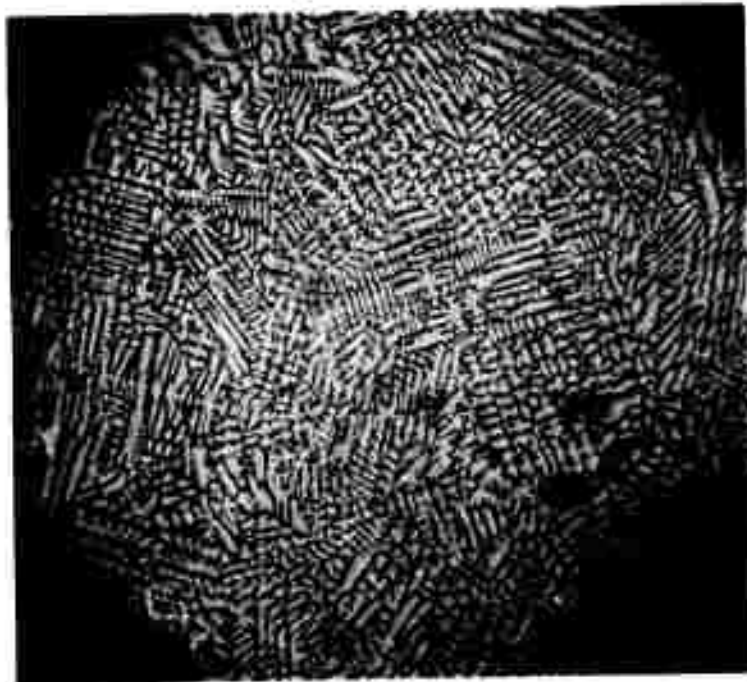


Figure 3b - Polished and etched sections of above powders. 350x.

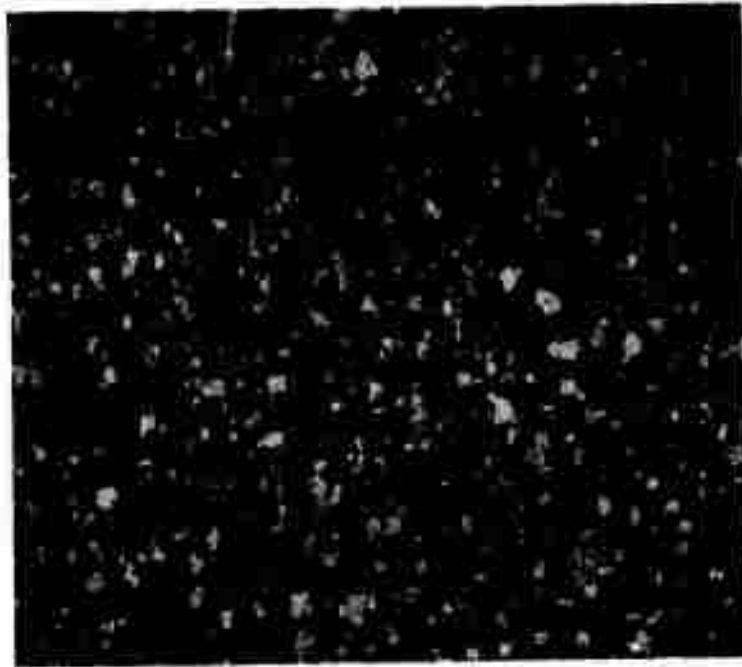


Figure 4 - Longitudinal section of as-extruded Federal Mogul powders. 200x.

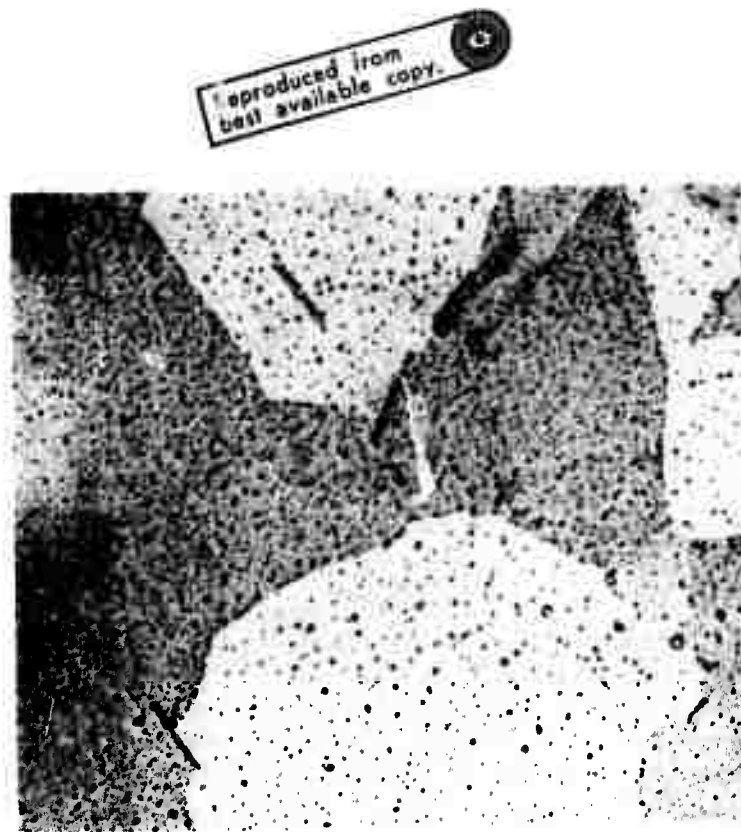


Figure 5 - Grain-coarsened Nuclear Metals powder extrusion. 24 hours at 2270°F. 500x.

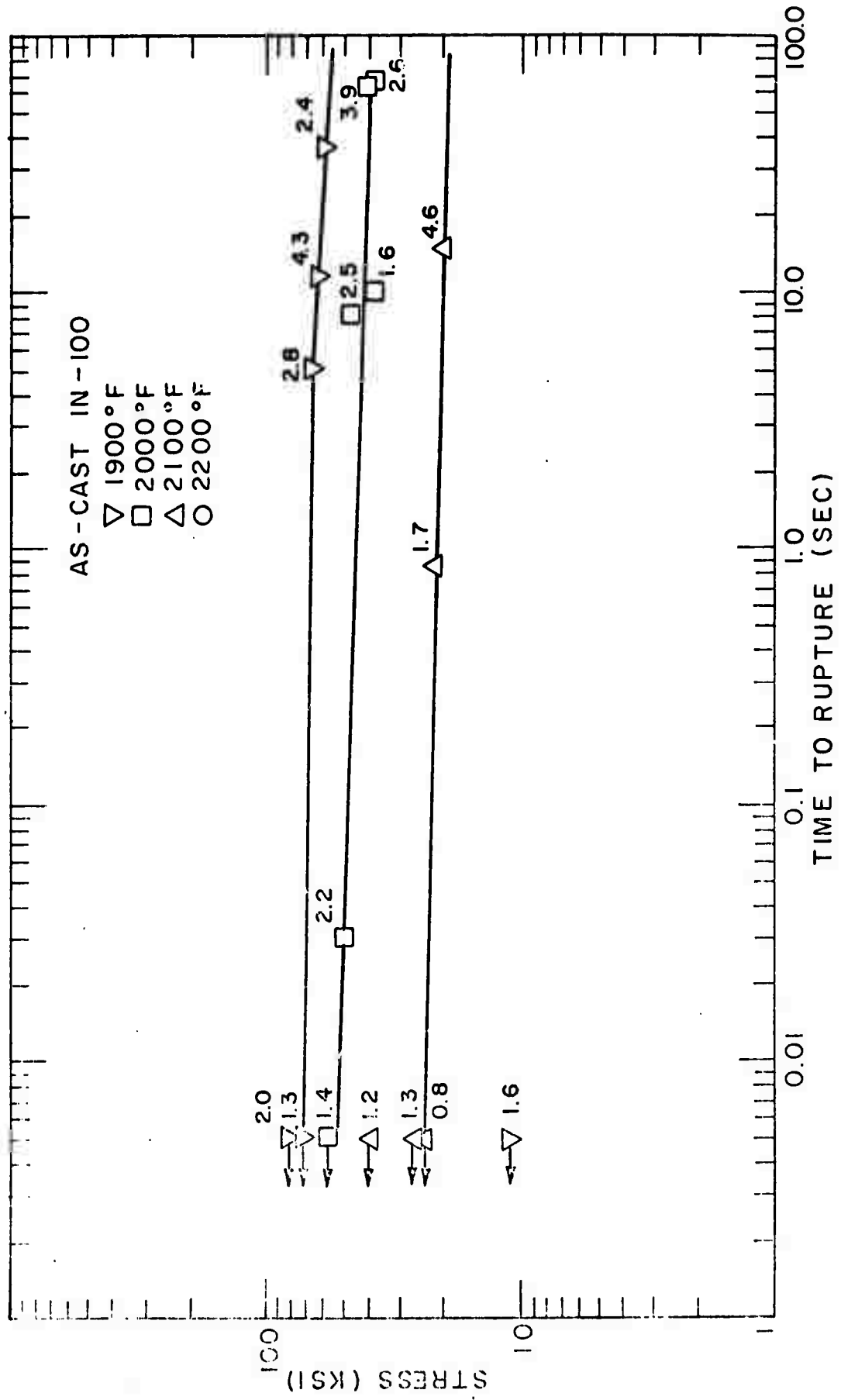


Figure 6 - High strain rate log stress vs. log rupture time at various temperatures for as-cast IN-100.

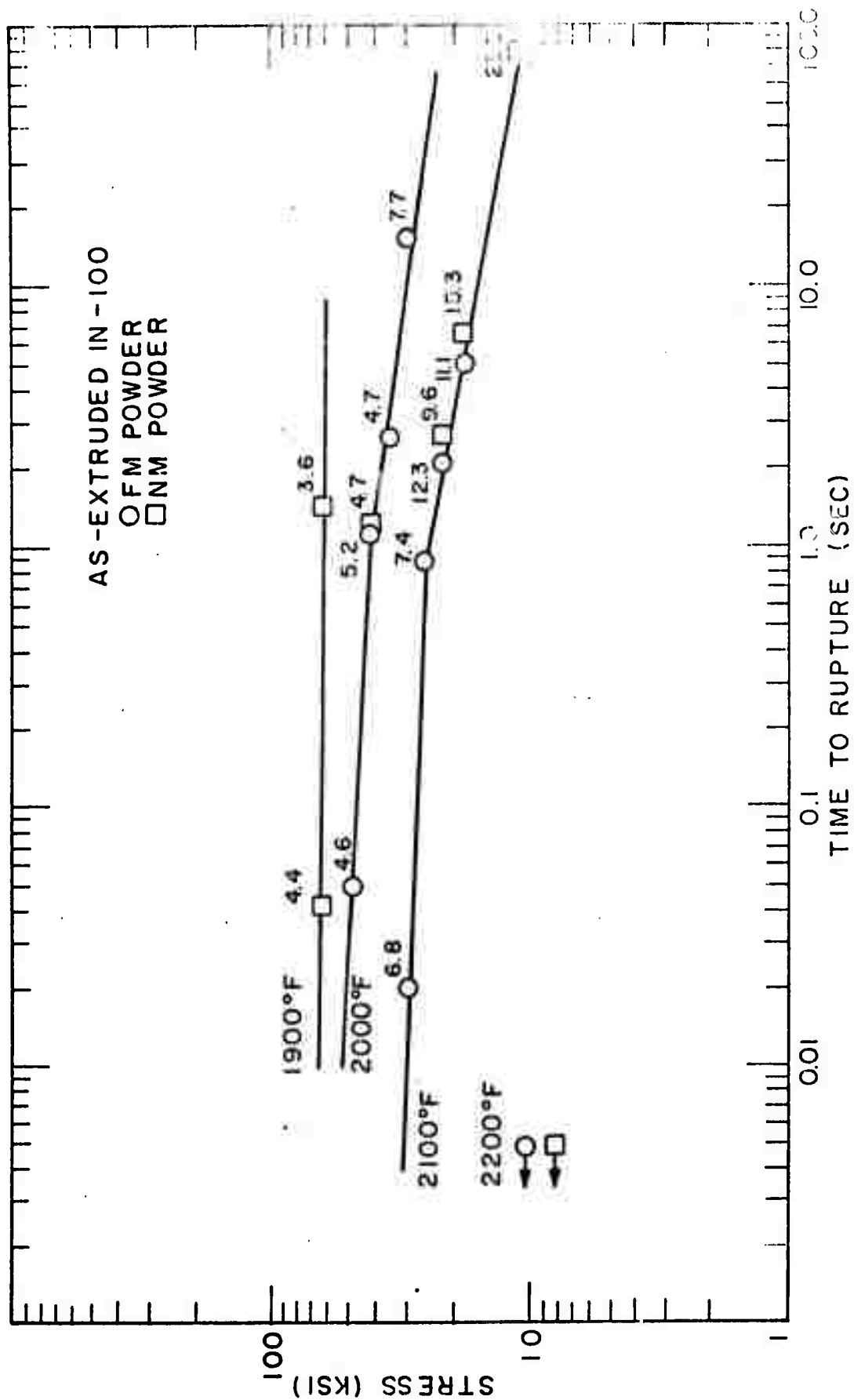


Figure 7 - High strain rate log stress vs. log rupture time at various temperatures for as-extruded IN-100.

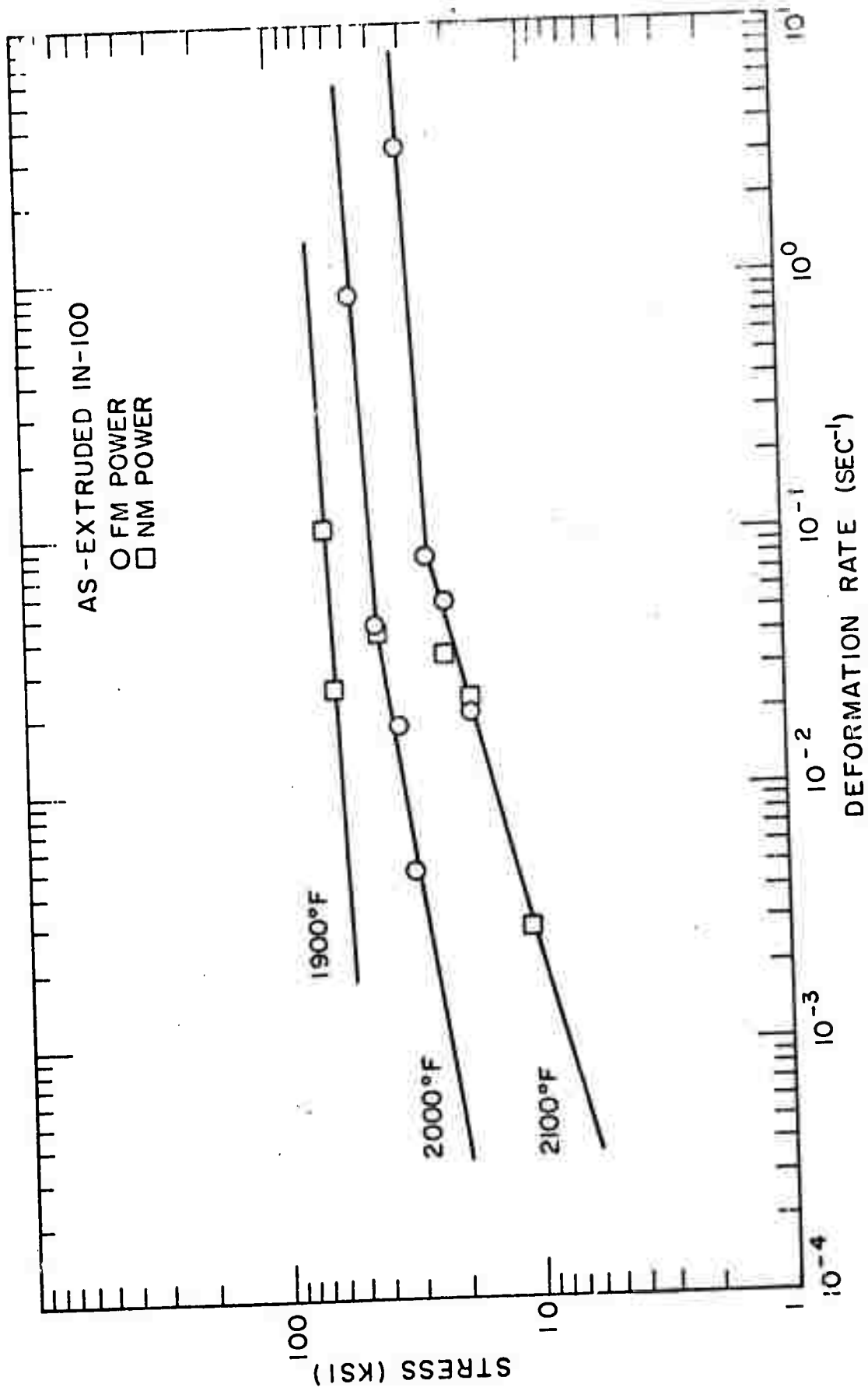


Figure 8 - High strain rate log stress vs. log deformation rate at various temperatures for as-extruded IN-100.

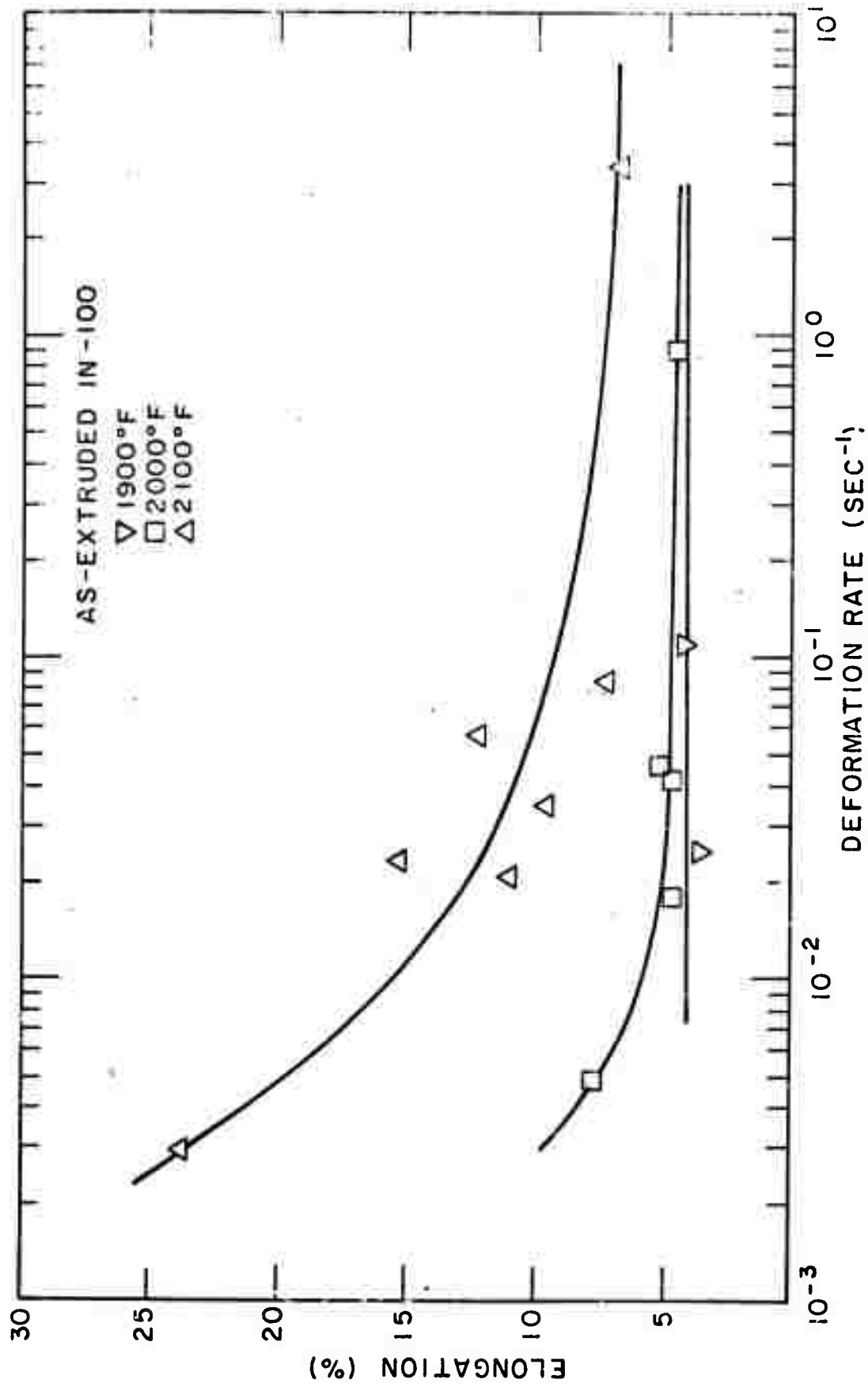


Figure 9 - High strain rate effect of deformation rate on elongation at various temperatures for as-extruded IN-100.

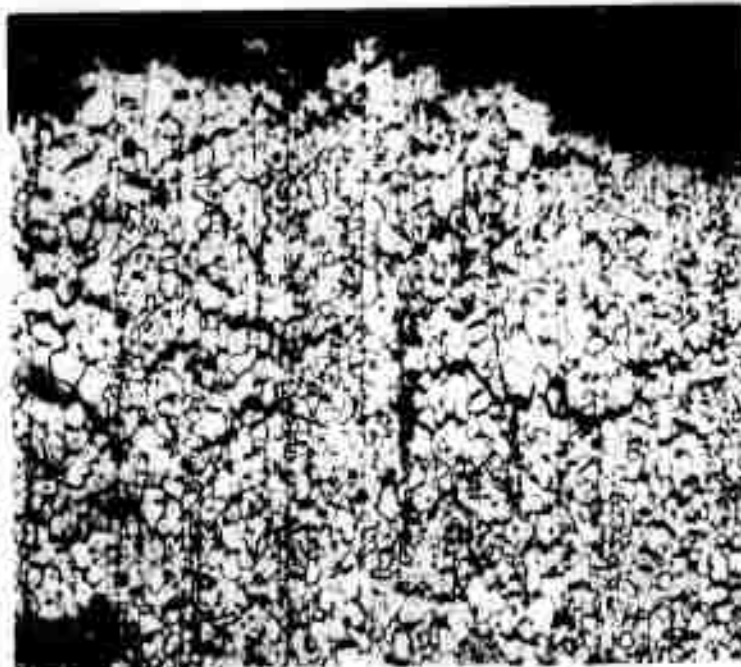


Figure 10 - High strain rate fracture cross-section of extruded Federal Mogul powder test bar. 200x.

Reproduced from
best available copy.



Figure 11 - As-extruded tensile bars superplastically deformed at 1900°F at indicated strain rates.

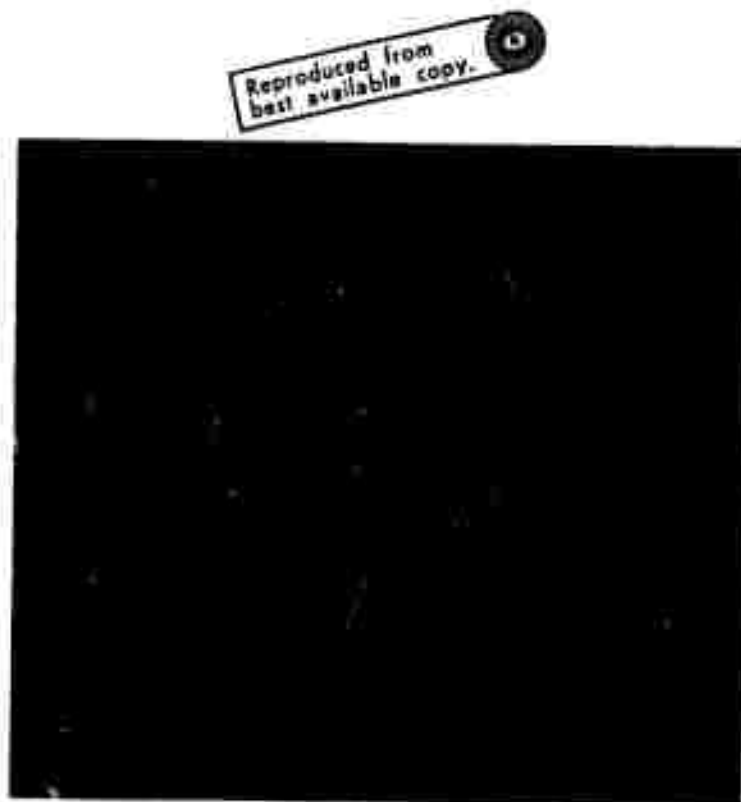


Figure 12 - Microstructure of a superplastically deformed as-extruded IN-100 tensile bar. 1000x.

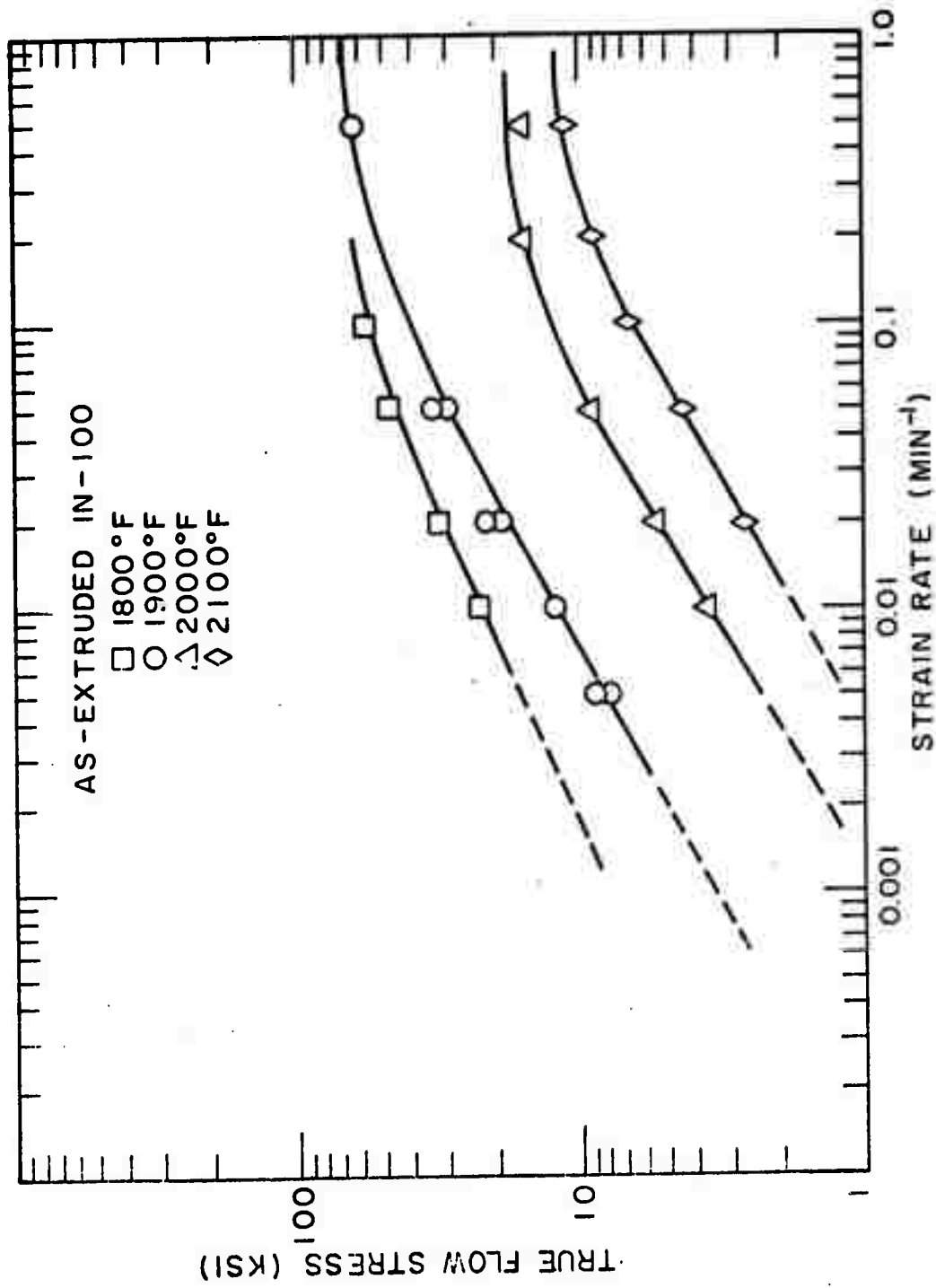


Figure 13 - Superplastic deformation of as-extruded IN-100 at various temperatures plotted as log true flow stress vs. log strain rate.

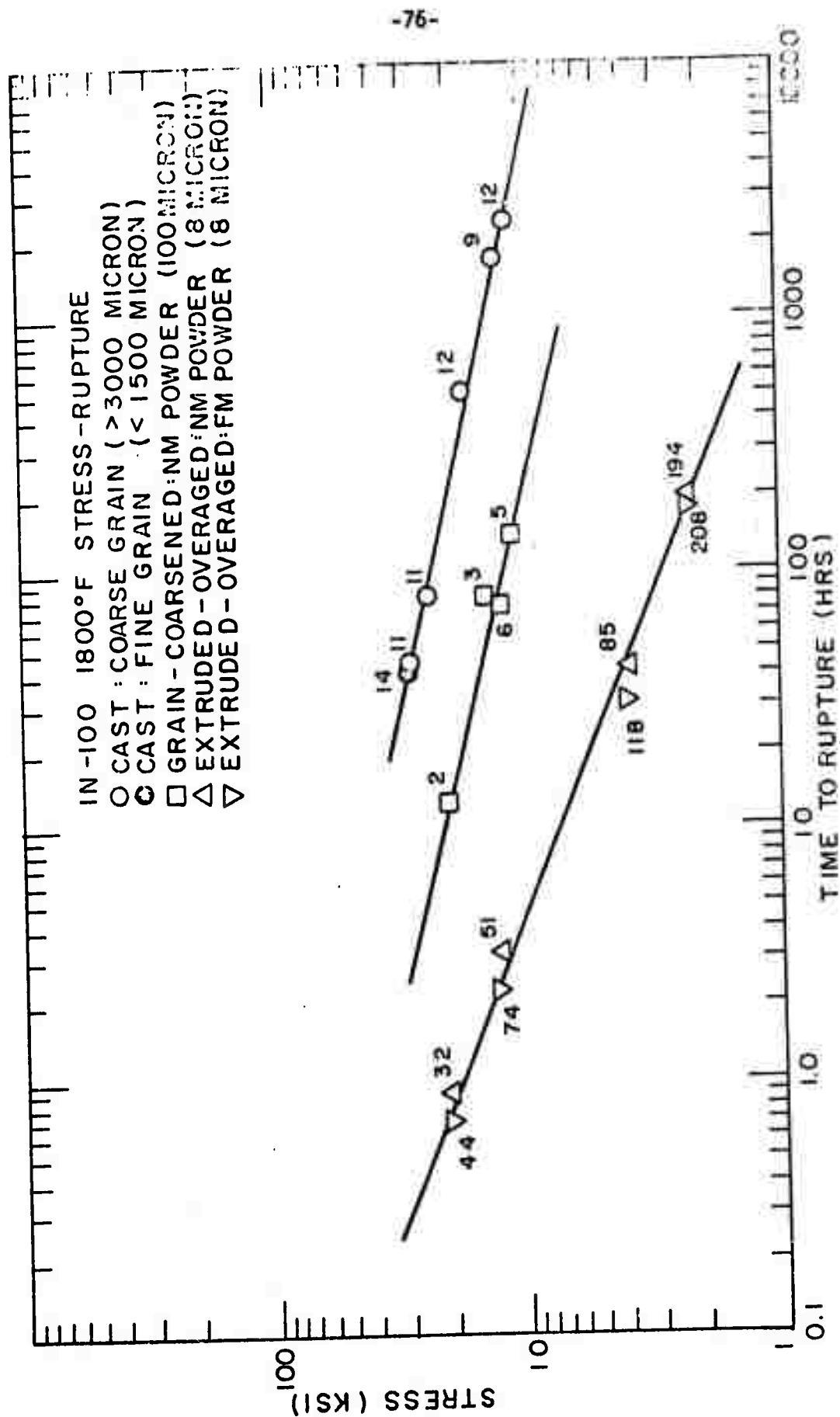


Figure 14 - 1800°F stress-rupture properties for various grain sizes of cast IN-100 and extruded IN-100 powders.

THERMOMECHANICAL TREATMENT, MICROSTRUCTURE AND MECHANICAL PROPERTIES OF COBALT-BASE SUPERALLOYS

INTRODUCTION

Progress made in this program area since the last report¹ includes the following:

New Compositions²

(1) A nominal three atom percent HfC-Co base alloy was prepared (a) by rapidly quenching in copper molds; (b) by steam atomization with and without minor silicon and boron additions; and (c) by vacuum atomization using dissolved hydrogen gas to break up the melt into droplets.

Thermomechanical Treatment and Processing

(1) A powder metallurgy (P/M) commercial alloy, MAR-M-509, was steam atomized into coarse powders, hot isostatically pressed (HIP) and hot rolled with intermediate anneals to a 6:1 reduction in area (RA).

(2) A 3 atom % HfC-Co base alloy, rapidly quench-cast into 5/16" square x 4" long rods was (a) hot rolled to a 5:1 RA; (b) HIP to close internal porosity from the casting operation; and (c) closed-die forged² to consolidate a nested group of four bars for subsequent extrusion and processing.

(3) Several heat treatments were used on available cobalt alloy product to determine (a) softening and aging characteristics

and (b) particle and grain coarsening kinetics. Temperatures under 2300°F for short times (1-2 hours) result in sporadic response to softening and grain coarsening. Secondary recrystallization was frequently observed after exposures at temperatures under 2300°F.

(4) Coarse powders of cobalt alloys were examined for dendrite arm variations and shape and structure anomalies. Calculations were made to correlate type, size, and % solid of atomized droplet with solidification time.

Structure and Properties

(1) Room temperature hardness and tensile strength values were determined on all compositions after each major TMT or processing change. Microhardness tests and metallographic examination indicated all structures were recrystallized with the exception of HIP material processed at less than 2300°F.

(2) Hot plasticity potential of HIP and HIP + extruded cobalt base alloys was assessed using strain rates up to 10 sec^{-1} at 1900 - 2100°F in a constant load test device. The commercial P/M alloy, MAR-M-509, exhibited up to 50% elongation at strain rates exceeding conventional forging practice.

(3) Stress rupture testing was performed on all consolidated powder products and cast material at 1800°F. Load-elongation-time data from all tests to date provided meaningful extrapolation according to the Monkman-Grant³ relationship.

(4) Hafnium-containing cobalt alloys are difficult to etch

for metallographic examination. Experimentation with a variety of etches resulted in a four-step electrolytic etch suitable for grain boundaries, twins, and several types of carbide phases.

COMPOSITION AND PROCESSING HISTORY

The compositions and initial processing history of the MAR-M-509 and cobalt-hafnium alloys used in this program are indicated in Tables I and II, respectively. All steam atomized MAR-M-509 compositions have yielded useful rounded powders for further processing. The 1 atom % Hf-Co alloy, CH2-01-HE (steam atomized) and the 3 atom % Hf-Co alloy, CH6-H1 (vacuum atomized) listed in Table II yielded round powders, all other steam atomized Co-Hf compositions resulted in flaky material. Both CH2-01-HE and the high-zirconium modification of MAR-M-509 (CZ1-01-HE) resulted in porous HIP and extruded product, the former subsequently being re-HIP into a sound product.

It has been speculated¹ that the silicon and/or boron additions plus the atomization superheat played an important role in the success of steam atomizing cobalt base alloys into the more desirable rounded morphology. A comparison of steam atomized cobalt-base powders versus tap temperature (super-heat) and chemistry is depicted in Figure 1. The first column relates morphology to tap temperature holding chemistry constant for an X-45 alloy containing relatively high silicon content (0.83%). Tap temperatures greater than approximately 2700°F were sufficient to produce rounded product for this chemistry. The second column

indicates morphology changes when the silicon and boron contents are varied for this same X-45 alloy at a constant $2920 \pm 40^\circ\text{F}$ tap temperature. Here the higher silicon (0.8 vs. 0.6) and boron (0.02 vs. 0.01) contents appear beneficial.

The MAR-M-509 and Co-Hf morphologies are indicated in the final two columns. Note that the MAR-M-509 P/M is rather insensitive to boron/silicon variations with rounded product being produced for each condition. There may be a subtle beneficial effect due to silicon as indicated in Table I where C51-01-HE composition containing 0.8% silicon yielded much lower oxygen (200 vs. approximately 1000 ppm) than those alloys not containing silicon. Silicon and boron additions improved the morphology of the 1 atom % HfC-Co (#217 vs. 185). Again the presence of silicon provided for easier descaling and subsequent lower oxygen analysis as can be noted in Table II.

A tentative conclusion is that a certain minimum tap temperature is a necessary but not sufficient condition for rounded steam atomized cobalt base powders containing reactive group IV elements. Silicon additions appear desirable to aid in producing rounded morphologies and in providing for easier descaling of the powder thereby producing lower oxygen contents. The minimum silicon additions to improve morphology and the maximum desirable silicon additions prior to generating undesirable secondary effects are not well defined.

The 3 atom % HfC-Co base alloys, indicated in Table II as

those alloys containing 9 - 11 Wt. % Hf, were added to the program since the last report. The purpose was to provide a higher volume fraction (Figure 2) of a stable carbide phase such that the relative merits of the structure refinement due to rapid quenching of liquid metals could be better utilized. Also, this compositional change puts the MAR-M-509 alloy and the Co-Hf alloy on an equal carbon basis providing more meaningful comparisons.

THERMOMECHANICAL TREATMENT

Hot Work

Two alloys, C51-05-HR and CH4-M1-CR, were hot rolled 10% per pass at 2100°F for a total reduction in thickness of 6:1 and 5:1, respectively. The MAR-M-509 alloy (C51-05-HR) was given three passes per heating cycle except for the final three passes. The Co-Hf alloy and the last three passes of the 509 alloy were reheated to 2100°F after each 10% reduction. Both alloys were examined metallographically, tensile tested at room temperature and stress rupture tested at 1800°F.

Re-HIP

The steam atomized, HIP, and extruded Co-Hf alloy, CH2-01-HE was re-HIP to close up porosity resulting from the initial processing. A 9" long bar was given a four hour HIP treatment at 2200°F and 26.5 ksi which successfully closed the porosity and partially coarsened the microstructure. Therefore the remaining four feet of this extrusion was cut into six, 8 - 9" long rods and re-HIP for 1 hour at 2300°F and 29 ksi. Microstructures

showing the duplex grain size and dense material after these re-HIP treatments are indicated in Figure 3. The nominally 5 micron grains after extrusion have coarsened parasitically and/or undergone partial recrystallization during the re-HIP step. Microhardness values of HK_{500} 320-338 (Rc 31-33) over fine and coarse grain areas indicate complete recrystallization after re-HIP.

HEAT TREATMENT

Fourteen heat treatments were performed since the last report to evaluate the stability of the microstructure and to coarsen the grains. These heat treatments ranged from 1 to 121 hours in duration at temperatures scanning 2170°F to 2400°F and are summarized in Table III. The initial hardness values of the Co-Hf P/M and cast material prior to heat treatment are Rc 36/39 and Rc 40, respectively. The P/M 509 and high-zirconium material had initial hardness values of Rc 43 each. All the P/M product had as extruded grain and particle sizes of approximately 3-5 microns and 1-3 microns, respectively.

Heat treatment tests were conducted on de-canned specimens encapsulated in Vycor tubing. Some sample contact and interdiffusion was observed in treatment #9 (2285°F), but no significant contact was allowed in all other tests. Analyses of the microstructures from all heat treatment tests resulted in the following tentative conclusions:

MAR-M-509

Between 2225 and 2300°F, parasitic grain growth and secondary

recrystallization occur generating a duplex grain size from the original uniformly fine (approximately 3 microns grain size), as-extruded structure. The fine grains coarsen at an approximate parabolic rate (Figure 4) from 3 microns to about 50 microns after 121 hours exposure at 2285°F. The coarse or abnormal grains grew very rapidly up to several millimeters in size even at the lower (2225°F) temperature. At 2170°F, grain coarsening was uniform and extremely slow taking more than 100 hours to double the original 3 micron grain size. Treatment #12 at temperatures exceeding 2300°F, uniformly coarsened the grain size to several millimeters. Examples of these structures are shown in Figures 5 and 6. Note that the particles coarsened similarly with time and temperature but to a much lesser extent.

Co-Hf

The coarsening behavior of the Co-Hf alloy (CH2-01-HE) was the reverse of the MAR-M-509. At 2170°F, secondary recrystallization occurred forming a duplex structure. At 2225°F to 2325°F, uniform but slow coarsening occurred with the grain size varying from an initial 5 microns to only approximately 40 microns after 121 hours at 2285°F (Figure 7).

In both alloys, secondary recrystallization preferentially occurred in bands between extrusion stringers of interparticle boundaries. The mechanisms postulated for the reverse behavior of the two types of alloys are that in MAR-M-509, the second phases go into solution over the temperature range 2200-2300°F,

whereas in the Co-Hf alloy, mass action effects may tend to convert initially metastable chromium carbides to the more stable hafnium carbides.

ATOMIZED COBALT-HAFNIUM POWDERS

Steam atomized, coarse cobalt powders were examined to determine dendrite arm spacings as a function of particle size (Table IV). During the course of this evaluation it was noted that there was a large fraction of hollow rounded particles. Previously¹, secondary dendrite arm spacing had been observed to vary from the outer surface to the core of atomized maraging steel powders. These observations plus the qualitative observation that steam atomization appeared to produce higher yields of rounded product in going from nickel to cobalt to iron base alloys led to an evaluation of the atomization process based on a radiation heat transfer model of Szekely⁴. This model is based on the transient heat conduction equation in spherical coordinates:

$$\frac{dT}{dt} = K \left[\frac{d^2T}{dr^2} + \frac{2}{r} \frac{dT}{dr} \right] \text{ where } R \leq r \leq a$$

Where: t is time in seconds,

$T = R(t)$ is the time dependent position of the solidification front moving from the surface of a liquid metal droplet inward

r = radial distance measured only within the solidified crust, cm.

K = thermal diffusivity of the solid

T = temperature, °K

Applying the boundary conditions and applying the simplifying assumption that the temperature distribution is spatially independent within the sphere, an asymptotic solution is derived by Szekely:

$$\frac{R}{a} = (1 - ct)^{1/3}$$

or, $t = \% \text{ solid}/c$

$$\text{where } c = - \frac{3\sigma\epsilon}{A\Delta H_p} \left[T_e^4 - (T_{mp} + 273)^4 \right]$$

and: ϵ = emissivity

σ = Boltzmann's constant

H = heat of fusion

a = radius of particle

T_e = temperature of the environment

A plot of R/a and % solidified against time and distance with the particle size as a parameter for steel powder is shown in Figure 8 with the data for the steam atomized powders shown by a dotted line. Some interesting results were generated when these equations were applied to hypothetical Fe, Ni, and Co alloys assuming (a) a 2-1/2 foot drop height to the water tank in steam atomization; (b) zero initial velocity; (c) no superheat; and the following property values:

<u>Property Values</u>	<u>Steel</u>	<u>Cobalt</u>	<u>Nickel</u>
density, g per cc	7.3	9.0	9.0
thermal cond, cal/sec-cm-°K	0.124	0.124	0.124
latent heat of fusion, cal/g	108.3	107	124

<u>Property Values</u>	<u>Steel</u>	<u>Cobalt</u>	<u>Nickel</u>
heat capacity, cal/g°K	0.09	0.09	0.09
melt temp, °C	1500°C	1400°C	1350°C
emissivity	0.58	0.6	0.6
temp of the environ, °C	0	0	0
Boltzmann's constant, cal/cm ² ·s·K	1.35×10^{-12}	ditto	ditto

To solidify a 1 mm diameter liquid droplet 98% in freefall requires:

$$S_{Fe} = 41.5 \text{ feet}$$

$$S_{Co} = 100 \text{ feet}$$

$$S_{Ni} = 167 \text{ feet}$$

In 2-1/2 feet:

$$R/a_{Fe} - 91.2\% \text{ Fe radius is molten}$$

$$R/a_{Co} - 94.5\% \text{ Co radius is molten}$$

$$R/a_{Ni} - 95.8\% \text{ Ni radius is molten}$$

The R/a calculated for cobalt (94.5%) compares very favorably with the experimentally measured low Hf alloy (Table IV). A tentative conclusion is that shells are produced by a partially solidified droplet (approximately 16% solid for a 1 mm diameter cobalt) reacting with the water in the collecting tank cracking the outer crust and releasing the remaining liquid. If there is sufficient solid to resist this action, a change in cooling rate occurs causing a duplex dendrite arm structure².

MECHANICAL PROPERTIES

Room Temperature

Room temperature tensile properties are indicated in Table V.

Note that as the grain size increases, the UTS, YS, and elongation all decrease accordingly. The tensile fractures for the HIP (only) material are shown in Figures 9-11. Interpowder fracture, interdendritic fracture and transgranular fracture are exemplified for the three HIP conditions: 2 hours and approximately 27 ksi at 2000, 2150, and 2300°F, respectively.

Note also in Table V that the hot rolled material has significantly higher YS and lower ductility than the as-extruded material.

Stress Rupture

Elevated temperature (1800 and 1850°F) stress rupture data are presented in Table VI and plotted in Figures 12 and 13. Grain coarsening, even if a duplex grain size resulted, was beneficial in all cases except for the as-cast specimens. Cobalt-hafnium extrusions which were re-HIP resulted in a duplex grain size in addition to closing the as-extruded porosity. The potential benefits derived from grain and/or structure modification via heat treatment are obvious from the summary of 100 hour stress rupture lives in Table VII.

Hot Plasticity (HP)

High strain rate test data on all material produced to date are listed in Table VIII and plotted in Figures 14 and 15. Unlike the IN-100 powder metallurgy alloy HP data discussed elsewhere in this report, the commercial cobalt base MAR-M-509 demonstrated excellent hot workability (2100°F) at high strain rates (up to approximately 10 in/in/sec) as indicated by elongations of 3^d and 50%.

REFERENCES

1. Semi-Annual Technical Report No. 2, ARPA Order #1608.
2. Semi-Annual Technical Report No. 3, Tasks I and II, ARPA Order #1608.
3. Monkman, F.C. and N.J. Grant: "An Empirical Relationship Between Rupture Life and Minimum Creep Rate In Creep-Rupture Tests", Proceedings, ASTM, 56 (1956) p. 593 ff.
4. Szekely, J. and R.J. Fisher: "On the Solidification of Metal Spheres Due to Thermal Radiation at the Bounding Surface", Metallurgical Transactions, Vol. 1 (May 1970) pp. 1480-1482.

Table I - MAR-M-509 Cobalt-Base P/M
Alloy Compositions and Processing History

Element Wt. %	C51-LIT- Cast Nominal	C51-01- HE	C51-03,4 H	C51-03-*** H	C51-04*** H	C51-05 HR	C21-01 HE
C	0.6	0.62	see	0.65	0.65	0.65	0.8
Cr	23.8	25.6	next	24.0	24.0	24.0	nom
Ni	10.0	12.4	two	11.0	11.0	11.0	nom
W	7.0	6.9	alloys	7.5	7.5	7.5	nom
Ta	3.5	2.75		4.0	4.0	4.0	nom
Zr	0.5	0.35		0.6	0.6	0.6	3.0*
Ti	0.2	0.14		0.25	0.25	0.25	nom
Si	< 0.4	0.8*					0.8*
B	0.01*	0.01*		0.05	0.05	0.05	0.01*
O**		200		960	1000		700
Bal Co	--	--	--	--	--	--	--
HIF-T(°F)		2175	2000	2300	2150	2300	2175
t(hrs)		1	2	2	2	1	1
p(ksi)		15	28	28.4	26.6	28	15
Extr-T(°F)		2000					2000
ratio		15.2					11.1
ROLL-T(°F)						2100	
RA						6	

* charged in the melt except for C and O

** in ppm

*** aim composition

Table II - Co-Hf P/M and Cast Alloy
Compositions and Processing History

Element Wt. %	CH1-A1- Cast	CH1-M1- Cast	CH1-01 Melt Dip	CH2-01 HE	CH3-01***	CH4-M1 Cast	CH5-01*	CH6-H1-***
C	0.24	0.28	0.25	0.20	0.55	0.65	0.58	0.6
Cr	19.9	18.6	19.9*	20.5	19.0	21.3*	20.0	21.3
Ni	9.2	8.5	9.2*	9.18	8.5	10.2*	9.0	9.9
Mo	5.6	6.8	5.6*	5.5	5.3	5.0*	5.0	5.0
Hf	4.0	2.5	4.0*	2.6	9.4	10.5	11.8	9.2
Si	0.02		0.02*	0.84			1.0	
B				0.04*	0.05		0.05	
O**	24	82	49	460	3300	90	2200	
Bal Co								
HIP-T(°F)				2100				
t(hrs)				1				
p(ksi)				14.5				
Extr-T(°F)				2000				
ratio				16				
ROLL-T(°F)						2100		
RA						5		

* charged to melt except C and O

** in ppm

*** aim composition except C and O

Table III - Cobalt Base Alloys -
Heat Treatment and Hardness Data

	P/M MAR-M-509 (as-extr)	P/M HiZr MAR-M-509 (as-extr)	P/M 1 atom % Co-Hf (as-extr)	cast 3 atom % Co-Hf (Melt Dip)
No Heat Treatment	43/-*	43/-	36/39	40/-
2170°F (#10)				
25 hours	38/41	38.5/-	32/34	--
119 hours	36/38	37/-	30/31	28/-
2225°F (#11)				
25 hours	28/34	37.5/-	27.5/30	--
120.5 hours	31/35	36.5/-	27/34	--
2285°F (#9)				
4 hours	32/34	39/-	26/32	26/-
24 hours	32/39	30/-	30/33	31/-
121 hours	24/27	26/-	25/33	33/-
2395°F-1 hr + 2325°F (#12)				
4 hours	31/36	36/31.5	-/35	--
25 hours	31/30	37/39	-/36	
2280°F-116 hours (#13)				

* xx/xx - first number is R_c ; second number is HK_{500} microhardness converted to equivalent R_c .

Table IV - Dendrite Arm Spacing Measurements in Co-Hf Alloy

<u>Alloy</u>	<u>Composition/History</u>	<u>Location or Size (mm)</u>	<u>DAS (μ's)</u>	<u>R/a*</u>
CH4-M1-C	3 atom % HfC/quench cast	Bot Trans sect near Edge	1.7	
		Top Trans sect near center	5.0	
		Bot Long. sect	2.0	
		Top Long. sect	4.4	
CH5-01-powder (#228)	3 atom % HfC/steam atom Hollow particle	OD = 2.4 wall = 0.10		0.92
		outer surface	2.4	
		inner surface	1.7	
		mid thick wall	1.4	
		mid thin wall	2.7	
		OD = 2.4 wall = 0.13	2.0	0.90
CH2-01-powder (#217)	1 atom % HfC/steam atom Hollow particle	OD = 1.3 wall = 0.053	1.1	0.92
		OD = 5 wall = 0.33		0.87
		outer surface	4.5	
		inner surface	2.9	
		mid wall	3.7	
		OD = 1.5 wall = 0.1		0.87
	Hollow particle	OD = 0.37 wall = .03	2.2	.84
		OD = 1.13	2.8	
		OD = 0.75	1.6	

*R/a = radial thickness of fraction liquid divided by particle radius or for hollow spheroids equal to wall thickness divided by radius.

Table V - Cobalt Alloy - Room Temperature Tensile Properties

<u>Alloy</u>	<u>Prior History</u>	<u>UTS</u> (ksi)	<u>0.2% YS</u> (ksi)	<u>Elong</u> (%)	<u>RA</u> (%)	<u>Grain Size</u> (microns)
<u>MAR-M-509</u>						
C51-01-HE	HIP + Extr	190	135	11	8	3-4
C51-01-HE	HIP + Extr	195	123	17	13.6	3-4
C51-01-HET13A6	N + HT Treated and Aged	166	94	11	8	6-10
C51-05-HR (Long)	HIP + Hot Rolled	188	150	2.2	2.0	3-5
C51-05-HR (Trans)	HIP + Hot Rolled	193	155	2.3	2.3	3-5
C51-03,4-H7	HIP	119	98	0.7	0.0	-
C51-03-H8	HIP	94	68	1.2	0.0	-
C51-04-H9	HIP	110	78	1.5	1.2	-
CZ1-01-HE	HIP + Ext. (HiZr)	188.5	129	5.6	7.3	3-4
<u>Co-Hf</u>						
CH1-M1-C	Cast	68.5	55	3	11	coarse
CH1-M1-C	Cast	82.3	60	11.5	10.6	coarse
CH2-01-HE	HIP + Extr	141.5	98	4	5.5	5
CH2-01-HEH 1	HIP + Extr + REHIP	137	97	10.8	9.5	duplex
CH2-01-HEH 2	HIP + Extr + REHIP	111.0	70	5.1	5.1	duplex

Table VI - Stress Rupture Data

<u>Alloy</u>	<u>Temp.</u> (°F)	<u>Stress</u> (ksi)	<u>Rupt. Life</u> (hours)	<u>Rupt. Ductilities</u> <u>Elong.</u> (%)	<u>R.A.</u> (%)	<u>Min Creep Rate</u> <u>in/in/hr</u> ($\times 10^{-3}$)	<u>Time for</u> <u>1% Total</u> <u>Creep Strain</u> (hours)
<u>Co-Hf Alloys</u>							
CH1-M1- casting	1800	6*	(281)	1.0		.074	281
	1800	10	47.5	38.8		6	1.7
	1800	12	2.4				
	1800	14	6.37	43.2		37	0.1
	1800	17	1.8	43.3		260	0.02
	1850	8*	1.97	8.9			
	1850	10*	10.8	19.9		12	0.8
	1800	5	51.8		18.3	3.2	0.5
	1800	6.5	26.1	32.0	18.3	6.8	1.4
	1800	10	5.17	65	32	40	0.15
CH2-01-HE (atomized, HIP, and extruded)	1800	10	9.22	60	27.8		
	1800	4	1005	23	7.5	.0645	150
	1800	15	1.97			200	0.03
	1800	6	120+	8.7	10.4	0.34	4.7
	1800	8	11.1	53.0	40	3.25	2.57
CH4-M1-CR (cast and hot rolled)	1800	6	36.5	18.5		3.9	0.83
	1800	10	3.94	35.3	18.4	82.5	0.03
<u>MAR-M-509 Alloys</u>							
C51-01-HE (atomized, HIP, and extruded)	1800	2.75	72.5	98	57	5.1	1.7
	1800	4	15.3	95	57		
	1800	10	0.85	120	57	480	0.02
	1800	17	0.095	56	50		

Table VI - Stress Rupture Data - cont'd

Alloy	Temp. (°F)	Stress (ksi)	Rupt. Life (hours)	Rupt. Ductilities Elong. (%) R.A. (%)	Min Creep Rate in/in/hr ($\times 10^{-3}$)	Time for 1% Total Creep Strain (hours)
" + Ht. Treat. (T 13A6)	1800	6**	33.5	36	5.1	2.0
	1800	10**	4.23	47.3	32	0.33
" + Ht. Treat (T 8A4)	1850	10*	17	10	1.6	6.0
	1850	17*	0.762	10	94	
C51-05-HR (Long) (atomized, HIP, and extruded)	1800	4	63.6	21.8	1.7	4.17
" (Long)	1800	6	20	20	8.3	1.13
" (Trans)	1800	6	18.5	17.3	6.65	0.5
CZ1-01-HE (HiZr, atomized, HIP, extruded)	1800	5	104	41.7	1.7	6.5
	1800	6	73 1/2	31.5	3.5	2.9
	1800	10	5.13			
	1800	15	0.58	45	500	0.02
Typical Commercial 509-castings	1800	10	3218	8		
	1800	13	1000			
	1800	17	100			
	1800	17.5	27	10		
				9.6		

* Sol. 8 + 20 hour age at 1450°F

** Sol. 13 + 20 hour age at 1650°F

Table VII - Cobalt Alloys -
1800°F, 100 Hour Life Stress Rupture Data

	Stress (ksi)	Elong. (%)
<u>MAR-M-509</u>		
as cast*	17	8-10
as ext.	2.5	50-120
as ext. + Heat Treat**	7.5	10
as Hot Rolled	3.75	20
<u>Co-Hf</u>		
as cast	9	20-40
as ext.	4	30-70
as ext. + Re HIP	6.5	20-50

* literature values

** Tested at 1850°F. Heat treatment 1 hour at 2280°F
plus 20 hours at 1450°F.

Table VIII - Cobalt Alloys -
Hot Plasticity Data

HP Test Conditions	P/M MAR-M-509				Co-Hf (1 atom %)	
	HIP 2000°F	HIP 2150°F	HIP 2300°F	HIP/Extr	HfZr HIP/Extr	Cast HIP/Extr
<u>1800°F</u>						
69 ksi			3.8/7.5*			
<u>1900°F</u>						
35 ksi	1.6/.08	4.7/.07				
45 ksi			9.5/0.3			
<u>2000°F</u>						
23 ksi			6.2/.03			
36 ksi			5.3/0.8			
<u>2100°F</u>						
12-17 ksi	1.6/.01	2.0/.01	2.5/.01		32/.08	10/0.4
21-26 ksi	1.2/2.5	2.0/4.0	3.3/0.2	50/0.5	34/1.1	8.5/1.1
34-37 ksi			1.2/2.5	34/9.6		8.8/.05 1.6/3.2**

* xx/x first number is % elongation/second number is strain rate (sec.⁻¹)

** ReHIP to close porosity

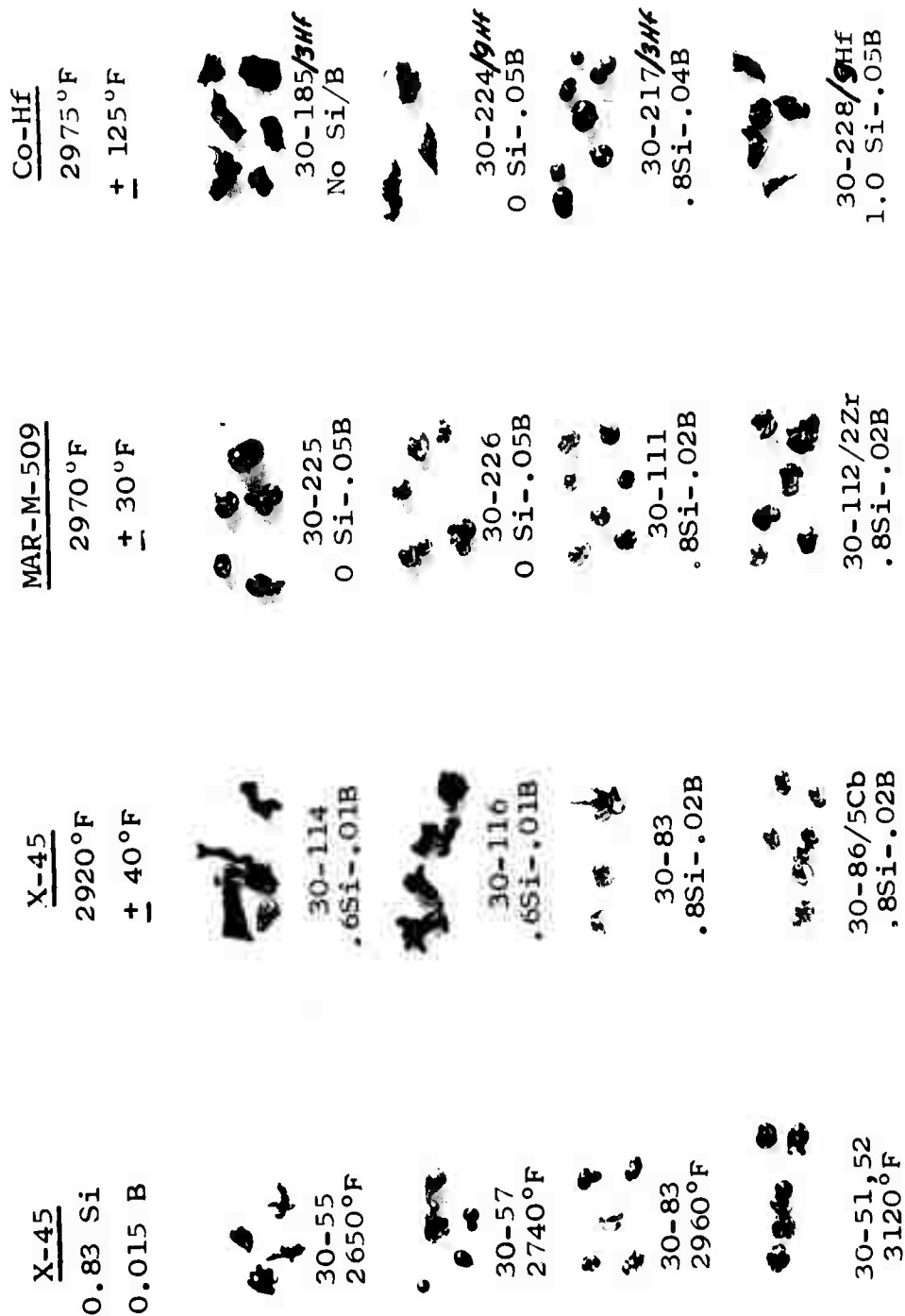


Figure 1 - Effect of Tap Temperature and Chemistry on the Morphology of Steam Atomized Coarse Cobalt Powders.

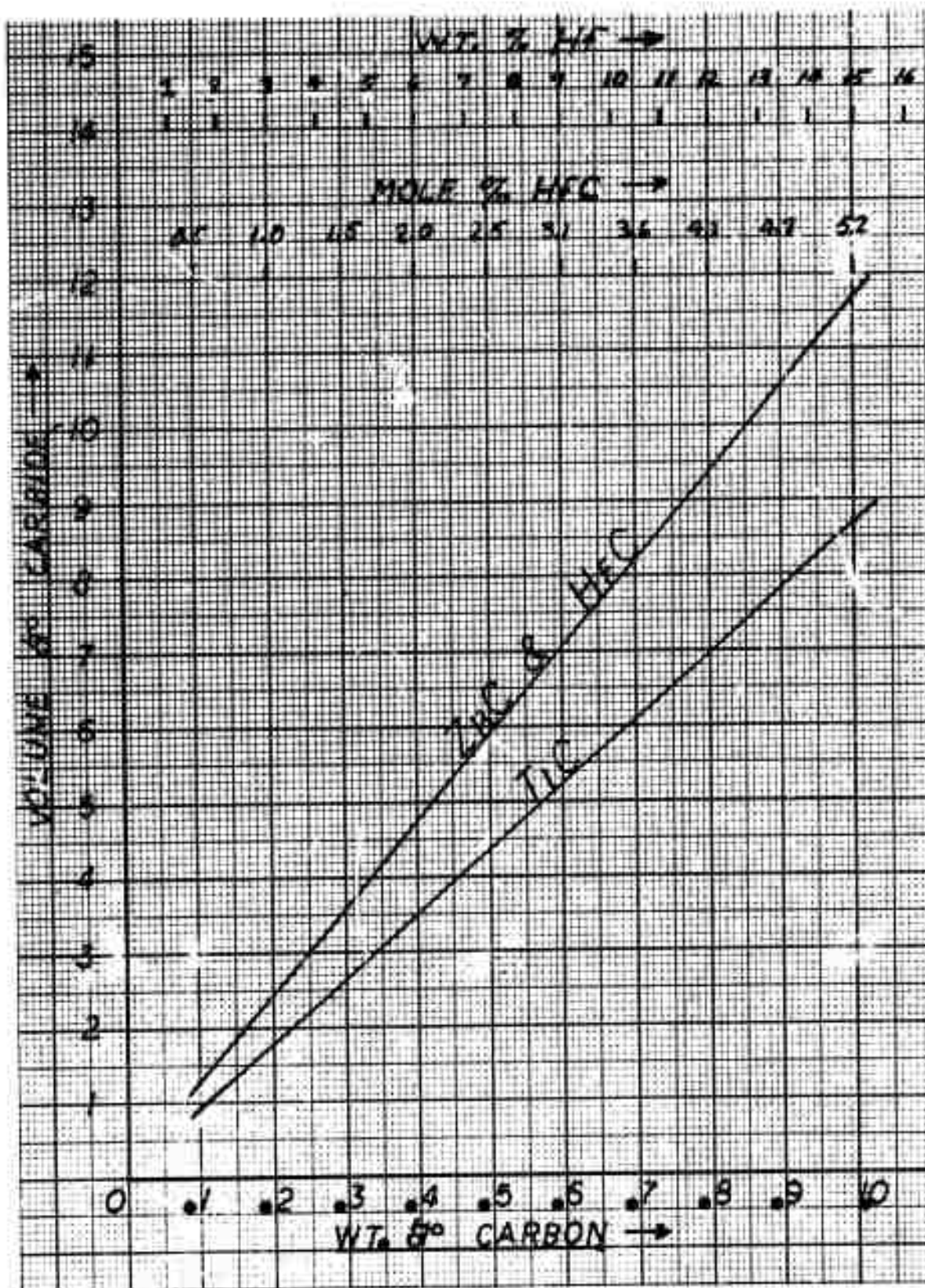
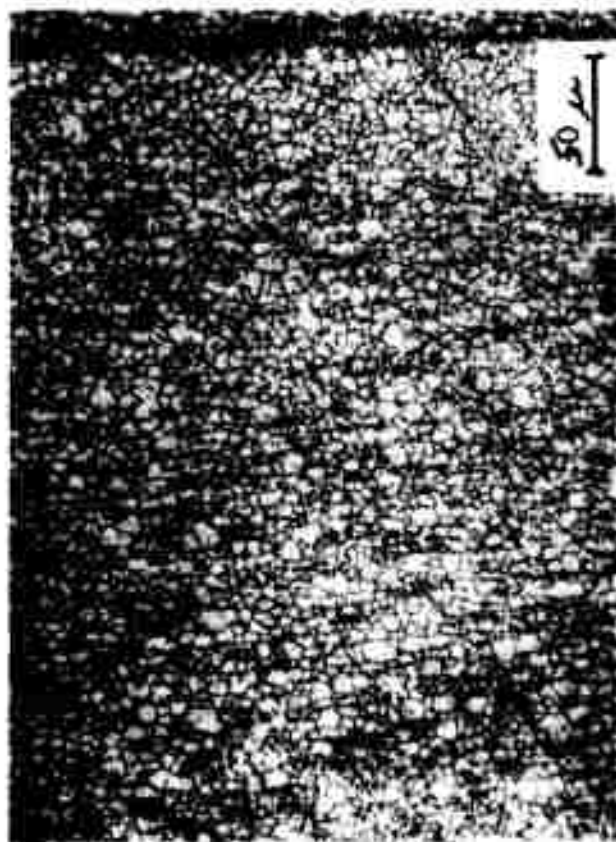
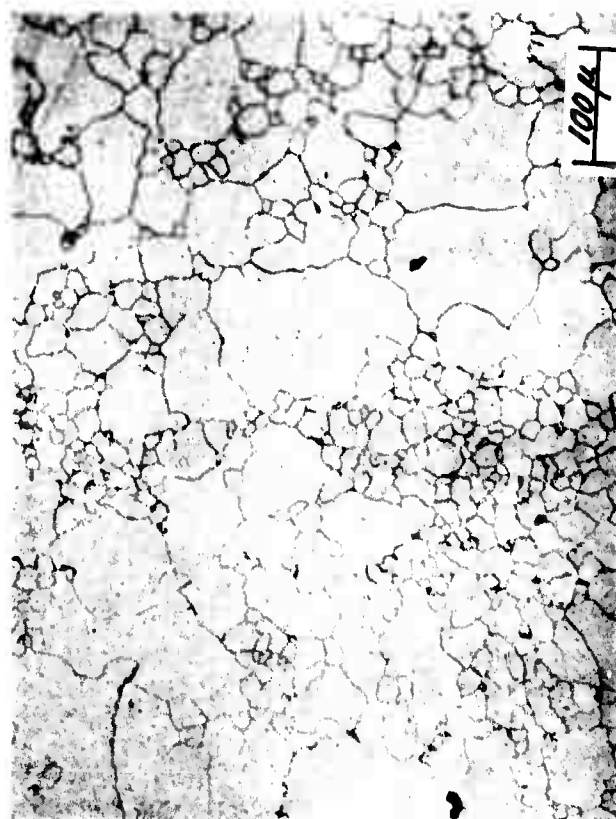


Figure 2. Stoichiometric Mono-Carbides in Cobalt Alloys

Reproduced from
best available copy.



a. Co-Hf alloy after extrusion showing uniformly fine grain size.



b. Co-Hf alloy after RE-HIP for 1 hour at 2300°F showing duplex grain size.

Figure 3 - Cobalt-1 atom % HfC P/M alloy comparing HIP + Extr. structure with the HIP + Extr. + RE-HIP structure.

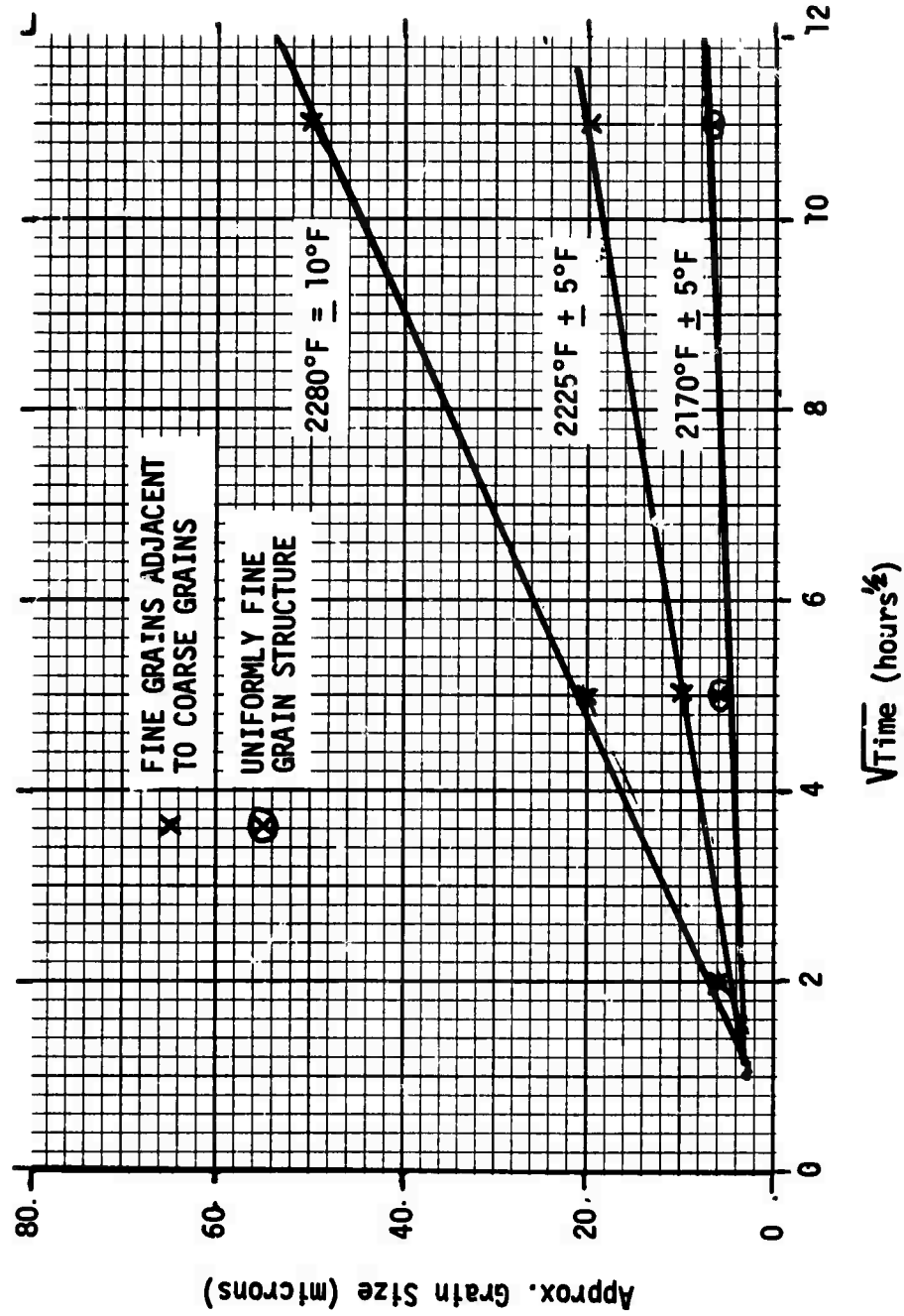
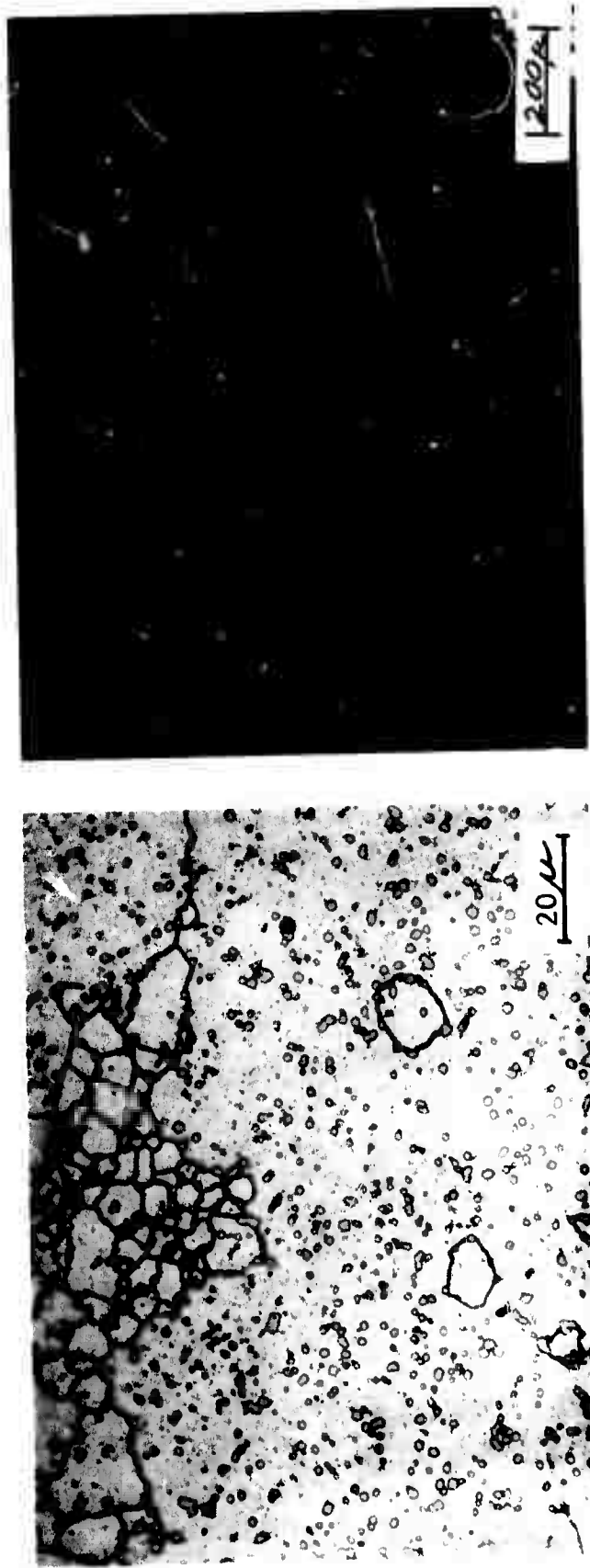


Figure 4 - Coarsening rate of fine grains in secondary recrystallized (2280°F and 2225°F) and in uniform (2170°F) MAR-M-509 (P/M) alloy structures.

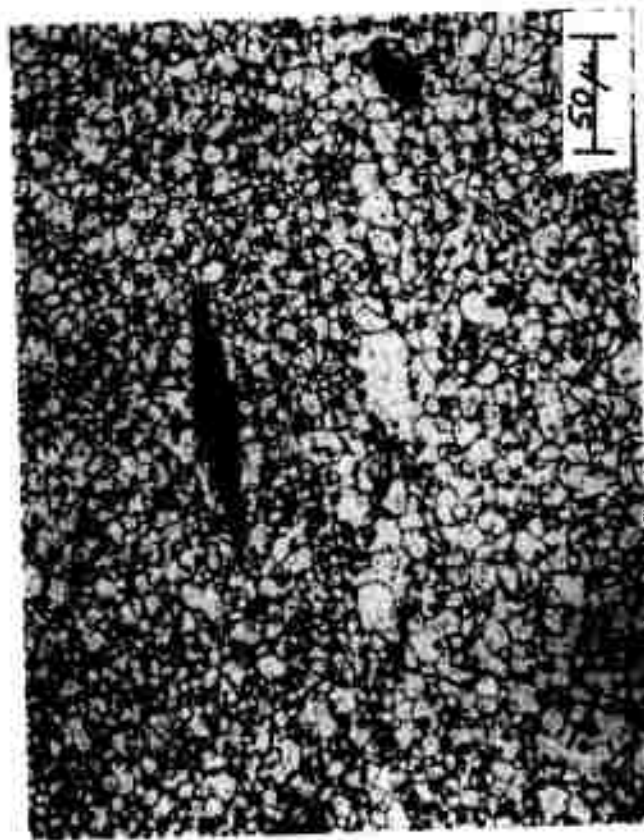
Reproduced from
best available copy.



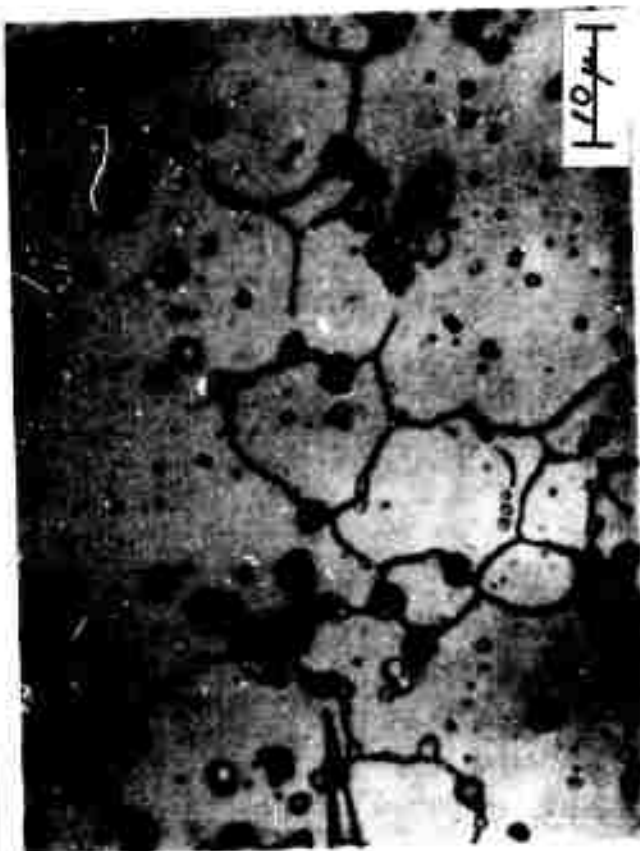
- a. One hour exposure showing duplex grain structure.
- b. 121 hour exposure showing typical coarse grains.

Figure 5 - Abnormal grain growth in MAR-M-509 P/M alloys heat treated at $2280 \pm 10^\circ\text{F}$.

Reproduced from
best available copy.



a. 2170°F exposure showing uniform coarsening of grains and carbides.



b. 2225°F exposure showing fine-grained area of duplex grain structure.

Figure 6 - Microstructures of MAR-M-509 P/M alloys heat treated for 121 hours at approximately 25°F above and below the secondary recrystallization temperature.

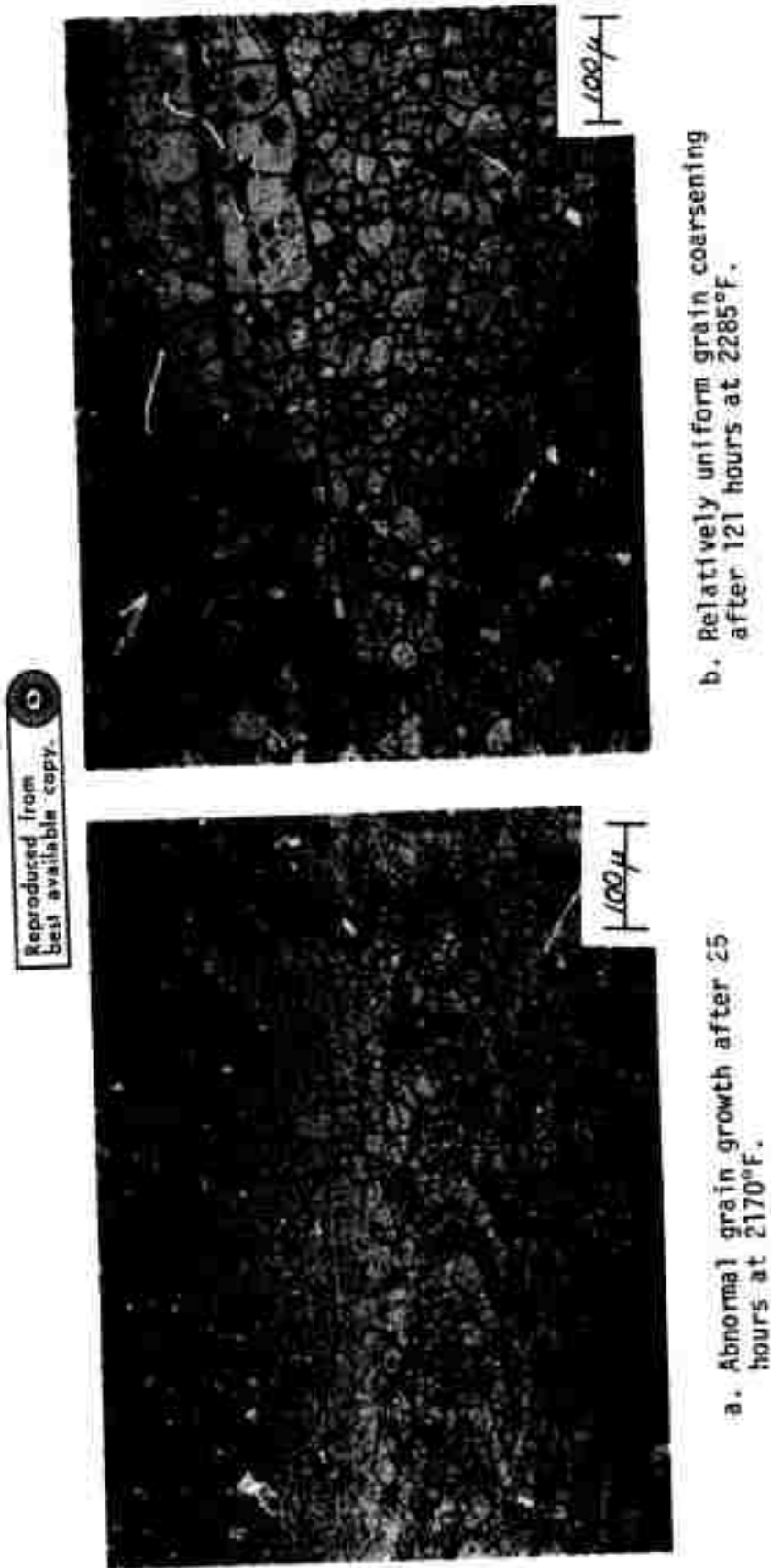


Figure 7 - Grain coarsening behavior of as-extruded Co-1 atom % HfC alloy.

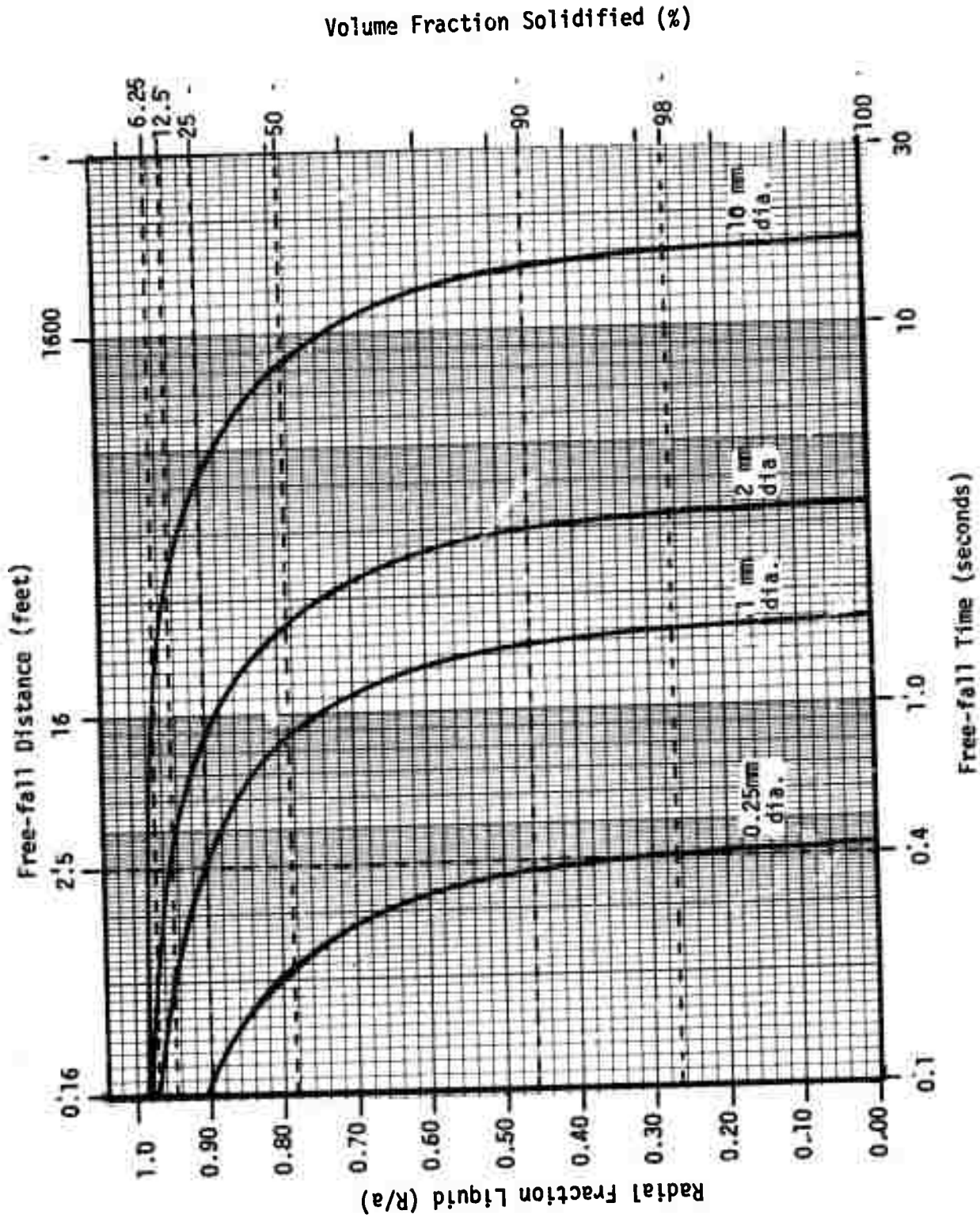


Figure 8 - The radial fraction liquid (or vol % solid) versus free-fall time or distance for spherical liquid droplets of steel.

Reproduced from
best available copy.



a. SEM photograph showing interpowder (pull-out type) fracture.



b. Fracture profile micrograph showing original dendrite structure (unrecrystallized area) of steam atomized powders.

Figure 9 - Fracture topography and profile of MAR-M-509 P/M alloy HIP at 2000°F and 28 Ksi for 2 hours and subsequently tensile tested at room temperature.

Reproduced from
best available copy.



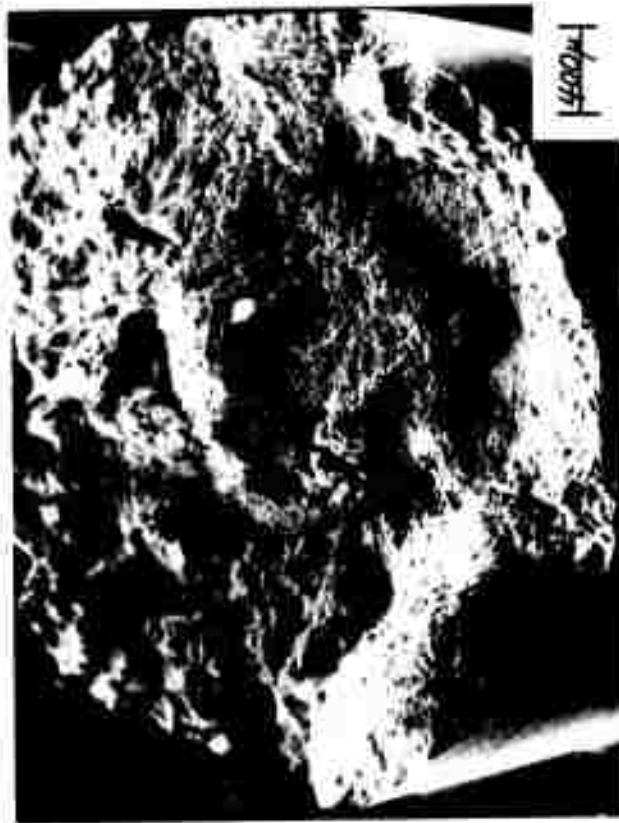
a. Fracture topography showing inter-dendritic and interpowder (pull-out) fracture.



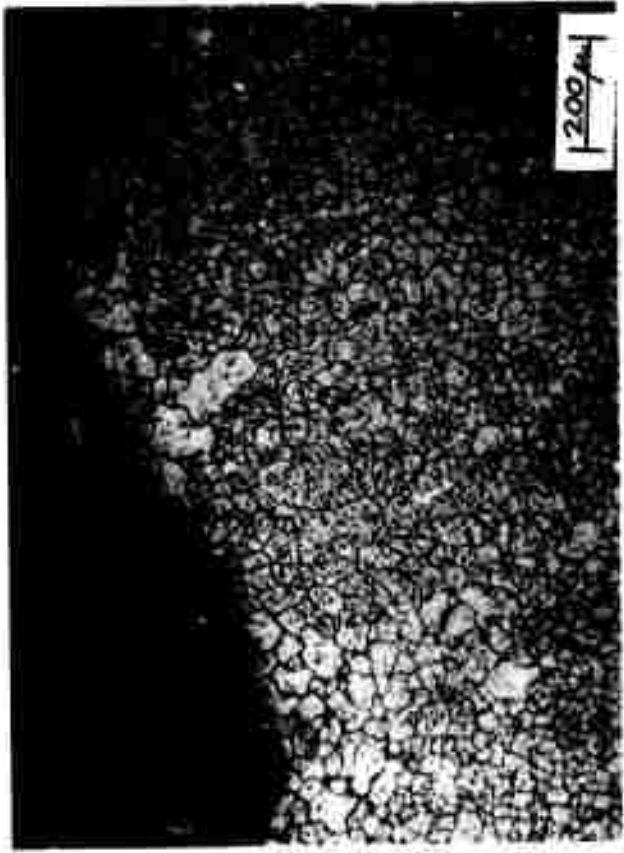
b. Partially recrystallized structure.

Figure 10 - Fracture topography and profile of MAR-M-509 P/M alloy HIP at 2150°F and 27 Ksi for 2 hours and subsequently tensile tested at room temperature.

Reproduced from
best available copy.



a. Fracture topography showing pre-dominantly trans-crystalline type fracture.



b. Fully recrystallized structure.

Figure 11 - Fracture topography and profile of MAR-M-509 P/M alloy HIP at 2300°F and 28 Ksi for 2 hours and subsequently tensile tested at room temperature.

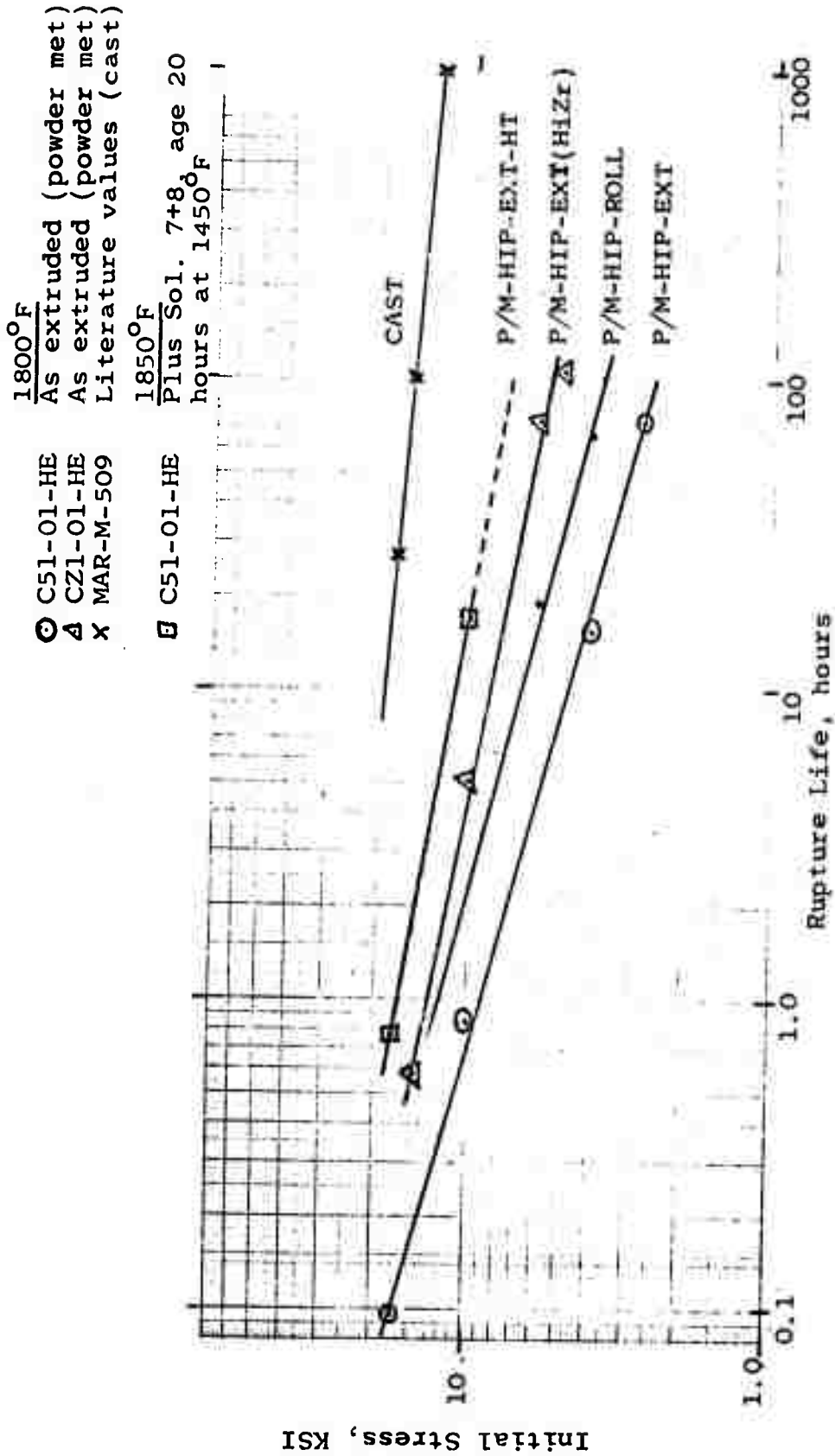


Figure 12 - MAR-M-509 and HiZr-509 Stress Rupture Data at 1800°F and 1850°F

- CH1-M1-C As precision cast
- CH2-01-HE As extruded (powder met)
- △ CH2-01-HEH Extruded + re-hot press

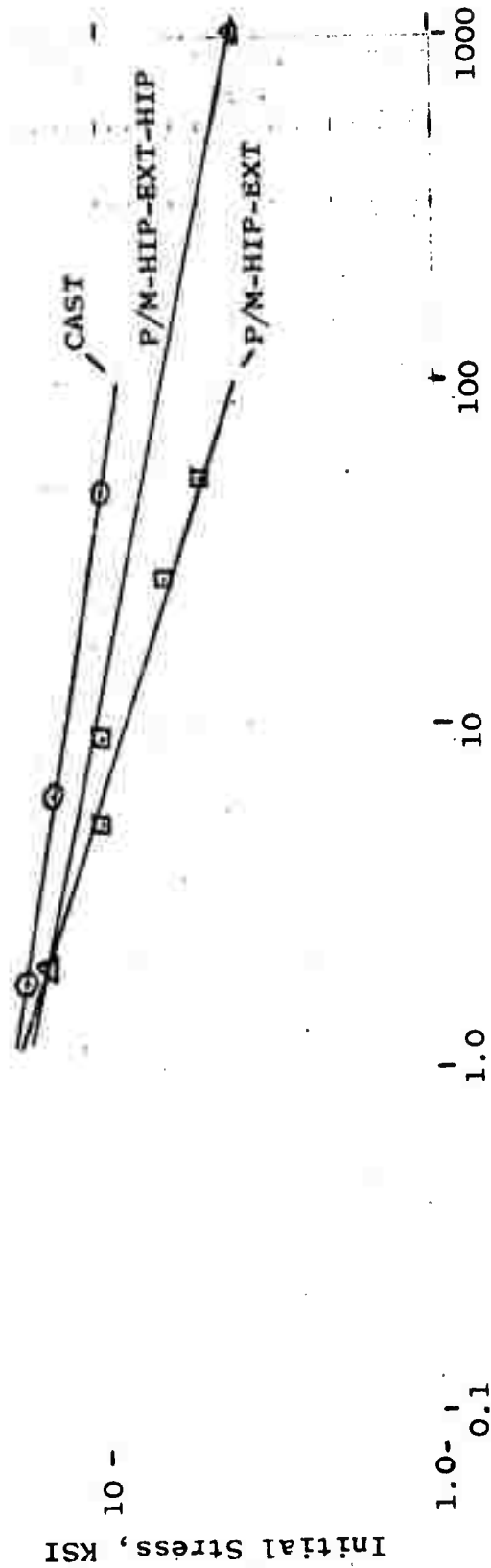
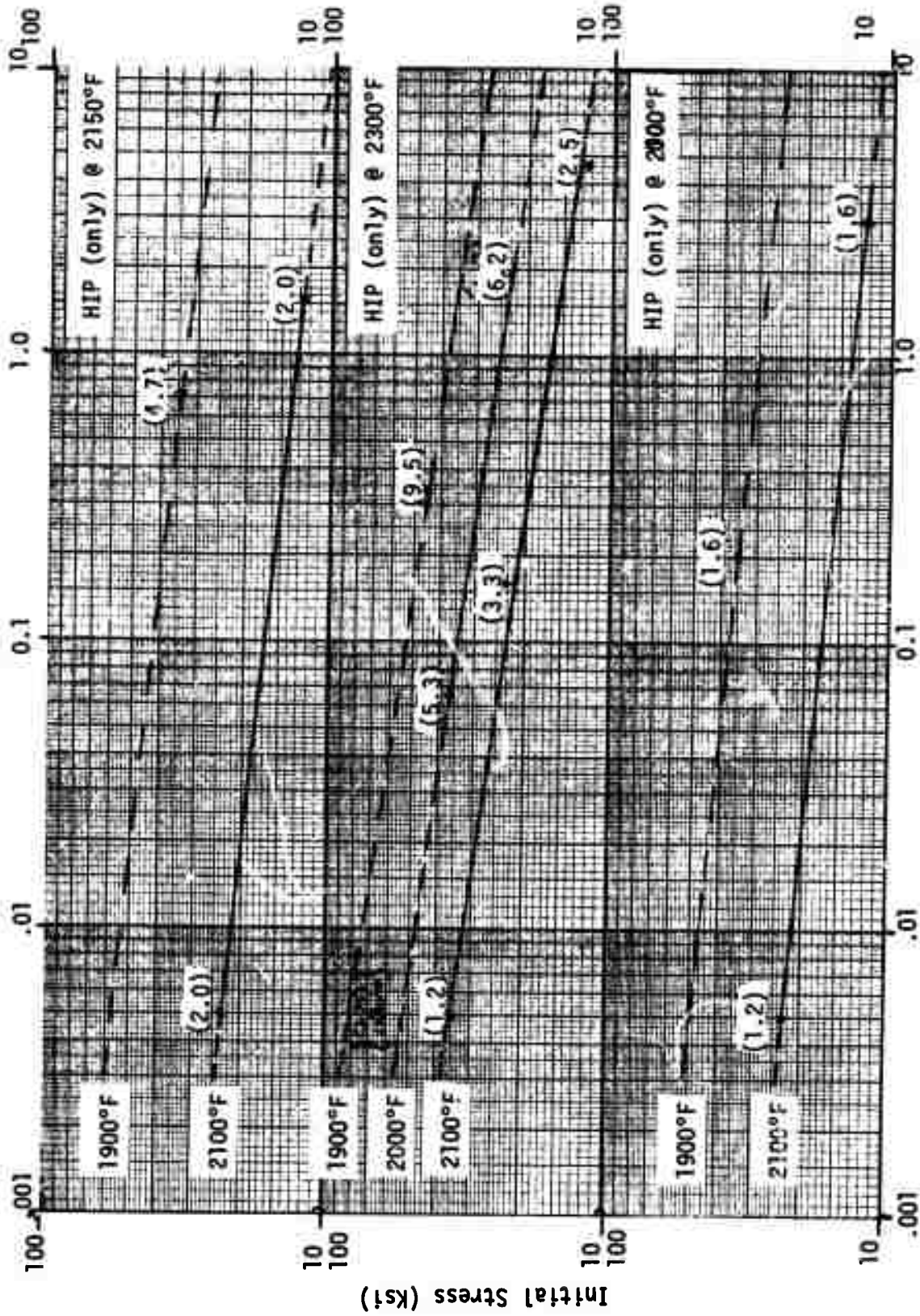


Figure 13 - Cobalt-Hafnium Alloys Stress Rupture Data at 1800°F



Rupture Time (seconds)

Figure 14 - High Strain rate stress-rupture data for MAR-M-509 P/M alloys in the as-HIP condition.

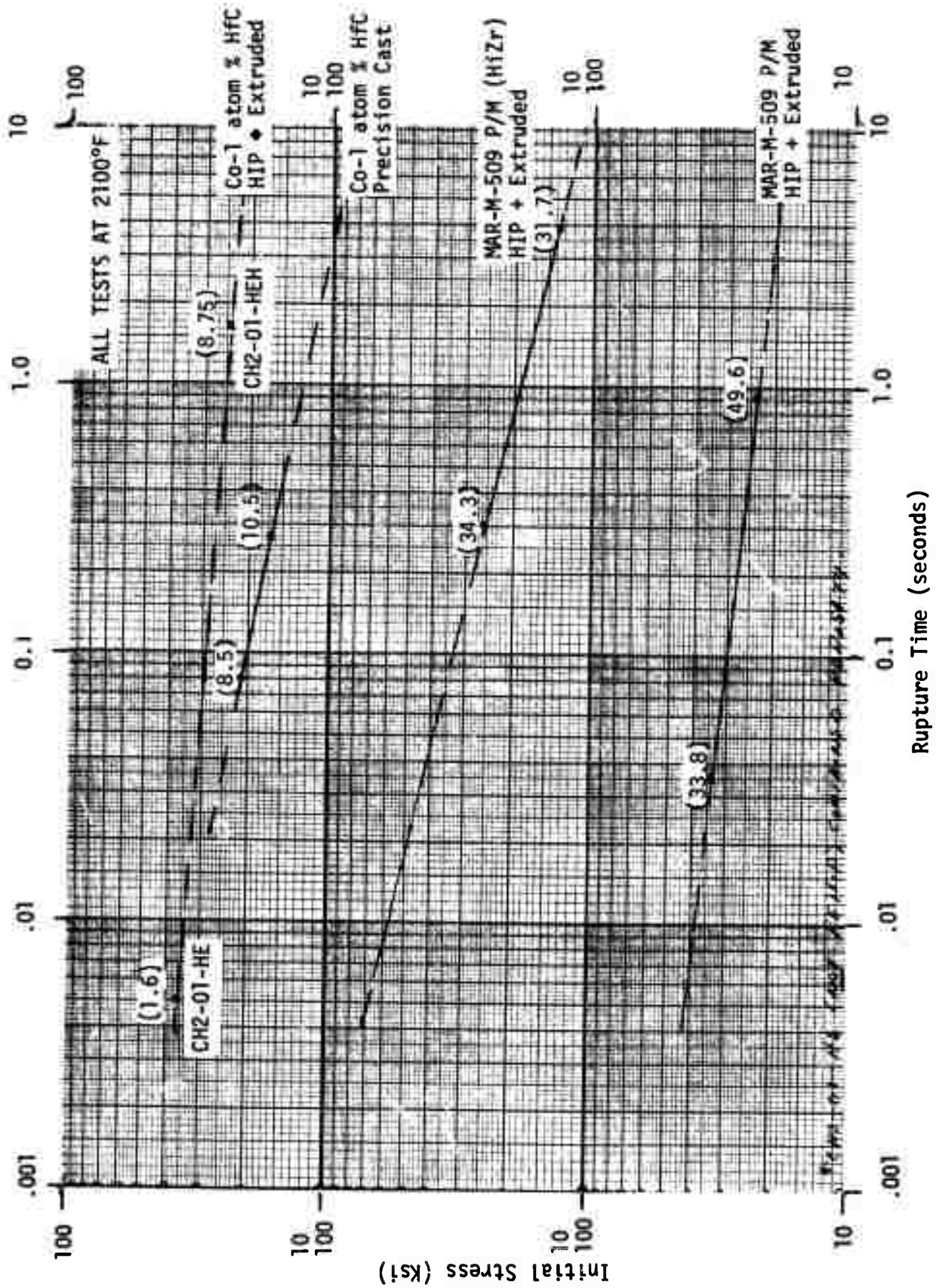


Figure 15 - High strain rate stress-rupture data for cobalt-base alloys in the cast or extr. condition.